·eesa

EARTH EXPLORER 11 CANDIDATE MISSION SEASTAR REPORT FOR ASSESSMENT

Reference	ESA-EOPSM-SEAS-RP-4374
Issue/Revision	1.0
Date of Issue	15/09/2023
Status	Issued

→ THE EUROPEAN SPACE AGENCY

·esa

Recommended citation:

ESA (2023). Report for Assessment: Earth Explorer 11 Candidate Mission Seastar, European Space Agency, Noordwijk, The Netherlands, ESA-EOPSM-SEAS-RP-4374, 116pp.

Cover image design: Earth Observation Graphics Bureau (EOGB). Inset by David McCann. Background by Christine Gommenginger and Fabrice Collard.

ACKNOWLEDGEMENTS

EXECUTIVE SUMMARY

Seastar is a new Earth Explorer mission concept dedicated to observing fast-evolving small-scale ocean surface dynamics in all coastal seas, shelf seas and marginal ice zones. Its science goals are: 1/ to understand the role of fast-evolving small-scale ocean dynamics in mediating exchanges between land, the cryosphere, the atmosphere, the marine biosphere and the deep ocean; 2/ to determine the ocean circulation and dominant transport pathways in the global coastal, shelf and marginal ice zones; and, 3/ to improve understanding of coastal, shelf and marginal ice zones contributions to the global climate system. Through its goals, Seastar contributes to the ESA Living Planet Ocean Challenge O1, O2, O3 and O4, together with Land Surface Challenge L2 and Cryosphere Challenge C1.

The ocean forms a central part of the climate system, with the capacity to store, transport and exchange vast quantities of carbon, heat, water, nutrients and other dissolved, suspended or floating matter. At its margins – in coastal, shelf and marginal ice zones – the ocean interacts with land, the cryosphere, the atmosphere and the marine biosphere, making these regions key interfaces of the Earth System. Within ocean margins, high-resolution satellite images reveal an abundance of ocean fronts, swirls, vortices and filaments at horizontal scales below 10 km that decorrelate rapidly within a few days. These fast-evolving small-scale features are the fingerprints of dynamic interactions and exchanges between the ocean, land, the cryosphere, the atmosphere, the marine biosphere and the deep ocean. Research shows that small-scale processes have far-ranging impacts on lateral dispersion, vertical stratification, ocean carbon cycling, and marine productivity, and play a key role in exchanges across these interfaces of the Earth System and in regulating climate.

Small-scale ocean processes play a dominant role in coastal seas, where dynamics are more intense and spatially variable due to the influence of coastlines and bathymetry. Interactions with the sea floor, underwater topography and coastlines produce complex current patterns that transform and transport sediments, nutrients, carbon, water and pollutants between coastal seas and the open ocean. Ocean surface winds exhibit greater heterogeneity in coastal seas, with localised effects near land linked to orographic steering, funnelling or temperature, elevation or roughness differences. Strong current-wind-wave interactions further modify air-sea fluxes, and cause marine hazards like coastal erosion, rip currents and dangerous sea states. Seastar would deliver frequent high-resolution data to advance scientific understanding, improve predictive skills and support sustainable developments (e.g., wind farms), effective coastal management and conservation strategies.

Shelf seas connect coastal seas and the open ocean through multiple physical, chemical, and biological processes, prompting some of the most productive and diverse ecosystems on Earth. Submesoscales act as conduits between the turbulent air-sea boundary layer and the deep ocean, affecting ocean heat and carbon uptakes and replenishment with nutrient-rich deep waters that sustain the ocean food chain. At the sea ice edge, atmosphere-ice-wave-sea interactions at scales below 10 km affect mixing, heat balance, momentum transfer and the dynamics of sea ice growth and decay. Small-scale processes also govern the delivery of heat to Antarctic ice shelves, with potentially critical implications for sea level rise globally. The scales, proximity of ice, remoteness and harsh conditions in these regions limit the availability of observations. New high-quality high-resolution current, wind and wave images are needed to better understand these processes, improve their representation in models, increase the reliability of forecasts and reduce uncertainties in projections about the ocean margins response to climate change.

The fast-evolving nature, small scales and spatial intricacy of these phenomena present formidable challenges for oceanographic observations, resulting in a striking scarcity of data at relevant temporal and spatial scales, even in coastal seas. The observational challenges of measuring fast-evolving small-scale dynamics at the boundaries of the global ocean means our knowledge of how the ocean interacts with other parts of the climate system is incomplete.

Seastar proposes to observe fast-evolving small-scale ocean dynamics with daily revisits and 1 km resolution to study exchanges of heat, carbon and nutrients at boundaries between land, the cryosphere, the atmosphere and the deep ocean. Seastar would measure two-dimensional fields of Total Surface Current Vectors (TSCV), Ocean Surface Vector Winds (OSVW) and Directional Ocean Wave Spectra (DOWS). With its highly innovative technology on a single independent satellite, Seastar is the first mission to offer the ability to characterise fast-evolving processes on daily to multi-annual scales over all coastal and shelf seas and Marginal Ice Zones. Existing and planned satellite missions like EE10 Harmony are unable to fulfil the rapid revisit, systematic coverage, and measurement sensitivity needed to satisfy the Seastar mission objectives.

Seastar's scientific goals are substantiated by nine mission objectives, including (amongst others): the quantification of the short-term variability of ocean surface dynamics on all scales relevant to ocean energy cascades from 100 km to 1 km and finer, to improve estimates of air-sea fluxes in open waters and in the vicinity of land and sea ice; and the delivery of the first comprehensive high-resolution description of ocean surface currents, winds and directional waves in all coastal, shelf and marginal ice zones, quantifying the magnitude, variability and dominant ocean transport pathways across seasons and multiple years. These mission objectives impose stringent observation requirements, notably on Level 2 uncertainties at 1 km resolution for TSCV (0.1 m/s) and OSVW (1 m/s) across the 100 km (or more) swath, in all sea state conditions, including sheltered coastal regions.

This level of performance is attained using a high-squint Ku-band Synthetic Aperture Radar (SAR) system with three azimuth beams dedicated to Along-Track Interferometry (ATI), onboard a single satellite in sun-synchronous Low-Earth Orbit scheduled for launch on a Vega-C rocket. Amongst several innovations, Seastar uses along-track interferometry in two highly squinted beams pointing ±45° in azimuth fore and aft of the satellite. By operating at Ku-band on a single satellite, Seastar achieves optimal angular diversity that delivers quasi-orthogonality (~ 90 degrees) between the two squinted looks. A broadside beam adds a third look in azimuth to support unambiguous simultaneous retrieval of current and wind vectors, giving Seastar the combined benefits of scatterometer-type sensitivity to wind vectors with the fine spatial resolution of SAR imagers. The required Level 2 performance is demonstrated achievable with the proposed instrument specifications and bespoke Level 2 geophysical inversion using high-resolution numerical simulations and OSCAR airborne campaign data. Seastar would be the first mission to implement high-squint three-azimuth along-track interferometry in space, the first payload and mission of its kind.

Seastar's sampling and coverage requirements are fulfilled with a single-sided swath of at least 100km. Full coverage of coastal, shelf and marginal ice zones is realised with slow-drifting orbits repeating every ~ 91 or 271 days, providing series of daily observations in all areas of interest, and sub-daily revisits at orbit crossovers. Seastar's sampling offers unmatched flexibility, with the ability to transition in-flight between the ~91 days, ~271 days and exact 1-day repeat cycles with very low impact on mission lifetime. This remarkable combination of sampling flexibility, systematic coverage of all ocean margins and high-performance makes Seastar uniquely able to attain its scientific objectives – capabilities unmatched by any other existing or planned mission.

With its unparalleled sampling and systematic mapping of global ocean margins, Seastar represents a leap forward in spaceborne ocean observing capability that would deliver ground-breaking understanding of fast-evolving small-scale ocean surface dynamics and their role in the climate system, and invaluable timely data of utmost significance for a multitude of practical applications and pressing societal needs. In the data-rich environment of the 2030s, Seastar would complete the Earth Observation portfolio of observations of the upper ocean, providing new opportunities for synergy across multiple data sources, and to harness advanced AI technologies to contribute to the advancement of knowledge in a new digital age.

Table of Contents

1. INTRODUCTION

1.1. Earth Explorer 11 candidates

ESA Research missions drive the Earth science agenda, technical innovation in Earth observing capabilities and future applications perspective within the Future Earth Observation (FutureEO) Programme. Earth Explorer missions focus on the atmosphere, biosphere, hydrosphere, cryosphere and the Earth's interior with emphasis on the interactions between these components and on the impact that human activities have on the Earth's processes. ESA's Earth Observation Science Strategy aims to cover all areas of science to which Earth observation missions can contribute. The Earth Observation Science Strategy for ESA (SP-1329/1) provides key elements and scientific direction for the future progress of ESA's Living Planet Programme. The context and specific scientific challenges to increase knowledge and capabilities in the five Earth science disciplines – atmosphere, cryosphere, land surface, ocean and solid Earth – are identified in the complementary volume (SP-1329/2).

The Call for Earth Explorer 11 (EE11) Mission Ideas was released in May 2020 and four mission candidates were selected for a Phase 0 study out of 15 proposals in June 2021. The four candidate missions selected for assessment phase study activities are outlined hereafter:

CAIRT would provide the measurements needed to unravel the intricate connections between circulation and composition throughout the middle atmosphere, and the role they play in climate dynamics, forcing and feedbacks. By tomographic imaging of many atmospheric trace gases and wave imprints at unprecedented spatial resolution, CAIRT would enhance our understanding of global atmospheric dynamics, chemistry, and transport of greenhouse gases and ozone-depleting substances. The mission would further explore the coupling of our atmosphere with space weather and help to constrain climate impacts by stratospheric aerosols. CAIRT would be the first limb-sounder with imaging Fourier-transform infrared technology in space.

Nitrosat would provide measurements and maps of atmospheric NH_3 and NO_2 at an unprecedented spatial resolution, which would allow exposing and quantifying individual nitrogen emission sources on a global scale. The two compounds account for 90% of all reactive nitrogen emissions and are major contributors to pressing environmental issues, including air quality deterioration, soil and water ecosystem contamination, biodiversity loss, and climate change. When combined with atmospheric models, Nitrosat would advance understanding of the human-induced disruptions to the nitrogen cycle and provide crucial scientific data to support the objectives of major international programs and environmental assessments.

Seastar would measure fast-evolving small-scale ocean dynamics with critical 1 day revisit time and 1 km resolution to study exchanges of heat, carbon and nutrients at boundaries between land, the cryosphere, the atmosphere and the deep ocean. It would deliver the first comprehensive high-resolution description of currents, winds and waves in the global coastal, shelf and marginal ice zones to improve their representation in models and identify coastal hazards, pollution pathways and impacts on marine energy, food and ecosystems. Seastar would carry a high-squint three-azimuth along-track radar interferometer, enabling the simultaneous observation and separation of ocean surface total currents and vector winds with unmatched revisit, coverage, and sensitivity.

WIVERN would deliver the first space-based observations of in-cloud winds and would complement the winds in clear air and thin clouds from the Aeolus follow-on mission in 2030. Equipped with its conically scanning 94 GHz Doppler radar, and its broad swath of width 800 km, WIVERN is designed to provide a global coverage of winds quasi-daily on average. These observations are expected to have a significant positive impact on Numerical Weather Prediction (NWP), as demonstrated by the first Aeolus

mission's winds, which showed one of the largest reductions in global NWP errors among others. Moreover, WIVERN would extend and continue the observations of CloudSat and EarthCARE radar reflectivities for cloud and precipitation profiling.

At the end of the Phase 0 study activities a down-selection will be performed. Up to two candidate mission(s) compatible with the scientific, technical and programmatic boundary conditions will be selected to proceed to Phase A study.

The Reports for Assessment capture the status of the respective mission idea at the end of Phase 0 activities. The four reports will be provided to the Advisory Committee for Earth Observation as a basis for a subsequent recommendation for up to two mission candidates to enter Phase A.

Each Report for Assessment follows a common format and logic. Each identifies the scientific questions and related key societal issues motivating the mission and its objectives. After establishing the scientific basis and rationale, the specific mission objectives are outlined and traced to a set of requirements used for system concept definition.

Each report comprises this introductory first chapter and eight subsequent chapters as follows:

- Chapter 2 identifies the background and scientific issues to be addressed by the mission. It provides justification for the mission and includes a review of the current scientific understanding of the issue in question while identifying the potential advances in knowledge that the mission could provide.

- Chapter 3 draws on arguments presented in Chapter 2 and summarises specific scientific goals and related mission objectives.

- Chapter 4 outlines the mission requirements, through providing quantitative descriptions and justification, including prioritisation, of the geophysical, observation and measurement requirements that would allow to fulfil the mission objectives.

- Chapter 5 provides an overview of the preliminary mission architecture and the system elements, including the space segment, ground segment, and operations.

- Chapter 6 gives a qualitative description of the data products at Level 1 and Level 2, the operational data processing and how the data acquired by this mission would be used - and includes a description of the data user communities.

- Chapter 7 briefly presents the retrieval approach, performance estimation with simulated and/or experimental data, and the validation concept.

- Chapter 8 describes the synergies and international context of the mission.

- Appendix A documents the scientific readiness self-assessment

- Appendix B documents the relevance of the mission to the evaluation criteria.

1.2. The Seastar mission

Seastar is a new Earth Explorer mission concept dedicated to observing fast-evolving small-scale ocean surface dynamics in all coastal seas, shelf seas and marginal ice zones. Its science goals are: 1/ to understand the role of fast-evolving small-scale ocean dynamics in mediating exchanges between land, the cryosphere, the atmosphere, the marine biosphere and the deep ocean; 2/ to determine the ocean circulation and dominant transport pathways in the global coastal, shelf and marginal ice zones; and, 3/ to improve understanding of coastal, shelf and marginal ice zones contributions to the global climate system.

"Ocean margins" (i.e., coastal, shelf and marginal ice zones) are fundamental interfaces of the Earth System where the ocean interacts with land, the cryosphere, the atmosphere and the marine biosphere. These regions frequently present a multitude of ocean jets, fronts, swirls and filaments at horizontal scales below 10km – fingerprints of dynamic interactions and exchanges between the ocean, land, the cryosphere, the atmosphere, the marine biosphere and the deep ocean. State-of-the-art models indicate that fast-evolving small-scale processes have far-ranging impacts on lateral dispersion and pathways, vertical stratification, air-sea fluxes, ocean carbon cycling, nutrient supply and marine productivity, and therefore play a central role in exchanges across key interfaces of the Earth System and in regulating climate.

Satellite images from ocean colour, thermal and active microwave sensors reveal complex spatial structures below 10 km scales that decorrelate within a few days. The fast-evolving nature, small scales and spatial intricacy of these phenomena present formidable challenges for oceanographic observations, resulting in a striking scarcity of ocean data at relevant temporal and spatial scales. Despite this pivotal role, small-scale ocean surface dynamics are poorly observed, even in coastal regions. The observational challenges of measuring fast-evolving small-scale dynamics at the boundaries of the global ocean means our knowledge of how the ocean interacts with other parts of the climate system is incomplete.

Seastar proposes to measure fast-evolving small-scale ocean surface dynamics with daily revisits and 1 km spatial resolution. With its highly innovative technology on a single independent satellite, Seastar is the first mission to offer the ability to characterise fast-evolving processes on daily to multi-annual scales over all coastal and shelf seas and Marginal Ice Zones. Existing and planned satellite missions like EE10 Harmony cannot provide the rapid revisit, systematic coverage, and measurement sensitivity needed to satisfy the Seastar mission objectives.

Seastar would deliver the first comprehensive high-resolution description of currents, winds and waves in the global coastal, shelf and marginal ice zones. Its data would support research of fast-evolving small-scale dynamics in these regions, improve understanding and their representation in models, and identify coastal hazards, pollution pathways and impacts on marine energy, food and ecosystems. Used in synergy with other satellite data and advanced Artificial Intelligence technologies, Seastar would enable a more complete interpretation of observed signatures in high-resolution optical, thermal and SAR images. In the context of Digital Twins, Seastar would complete the Earth Observation portfolio of observations of the upper ocean, to help bridge the scales gap between infrequent or low-resolution measurements from different data sources and the small, local scales that are relevant to users.

With its unparalleled temporal and spatial sampling and systematic mapping of global ocean margins, Seastar represents a leap forward in spaceborne ocean observing capability that would deliver ground-breaking understanding of fast-evolving small-scale ocean surface dynamics and their role in the broader climate system. Seastar would also delivering invaluable timely data of utmost significance for a multitude of practical applications and pressing societal needs.

2. BACKGROUND AND SCIENTIFIC JUSTIFICATION

In this chapter we present the science case for Seastar, providing a brief introduction for the mission justification, and going into detail for each specific science application in subsequent sections.

2.1. Introduction

The ocean forms a central part of the global climate system, with the capacity to store, transport and exchange vast quantities of carbon, heat, water, nutrients and other dissolved, suspended or floating matter. The global ocean margins (i.e., coastal and shelf seas and marginal ice zones) are key interfaces of the Earth System where the global ocean interacts with land, the cryosphere, the atmosphere and the marine biosphere. These dynamic climate-sensitive regions are characterised by an abundance of jets, eddies, fronts, vortices and filaments at scales below 10 km that decorrelate rapidly over a few days. Often seen in satellite ocean colour and sea surface temperature images, these fast-evolving small-scale features are the fingerprints of dynamic interactions, intense horizontal mixing and vertical exchanges that impact lateral dispersion and pathways, vertical stratification, heat fluxes, ocean carbon cycling, nutrient supply and marine productivity. State-of-the-art high-resolution models indicate that these fast-changing small-scale dynamics play a critical role in regulating global climate by mediating exchanges across fundamental interfaces of the Earth System.

Today, despite their paramount importance in the Earth system, fast-evolving small-scale processes at interfaces are not represented in Earth System Models and the roles of coastal, shelf and marginal ice zones in climate change are not well quantified. The spatial complexity, small scales and rapid evolution of these phenomena make them challenging to observe with oceanographic means. In coastal and shelf seas, there is a lack of ocean current, wind and wave data, despite the critical scientific, societal and economic relevance of these regions. In the MIZ, the remoteness and harsh conditions limit observing possibilities. Existing and planned satellite missions do not provide the rapid revisit, systematic coverage, and sensitivity to address these needs. This lack of relevant data inhibits complete interpretation of existing high-resolution satellite data (like SST), limits understanding and holds back our ability to represent these processes in models, forecasts and projections. Seastar would bring urgently needed new spaceborne capability to understand the role of fast-evolving small-scale ocean dynamics in exchanges at global ocean margins, and to deliver the first comprehensive high-resolution description of ocean surface currents, winds and directional waves in the global coastal ocean, shelf seas and marginal ice zones.

2.2. Coastal dynamic processes

Coastal regions, where land meets the sea, are dynamic interfaces of numerous interactions between the land, atmosphere and the ocean. Coastal dynamics play a crucial role in the global climate system, influencing weather patterns on nearby land, impacting coastlines, marine ecosystems and lateral and vertical processes. Coastal seas also provide vital resources and services to society including energy (oil & gas, renewables), transport (shipping, ferries) and recreation (sailing, tourism), whilst presenting mankind with some of the most challenging environmental hazards (sea level change, coastal erosion, coastal flooding). Enhancing our observations of coastal ocean dynamics is essential to advance understanding and improve the representation of coastal processes in the global climate system, to enable communities to identify sustainable coastal management and climate adaptation/mitigation strategies. Seastar represents a leap forward in coastal observing that is particularly timely, given the unprecedented industrialisation of the coastal and shelf seas in coming decades, in particular for large scale wind energy production (Koutsokosta & Chadwick, 2023), that will impact coastal environments and will require better data to achieve effective management and mitigation.

2.2.1. Fast-evolving coastal processes

The coastal ocean circulation is dominated by processes that occur on short spatial and temporal scales. Interactions with the sea floor, underwater features and the coastline result in complex current patterns and interactions that can change in a few hours (Schulz-Stellenfleth & Stanev, 2016). Key differences with the open ocean include stronger tidal flows, changing water depths, spatially varying ocean waves and sharp water density fronts associated with freshwater river plumes or upwelling.

High-resolution images from satellite ocean colour sensors in coastal seas frequently display complex spatial patterns of chlorophyll, turbidity or suspended sediments at scales below 1 km. Using data from multiple missions makes it possible to build sequences of daily or sub-daily images that show the rapid temporal decorrelation of these small-scale structures after a few days (Figure 2.1). Chlorophyll or suspended sediment concentration patterns respond to the action of ocean currents, winds and waves on short temporal and spatial scales. Short-lived storms and tidal streams cause resuspension of bottom sediments and mixing of the water column (Miller *et al.*, 2007; Chen *et al.*, 2020).
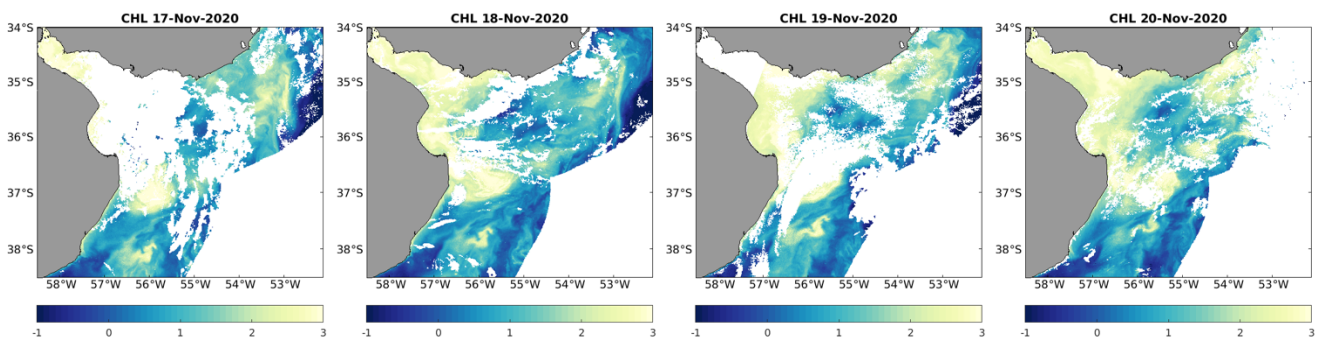
Figure 2.1: Sequence of Copernicus Sentinel-3 OLCI daily products over Río de la Plata (Patagonia) showing chlorophyll concentration structures advected and modified by long-shore currents. The space-time evolution of the structures is partially obscured by the presence of clouds (white pixels). [Credits: University of Liège, A. Alvera-Azcárate]

Accurate high-resolution information about ocean dynamics, vertical mixing and horizontal pathways is needed to disentangle the complex physical, biological and chemical processes that control concentrations of chlorophyll, sediments and other waterborne materials in coastal seas. New high-resolution measurements of total surface currents, winds and waves from Seastar – including details of their magnitude, spatial structure, short-term variability and interactions – will enable more advanced interpretation of ocean colour signatures in satellite data, to help determine more precisely how coastal dynamics affect exchanges of carbon, nutrients and other matter with shelf seas and the open ocean.

2.2.2. Air-sea fluxes in coastal seas

The ocean is a key component of the Earth System, especially regarding its influence on weather and climate at the timescales relevant to the next generations. Air-sea fluxes are the direct link between the atmosphere and the ocean and determine how the ocean modulates weather and climate. Air-sea fluxes also relate to marine hazards such as coastal flooding, marine heatwaves and hypoxia. The centrality of air-sea fluxes is recognised by the United Nations Decade of Ocean Science for Sustainable Development OASIS programme ("Observing Air-Sea Interactions Strategy"). In OASIS, Cronin *et al.* (2023) propose an action plan incorporating three "Grand Ideas", including one advocating "satellites optimised for air-sea fluxes". At the same time, sectoral reviews have looked at existing and future spaceborne Earth Observation capability, for example, relating to ocean carbon (Shutler *et al.*, 2020; Brewin *et al.*, 2023). For coastal seas, the combined action of surface fluxes and sub-surface

processes will determine transports within the shelf region and across the shelf edge, with the general lack of fine-scale information introducing major uncertainties about contemporary and future transports (Roobaert *et al.*, 2019; Dai *et al.*, 2022; Figure 2.2). Seastar would bring unique new capability to complement the observing system to address this important knowledge gap.
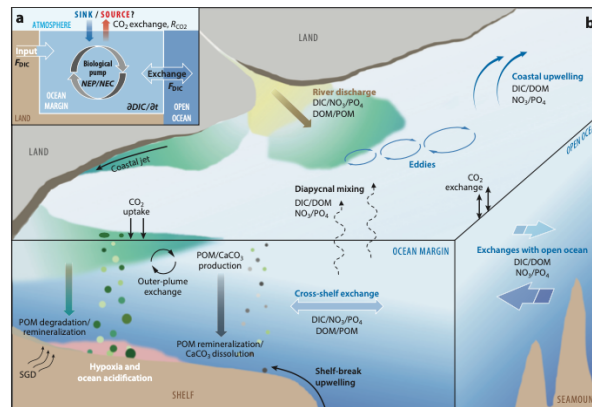
Figure 2.2: Conceptual schematics of air-sea CO_2 exchanges (*a*) and major physical and biogeochemical processes in the coastal ocean (*b*), highlighting the transport of matter between land, ocean margin, and open ocean [Credits: Dai *et al.*, 2022]

Air-sea fluxes depend on turbulent wind-driven processes, or more precisely, on the turbulence resulting from the interaction of winds, surface waves and currents. Currents can locally affect coupling of atmosphere and ocean, resulting in large anomalies in surface fluxes. This was demonstrated theoretically by Shin *et al.* (2022) for CO_2 transfer. Anomalies may be both positive or negative, and the net effect depends on the coherence of surface anomalies with sub-surface processes. For example, where a sustained downward anomaly in surface transfer coincides with a downwelling or depositional process, enhanced transport is implied. Observational confirmation of this hypothesis is missing though, and the required data must have sufficient resolution and duration. Observations of features (e.g., fronts) must be sustained over several days since flux anomalies accumulate in the surface ocean over time; in some cases, accumulation is relatively slow (e.g., dissolved inorganic carbon), calling for sustained systematic observations. The capabilities of Seastar are uniquely qualified to fill this knowledge gap thanks to three key mission characteristics: 1/ simultaneous measurements of current and wind vectors and surface waves; 2/ fine spatial resolution (1 km), revisit (1-day or better) and duration (sustained observations of given site for extended periods); and 3/ global coastal coverage.

Air-sea fluxes of heat, moisture and radiatively active gases play a crucial role in shaping weather and climate. Exchanges of gases, like carbon dioxide, impact the greenhouse gas composition of the atmosphere, influencing global temperatures. The coastal ocean is a challenging environment to estimate air-sea fluxes due to greater heterogeneity and variability of winds, waves, and currents at all scales. The coastal ocean and shelf seas are also disproportionately important with respect to global ocean carbon cycle with large sources, sinks and transports within these seas and across the shelf edge (Dai *et al.*, 2022; Regnier *et al.*, 2022). Seastar's ability to measure relevant dynamics would transform our understanding of fluxes and transports in coastal and shelf seas. The mapping of kilometre to sub-kilometre motion vectors, with frequent and sustained revisits, will make it possible to observe the evolution of fronts and other features to provide estimates of fluxes, downwelling, upwellings and transports in these regions. Estimating and understanding heat, carbon and water exchanges in the land-coastal-shelf-open ocean continuum are a societal imperative, to inform the direction and urgency of climate action and energy and environmental policy. Better estimates of fluxes will reduce uncertainties in projections of ocean warming and acidification, and the predictions of harmful extreme events such as marine heatwaves and deoxygenation.

2.2.3. Wind/wave/current interactions and coastal hazards

Wind/wave/current interactions are important in coastal regions also for coastal engineering, shoreline management and marine conservation (Wolf & Prandle, 1999). Waves travelling into coastal areas release enormous amounts of energy and momentum, accumulated over tens of hours and hundreds of kilometres, into shallow waters, sea floor, coastline and coastal structures. Momentum generates currents, long-period oscillations and wave setup that contribute to coastal flooding (Wolf, 2009; Staneva *et al.*, 2017). Interactions with currents or bathymetry can lead to rapid wave height changes over short distances (Ardhuin *et al.*, 2012) and dangerous sea states. Tidal and wave-induced long-shore and cross-shore currents cause patterns of erosion and accretion, sediments redistribution (Stanev et al., 2009) with wave-induced rip currents now the primary coastal hazard to life globally (Zhang et al., 2021). These processes represent important coastal hazards that impact water quality, marine ecosystems and coastal habitats and pose major challenges for coastal management and engineering (e.g., Luijendijk & van Oudenhoven, 2019).

Wind/wave/current interactions are relevant also to coastal erosion at high latitudes. As the Earth's climate warms, Arctic coastal regions are exposed to stronger coastal erosion through the combined action of sea level rise, stronger winds and greater wave action due to sea ice retreat (Nielsen *et al.*, 2022). In turn, high-latitude coastal erosion exposes previously frozen organic matter, such as peat, vegetation, and soil, to the marine environment, where it decomposes and releases carbon dioxide and methane into the atmosphere (Winterfeld *et al.*, 2018). This feedback loop of increased erosion, carbon release, and diminished carbon uptake underscores the complex interplay between climate change and coastal processes at high latitudes.

2.2.4. Marine renewable energy: resources, management and impacts

The requirement to move rapidly towards "Net Zero" implies an accelerated growth in renewable energy generation over the next decades, most likely including Terawatt-scale (TW) electricity production offshore (US Department of State, 2021; European Commission, 2023). For context, 1 TW offshore capacity can provide ~5% of global energy consumption. Clean energy generation is expected to be dominated by offshore wind farms (although wave, current and other resources will also grow), to be sited primarily in coastal and shelf seas. Offshore wind will be a global phenomenon, with China and its Asian neighbours, and Europe (especially North Sea) leading sectoral growth.

The proposed colonisation of coastal and shelf seas by large-scale industrial renewable infrastructure represents an unprecedented first-order disruption of the dynamics and energy budget of these sensitive environments, with an occupation of space exceeding oil and gas. Since global tidal energy in shelf seas and the global wave energy resource are also order of a Terawatt, characterisation of their resource and potential interactions will be needed. Better data and understanding are required across a range of engineering, scientific and policy areas to support the growth of offshore renewable energy and establish the practical "carrying capacity" of the marine environment with respect to offshore wind.

A key area of uncertainty regards how individual turbines and arrays of turbines will interact with winds, waves, currents, coastal mixing and sedimentation processes. Most early offshore wind developments were in shallow water, many fringing the North Sea, with some impacts already observed or modelled with reasonable confidence. For example, the scouring around the base of monopiles (supporting turbines) and sediment plumes are readily observed, as are wind shadows, visible in SAR images and coastal radar data (e.g., Ahsbahs *et al.*, 2020; Figure 2.3). These interactions and modification of the wind field are expected to reduce wind and wave resources (Fischereit *et al.*, 2022) and impact ecosystems and the food chain through large scale changes in primary production (Daewel *et al.*, 2022).
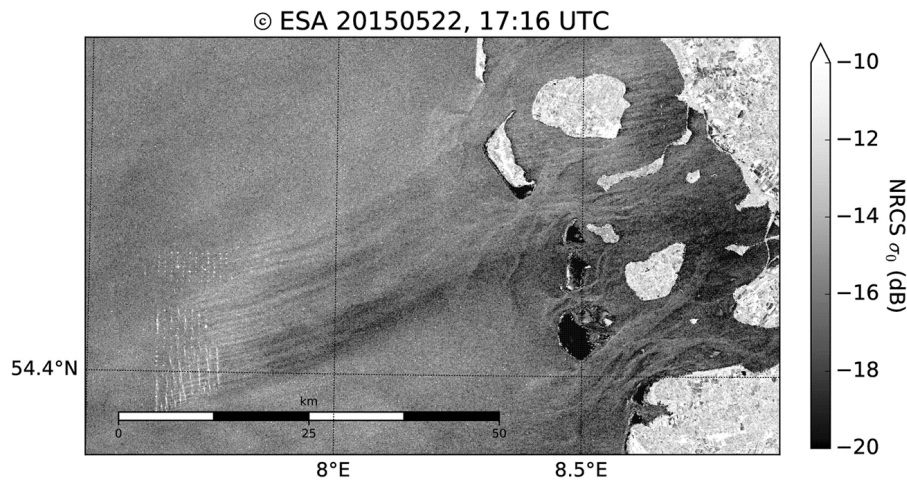
Figure 2.3: Copernicus Sentinel-1A roughness image over Wadden Sea on 22 May 2015 showing wind shadowing and variability downstream from wind farms and interactions with complex roughness patterns near the Danish coast. The scene is a little under 100 x 100 km^2. [Credits: Platis *et al.*, 2018]

At the same time, an entirely different paradigm emerged with the realisation that the underwater foundations and moorings act to stir the sea through interaction with a flow (e.g., tidal). As wave farms move into deeper waters, it is thought the stirring action could disrupt seasonal stratification in shelf seas (Dorrell *et al.*, 2022). The choice of foundations and moorings in deeper waters could have positive and negative effects and this should be studied and understood. Affecting ocean stratification and ecosystems could have serious consequences and observations must be appropriate to make informed choices. There is a clear deficit regarding current, wind and wave data at the scales relevant to wind farms that Seastar could fill. New offshore wind turbines are typically ~200 m in diameter (~10 MW capacity) and commonly gathered in arrays of 100+ turbines, with a steady upward trend in all parameters. With turbines usually spaced 7 diameters apart, the separations (~1.5 km) and array dimensions (~20 km) are compatible with the capabilities of Seastar (simultaneous data about currents, winds, and waves in the global coastal ocean; 1 km resolution; 100+ km swath) which are clearly relevant to address the observing and knowledge gap.

The successful and sustainable development of marine renewable energy is necessary to decarbonise the economy and maintain a healthy and habitable planet. But the implied scales and impacts of offshore wind are only now reaching the consciousness of policy and science leaders. The scale and speed of growth in this sector call for an improved observing system that can deliver all the required information, from resource assessment, to hazards, to operations and maintenance, to environmental impacts. The existing and planned observing system addresses some of these (e.g., Cronin et al., 2023), but there is a clear need for simultaneous measurements of currents, wind and waves at the scale of turbines and arrays, globally across coastal and shelf seas. Right now, there is incomplete scientific understanding of the effects of large-scale wind installations on the structure of coastal and shelf seas, and of their impact on marine ecosystems and the food chain that support commercial fisheries. The need to measure currents, winds and waves, their variability and the anomalies associated with offshore infrastructures, will become more pressing in coming decades, and could be addressed by Seastar at the time when offshore wind reaches the scales where local, regional-scale and global-scale effects start to emerge. Offshore renewable energy requires scientific supporting actions to inform industry about the scale and detail (e.g., siting, choice of foundations and moorings) that different environments can support, thus reducing risks to marine habitats, ecosystem diversity, fisheries, safety at sea and coastal protection.

2.2.5. Other coastal applications

2.2.5.1. Tides and bathymetry

Tides are long-period waves that appear to move through the oceans due to the gravitational pull of the Moon and the Sun. The dominant tidal components are the main lunar tide (M2) and main solar tide (S2) with periods of 12.42 h and 12 h respectively. In coastal seas, coastlines and seabed topography including shallow areas, channels, and narrow straits, can amplify or attenuate tidal amplitudes and currents (Andersen, 1999). As tides encounter different depths and obstacles such as islands or headlands, they undergo changes in amplitude, timing, and direction. Bottom friction modifies the progression of tidal waves, scaling down the tidal wave patterns as the tidal wave speed reduces. Where the natural period of the basin matches the tidal period, resonance or near-resonance can add complexity and produce some of the world's largest tidal amplitudes, for example in the Irish Sea, the Bay of Fundy (Canada) or the Severn Estuary (UK).

Traditionally, tides are predicted using numerical models whose accuracy in coastal seas depends on their spatial resolution, the quality of the bathymetry data and whether local effects are present (e.g., river plumes). Tidal water levels and currents can vary significantly over short distances, but fine-scale structures are difficult to observe and model. A recent study in the Severn Estuary (UK) used high-resolution Sentinel-3 fully focused SAR altimeter data (Egido & Smith, 2016) to estimate water height residuals in the state-of-the-art FES2014 tide model (Lyard *et al.*, 2021). Residuals up to 1.6 meters were identified along a 5 km stretch, equivalent to current speeds up to 4 m/s. Such uncharted currents are significant hazards for humans and shipping and modify erosion and sediment transport patterns.

Together, tidal models and bathymetry are used to understand and predict coastal erosion, sediment transport and the impacts of storms and tsunamis. Tides and bathymetry hold significant relevance to navigation safety, dredging, fishing and other economic and leisure maritime activities. High-resolution bathymetry data are in short supply, however. Bathymetric surveys with traditional acoustic systems, such as echo sounders and side-scan sonars, are time-consuming and prohibitively expensive. Satellite altimetry methods to estimate bathymetry are limited to water depths greater than 100 m, whilst spaceborne optical methods give reliable estimates only for shallow waters less than 30 m deep. Seastar's detailed mapping of coastal currents will bring additional information about coastal tides that complements satellite altimeter water level data, to improve models and the vital information they deliver for coastal zone management, including coastal engineering, hazard assessment, and the protection of marine biodiversity and habitats.

2.2.5.2. River input to the ocean

Rivers play a critical role in exchanges between land and the ocean, acting as conduits for the transport of water and various materials, including sediment, nutrients, organic matter, and pollutants, from terrestrial environments to the coastal and marine ecosystems. Riverine sediment input not only influences coastal morphology and sedimentation patterns but also provides essential nutrients and minerals to the marine environment, supporting coastal ecosystems and promoting biological productivity. Sadly, human activities like agriculture, urbanisation, and industrialisation, also inject pollutants, plastic waste and excess nutrients into rivers, with detrimental impacts on coastal and marine life, including eutrophication, harmful algal blooms, and plastic pollution (MacLeod *et al.*, 2021).

Riverine carbon input to the coastal ocean affects air-sea CO_2 fluxes, oxygen balance, and acidification level, with impacts on marine ecosystem health (Meybeck & Vörösmarty, 1999; Liu et al., 2021). Riverine transports of nutrients and carbon from inland waters to coastal and open ocean regions are poorly quantified but could play an important role in the global carbon budget (Gao et al., 2023). Seastar

measurements of coastal currents, winds and waves would provide valuable insight into the pathways and dispersion patterns of riverine water, carbon, plastics and other suspended or dissolved materials. Within the context of Digital Twins and multi-sensor synergy, integrating Seastar data with other relevant information (e.g., river discharge, sediment load, nutrient concentrations) could lead to improved estimates of riverine input that could benefit carbon cycle and climate studies and promote effective management and conservation strategies for coastal and marine environments.

2.3. Shelf and cross-shelf processes

Shelf seas are the oceanic regions that extend from the coastline to the edge of the continental shelf. Where the continental shelf is wide, shelf seas can span several hundred kilometres from land (e.g., west European shelf, Patagonian shelf, North Sea). The proximity of coastal seas provides access to nutrient-rich waters, resulting in abundant primary production that supports a diverse and thriving marine ecosystem and wide array of marine life, including fish, shellfish, marine mammals, and seabirds. The abundant food and sheltered conditions are favourable for the growth and survival of fish larvae and juveniles, making them nurseries for many commercially important fish species. Shelf seas connect coastal seas and the open ocean through multiple physical, chemical, and biological processes. Here, complex interplay of currents, winds and waves at different scales mingle tides with boundary currents, mesoscale eddies, fontal systems and sub-mesoscale structures, all influencing to a greater or lesser degree, the connectivity of the coastal and the open ocean.

2.3.1. Fast-evolving sub-mesoscale processes

High-resolution satellite ocean colour and sea surface temperature (SST) images tell us that the coastal ocean is filled with fronts, swirls, vortices and filaments at scales below 10 km (Figure 2.4). With scales of 0.1–10 km and variability of the order of 1 day, these so-called 'submesoscales' are characterised by loss of geostrophic balance, large vorticity and divergence (of the order of the Coriolis parameter f or higher) and large vertical velocities (McWilliams, 2016; Chelton *et al.*, 2019; Esposito *et al.*, 2021). Their characteristic signatures in chlorophyl and SST images are the fingerprint of intense air-sea interactions and vertical processes linking the atmosphere, ocean surface and ocean interior.

Sub-mesoscale dynamics have come into sharp focus in recent years in numerous high-impact scientific publications that highlight their importance for heat fluxes, ocean gas transfer, horizontal dispersion, vertical stratification, surface water nutrient supply and marine ecosystems (e.g., Lapeyre & Klein, 2006b; Capet *et al.*, 2008; Lévy *et al.*, 2012; Zhong *et al.*, 2017; D'Asaro *et al.*, 2020a; Siegelman *et al.*, 2020). State-of-the-art numerical models highlights their critical stirring role at kilometre scales, and radical dynamical changes when scales reach 1 km or less (Lapeyre & Klein, 2006a; Capet *et al.*, 2008). Different theories suggest complex direct and inverse energy cascades at scales between 1-100 km (Capet *et al.*, 2016; Klein *et al.*, 2019), making the case for new fine-resolution dynamical observations over continuous 100km scenes or more to validate these hypotheses.

Frontogenesis and wind/current interactions are key mechanisms invoked in ocean stratification and the generation of unusually large vertical ocean velocities (100 m/day instead of typical 1-10 m/day). These can penetrate deep into the mixed layer to transfer nutrients and heat between the turbulent surface boundary layer and the ocean interior (Lévy *et al.*, 2009; Klein *et al.*, 2011). Current research indicates that the structure and intensity of sub-mesoscale processes, and their contribution to ocean transport and mixing, varies seasonally and regionally (Brannigan *et al.*, 2015; Buckingham *et al.*, 2016). Seastar is uniquely placed to deliver the high-quality high-resolution observations of surface dynamic properties with the necessary sensitivity, temporal revisit and coverage, to test these theoretical ideas, assess models and validate these findings. Circumstantial evidence is mounting that

submesoscales also shape the trophic interactions between many marine organisms and impact the marine food web as a whole (Kai *et al.*, 2009; Woodson & Litvin, 2015). Given the central importance of marine resources for international food security, and the social and economic implications of fluctuations and redistributions, better understanding of these processes and their variability is needed. Seastar data will characterise the temporal and spatial variability of these phenomena across main primary production regions in coastal, shelf seas and Marginal Ice Zones (e.g., Southern Ocean), and work in synergy with other satellites and model data to explore the impact of small-scale dynamics on the marine food chain.
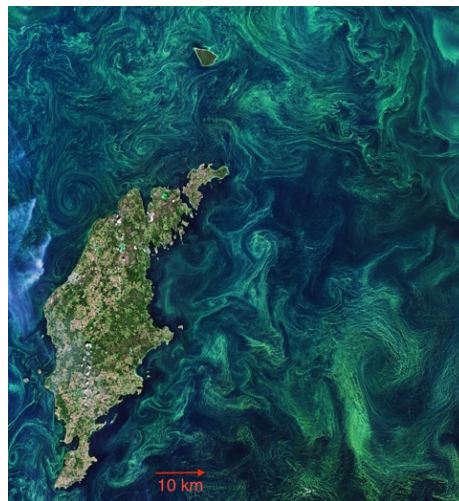
Figure 2.4: Copernicus Sentinel-2 image showing the characteristic signatures of sub-mesoscale dynamics in algae blooms in the Baltic Sea, July 2019. [Credits: ESA CC BY-SA 3.0 IGO]

On longer time scales, it is recognised that re-stratification by submesoscales is a leading-order process for climate (Fox-Kemper & Ferrari, 2008; Flato *et al.*, 2013). Long-term model simulations at different spatial resolutions demonstrate widespread impact of submesoscales on deep water formation, the Atlantic Meridional Overturning Circulation (AMOC), heat transport, mixed layer depth and ocean biogeochemistry (Lévy *et al.*, 2010). Resolving small scales in models dramatically alters how the ocean interacts with the rest of the climate system, changing ocean circulation pathways, air-sea fluxes, ocean carbon and heat uptake, and marine ecosystem response to climate change. Today's climate models remain too coarse to resolve small scales explicitly, relying instead on parameterisations. Improved parameterisations were used in IPCC AR5 CMIP5 models (Fox-Kemper *et al.* (2011); Flato *et al.*, 2013). But despite significant improvements in their parametrization over the last decade and significant improvement in some models, biases in mixed-layer representation generally persist (AR6 Chapter, Fox-Kemper *et al.*, 2021). Key aspects that still require parameterisation are front-wind and front-wave interactions which depend critically on the alignment between fronts, waves and winds. Because co-alignment and anti-alignment have qualitatively different and asymmetric impacts, systematic assessments of these phenomena and their statistics are needed. Here again, Seastar's regular observations of the spatial organisation of winds, currents and waves at small scales will directly inform these questions to validate and improve parameterisations for better future climate projections.

2.3.2. *Fast-evolving small-scale surface dynamics and buoyancy fluxes*

Surface winds play a central role in many aspects of the climate system and their variability and interactions with currents at short temporal and spatial scale are critically underexplored. Scatterometers will successfully track fast-evolving global winds down to ~20km scales (Stoffelen *et*

al., 2019), but do not observe the important interactions at km-scales that Seastar will address. Winds are both driving a direct ocean circulation response (i.e., Ekman currents, upwelling/downwelling) and a leading factor in air-sea fluxes of heat and water which set ocean surface buoyancy losses. Here, buoyancy losses have a major influence on dense water formation and the ocean overturning circulation, including the AMOC, a strong source of uncertainty in climate projections (IPCC AR6, 2021).

Right now, our understanding of high latitude Atlantic processes and their influence on the AMOC is undergoing a major transformation thanks to new in situ data from the past decade (Lozier *et al.*, 2019). The Labrador Sea (Figure 2.5), long believed to be a key driver of AMOC variability, is now thought to experience *density compensation* (where temperature and salinity effects on buoyancy cancel out). Eddies, cross-shelf exchanges and wind-driven buoyancy loss all relate to this process, but new fine-scale observations are needed to determine their respective contributions, a knowledge gap that Seastar could address. In contrast, the Irminger Sea (Figure 2.5) is now thought to play a central role in Atlantic deep-water formation, but which processes drive the buoyancy losses remains unclear, notably the contribution by eastward high velocity wind jets at the tip of Greenland (Tip Jets).
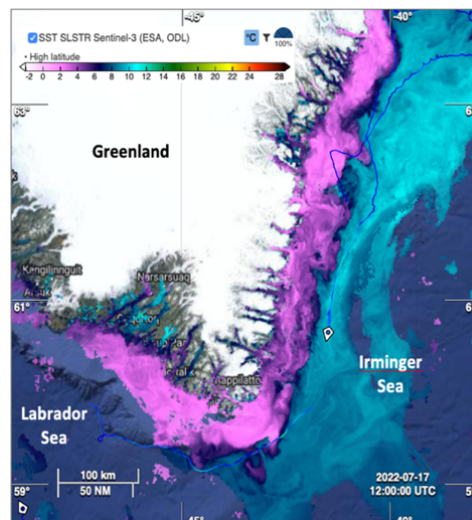
Figure 2.5: Copernicus Sentinel-3 Sea Surface Temperature over Irminger Sea and Labrador Sea with large SST contrasts and fine scale variability at the continental shelf break and the southern tip of Greenland. [Credits: OceanDataLab]

Seastar would provide the first robust characterisation of these fine scale effects, the mission's daily revisit being particularly relevant to their characteristic timescale (Josey *et al.*, 2019). Moreover, Seastar data would enable much-needed evaluation of how these phenomena are represented in new high-resolution atmospheric reanalyses (e.g., Copernicus Arctic Regional Reanalysis Service, 2023).

Surface winds and currents are important for ocean processes across the globe, also in the Southern Ocean, at mid latitudes and in the Tropics. The Mediterranean Sea is one of few regions globally where deep ocean convection occurs and provides a natural laboratory for studying this key ocean process. The NW Mediterranean (Gulf of Lions) is a key deep convection site which appears to be shutting down in response to climate change (Josey & Schroeder, 2023) with potentially far-reaching consequences for Mediterranean climate and marine life. Severe winter winds originating over Europe are key to this process and Seastar would provide the fine-scale resolution needed to observe and understand in greater detail the resulting ocean response; as for Tip Jets in Greenland, Seastar's daily revisits would better capture the rapid evolution of NW Mediterranean severe wind events and their effects on heat loss and convection.

2.3.3. From fjords to the open ocean: a Norwegian case study

The Norwegian Sea is of significant relevance in the global climate system due to its geographic location between the Atlantic and Arctic oceans. Along the coast of Norway, important long-shore transports and cross-shelf exchanges are enabled by the proximity of the fresh Norwegian Coastal Current, warm Norwegian Atlantic Slope Current and an energetic quasi-permanent anticyclonic structure in the deep western part of the Lofoten Basin known as the Lofoten Vortex (Figure 2.6 left). Large density gradients combined with strong westerly winds and waves produce complex meso- and sub-mesoscale circulation patterns that stimulate large primary production which provide rich feeding habitats for higher trophic marine life (e.g., Godø *et al.*, 2012). Synergy between multiple satellite sensors bring to light the fine scale eddies and fronts within the mesoscale field (Figure 2.6 right; Dong *et al.*, 2022).
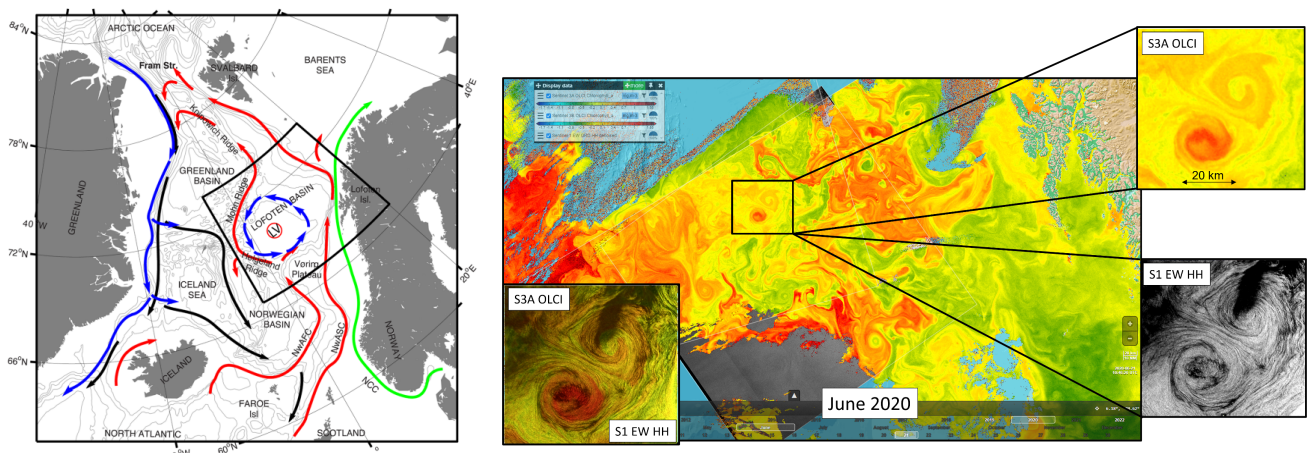
Figure 2.6: (Left) Main ocean circulation pathways in the Nordic Seas showing (red) warm inflowing Atlantic surface waters of the overturning circulation and (blue) cold and dense overflows to the North Atlantic. Green arrows show the fresh Norwegian Coastal Current (NCC) next to the warm Norwegian Atlantic slope current (NwASC). Gray isobaths are drawn every 600 m. The black frame outlines the Lofoten Basin [Credits: Raj *et al.*, 2020]. (Right) Sentinel-3 OLCI Chlorophyll-A in the Lofoten Basin on 21 June 2020 collocated with Sentinel-1 SAR EW HH roughness. The panels and inset show surface expressions of mesoscale mushroom-like pair of anticyclonic/cyclonic eddies with diameters around 20 km in OLCI and ASAR data. [Credits: Nansen Environmental and Remote Sensing Center, A. Bonaduce — OceanDataLab]

Nearest to the coast, the Norwegian Coastal Current (NCC) finds its primary source in the outflow of low salinity waters from Skagerrak (Johannessen *et al.*, 1989) and flows northward, maintained by the prominent freshwater inputs from the complex fjord systems along the coast of Norway. In places, tidal currents in excess of 3 m/s meet strong winds and heavy swells from the west (Halsne *et al.*, 2022), causing strong wave-current interactions and some of the most extraordinary sea states in the world. Water pathways and lateral dispersion of fish larvae, oil and pollution along the coast and across the shelf are strongly impacted by ageostrophic currents caused by winds and waves (van den Bremer & Breivik, 2018; Strand *et al.*, 2021). Inside fjords, water quality depends crucially on the exchange of water masses with the open ocean. With fish farms in almost every fjord in Norway, insufficient oxygenation and dead zones due to stagnant deeper layers in Norwegian fjords are major challenges for aquaculture. The combination of shallow sills near the open ocean and river runoff leads to a shallow, brackish layer near the surface and oxygen-depleted deeper layers, exacerbated by bacterial consumption of fish farm detritus below the euphotic zone. Major reoxygenation events depend on the passage of strong synoptic weather systems and exchanges with the open ocean.

Further offshore, the Lofoten Basin is the most eddy-rich region of the Nordic Seas, characterised by eddies spinning off the slope current that propagate westward, transporting heat and nutrients toward the deepest part of the basin (Rossby *et al.*, 2009). The eddy shedding also enables gradual cooling of the slope current on its way to the Arctic (Isachsen, 2015). Until now, these eddy-mediated exchanges

are estimated primarily from satellite altimeter sea surface height data (e.g., Raj *et al.*, 2020). But altimetry-derived geostrophic currents ignore ageostrophic motions, introducing large uncertainties in the ability to track eddy pathways over their lifetime. In addition, the nadir-pointing altimeters cannot resolve the fine scales of dynamic fields at these high latitudes. The Surface Water and Ocean Topography (SWOT) mission, launched in December 2022, targets this need for fine scale 2D sea surface height data. Already, early data from SWOT's 1-day repeat Cal/Val phase have confirmed the extraordinary day-to-day variability of the ocean at small scales (Figure 2.7). Although SWOT Sea surface height fields still exclude ageostrophic processes, its daily revisit set a new standard for future ocean missions by highlighting a wealth of ocean variability at small spatial and temporal scales.
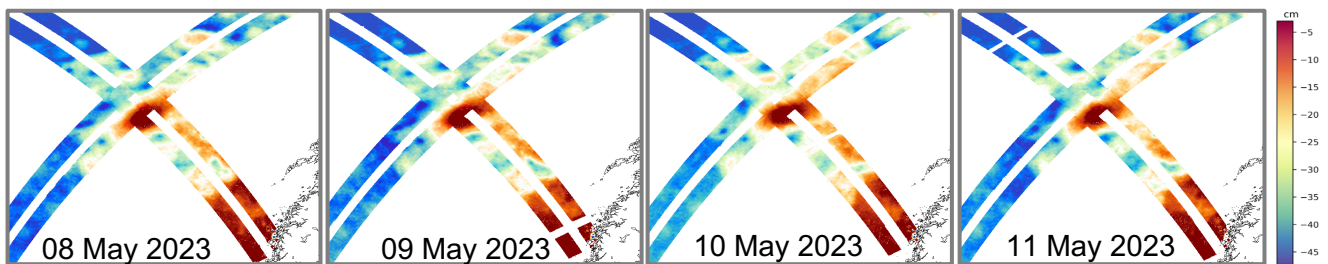
Figure 2.7: SWOT KaRIN Absolute Dynamic Topography (ADT) images for two tracks over the Lofoten Basin and Norwegian Coastal Current on four consecutive days between 08-11 May 2023 during the SWOT 1-day repeat CalVal phase. SWOT data are preliminary Level 2 Low-Resolution products made available to the SWOT Science team before public release. [Credits: Nansen Environmental and Remote Sensing Center, A. Bonaduce]

As well as high temporal and spatial resolution, ocean motion vectors must be precisely resolved to be useful. Numerical models present the ideal tool to evaluate the spatial sampling and accuracy needed to add value. Along the Norwegian west coast, the main tool is the Norkyst-800 model which features 800 m horizontal sampling (Sperrevik *et al.*, 2015). The model produces forecasts for sea surface temperatures and currents that support numerous practical operations including oil spill preparedness, Search-and-Rescue, and dispersion modelling. High-resolution knowledge of Total Surface Current Vectors (TSCV) with appropriate accuracy is critically important here. Figure 2.8 (top) shows the dramatic increase in representation error when resolution exceeds 1 km (Oke & Sakov, 2008). The ratio of the representation error and the current variability indicates how ocean currents in this region cannot be resolved when errors are larger than 0.1 m/s. These important results confirm the necessity of Seastar's demanding requirements for spatial resolution (1 km or finer) and uncertainty (0.1 m/s for total currents), surpassing the capabilities of all other existing and planned missions.

2.3.4. Validating and improving high-resolution coupled prediction systems

Accurate predictions of total ocean surface currents are crucial for users of ocean prediction system output, who depend on reliable information to support naval operations, search and rescue, navigation and shipping, and offshore energy activities. Remarkably, over 80% of search and rescue operations occur within 3 nautical miles of the coast (Futch & Allen, 2019) where data are generally unavailable. Accurate representation of currents is also important for weather predictions as forecasting centres increasingly move toward coupled prediction (Vellinga *et al.*, 2020) and coupled data assimilation systems (Lea *et al.*, 2015). Ocean, waves and atmospheric models have generally developed separately, with little or no crossover. Persistent biases and uncertainties observed in some systems have been traced to missing air-sea interactions (Sandu *et al.*, 2020). Coupled prediction systems allow explicit representation of feedbacks at the air-sea interface and make it possible to evaluate the sensitivity of coupled forecasts to exchanges between different parts of the Earth System (e.g., Belcher *et al.*, 2012; Renault *et al.*, 2019). Coupling has particularly pronounced impacts in sea-ice covered regions where ice pack motion is driven by surface winds, currents, waves and internal ice stresses.

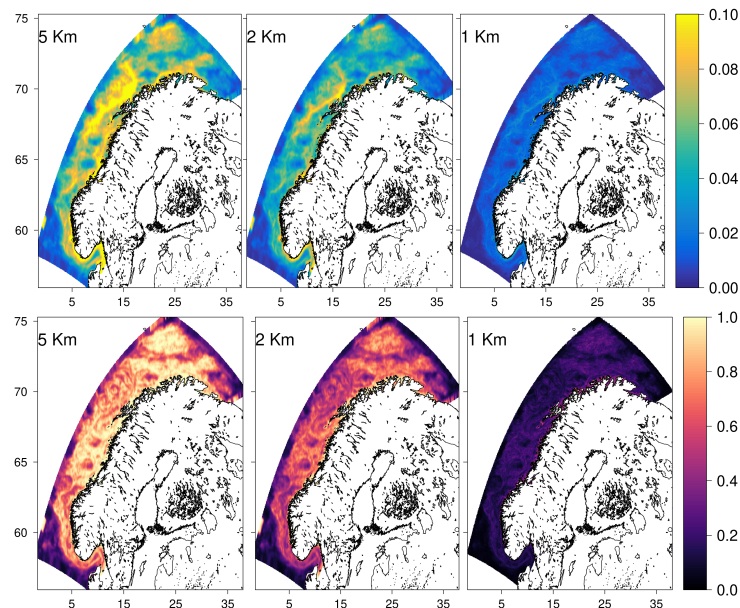Figure 2.8: (Top) Representation error, expressed as the standard deviation of the differences between the signal at a given grid cell and surrounding pixels, for spatial resolutions of (left to right) 5 km, 2 km and 1 km. (Bottom) Ratio of the representation error to the ocean current standard deviation, underlying the need for accuracies 0.1 m/s or better. [Credits: Nansen Environmental and Remote Sensing Center, A. Bonaduce - Norwegian Meteorological Institute, Øyvind Breivik]

Numerical Ocean Prediction (NOP) systems need observations to validate model parameterisations, assess the impact of coupling, improve initial conditions through data assimilation and verify predictions. Verification is essential to understand the quality of predictions and to provide uncertainty estimates for users. Today's operational regional ocean forecasting systems have km-scale horizontal grids and should reach O(100m) in the 2030s (Graham *et al.*, 2018). On the same timeframe, global ocean forecasting systems are likely to migrate towards 'shelf-enabled' configurations, whereby shelf-seas are represented at higher-resolution than the open ocean to better represent dynamic processes and exchanges between shelf-seas and the deep ocean (Holt *et al.*, 2017). Evaluating these predictions systems and the impacts of coupling will require accurate observations of ocean currents, winds and waves at fine horizontal resolution and high frequency across the continental shelves (De Mey-Frémaux *et al.*, 2019), an observational gap that Seastar is ideally placed to fill.

At present, the quality of NOP TSCV products provided to users is not well understood due to the severe lack of data with which to verify predictions. Verifications by operational prediction centres (e.g., in OceanPredict, https://oceanpredict.org) tend to assess forecasts of sea-surface temperature, sub-surface temperature and salinity, and sea level anomaly (Davidson *et al.*, 2019). Verification of TSCV predictions remains uncommon (Poulain *et al.*, 2013; Blockley *et al.*, 2014). While satellite altimetry can constrain geostrophic currents away from the coast, the data do not represent ageostrophic motions. High-frequency radar systems (HF radars) exist along some coastlines and km-scale HF radar data have been used for verification (Tonani *et al.*, 2019) and even assimilation in some regional systems (Yu *et al.*, 2012). But spatial coverage is limited to only a few sites worldwide, mainly in western industrialised countries. Currents from Acoustic Doppler Current Profiler (ADCP) are available from a few moorings, research ships and vessels-of-opportunity, and from surface drifters at the depth of their drogues (Lumpkin *et al.*, 2017). All are used for NOP verification, but the limited and uneven spatial and temporal coverage compared with the scales and variability of currents hampers their use.

It is surprising that coastal and shelf-seas, despite their economic and societal importance, are still poorly observed today. For instance, the North Sea is surrounded by prosperous countries with densely populated coastlines, hosting substantial economic activities across several sectors, including oil and

gas, fishing, and renewable energy. But even the North Sea is not sufficiently well observed (King *et al.*, 2018). Staneva *et al.* (2016) demonstrated how nonlinear feedback between strong tidal currents and wind-waves dominate in a coupled atmosphere-ocean system in the German Bight, but validation relied on a single ADCP at the FINO-1 research platform. The provision by Seastar of ocean current data in all coastal and shelf-seas across the globe would transform our ability to verify predictions and evaluate models in an unprecedented range of dynamical regimes, globally, and particularly in regions of the world which have seldom or never been observed or modelled so far.

Seastar's observations are especially relevant to the evaluation of coupling strategies in different environments. Today's systems use either uncoupled or weakly-coupled data assimilation schemes. By the 2030s, strongly coupled assimilation may be the norm, whereby observations within the ocean can directly affect the atmosphere analysis and vice versa (Storto *et al.*, 2018; de Rosnay *et al.*, 2022). Seastar's global coverage of coastal and shelf seas and concurrent observations of currents, winds and waves with daily and even sub-daily sampling at some latitudes, will be a rich resource to explore day-to-day variability in cross-fluid error covariances to inform strongly coupled data assimilation.

Seastar's sampling capabilities would also bring about a step change in our ability to observe, verify and predict fast-evolving small-scale dynamics and feedbacks in coastal and shelf seas. Nowadays, prediction systems used for seasonal, decadal and longer forecasts share the same fundamental framework as NOP systems, whose seamless integration across time present opportunities to improve both weather and climate forecasts using data. Improved representations of coupling and fast-evolving small-scale processes will transfer from NOP to models that inform our understanding of climate change. Altogether, Seastar data would bring new understanding to improve ocean and weather forecasting (and the associated safeguarding of life at sea and prevention of hazards) and reduce uncertainties about the dynamics and evolution of the fully coupled climate system.

2.4. Small-scale processes in Marginal Ice Zones

2.4.1. Atmosphere-wave-ice-ocean interactions at the sea ice edge

The high latitude ocean plays a critical role in the Earth system, both for deep-water formation that drives the global overturning circulation, and intense air-sea fluxes and atmospheric carbon drawdown through the ocean carbon pump. The Southern Ocean is thought to represent about 40% of the global oceanic CO_2 sink (Mayot *et al.*, 2023). Here, lateral and vertical mixing is organised by mesoscale eddies (Horvat *et al.*, 2016) with scales defined by the Rossby radius of deformation, typically smaller than 10 km in deep water (Chelton *et al.*, 1998), less on continental shelves. Evidence also points to the role of small scales of 1 km or less (Carmack *et al.*, 2015; Manucharyan & Thompson, 2017). In the Arctic Eurasian sector, eddies are typically smaller than 5 km (Nurser & Bacon, 2014). As a result, most eddies are undetected by satellite altimetry. A recent survey of eddy signatures in SAR and optical surface roughness and sea ice images by Kozlov *et al.* (2019) confirmed that most eddies detected with their method have diameters below 10 km. However, such analyses cannot provide the quantitative estimates of surface current and eddy kinetic energy needed to estimate vertical mixing and transports (Armitage *et al.*, 2020). Seastar would bring new insight about these processes and their influence on heat fluxes, the meridional overturning circulation and the biological and physical ocean carbon pump.

Air-sea exchanges and vertical processes at the sea ice edge generate eddies and jets (Bulczak *et al.*, 2015; Rynders, 2017) which interact with surface waves and affect mixing, heat balance and air-ice-sea momentum transfer (Giles *et al.*, 2012). The Marginal Ice Zones (MIZ), defined as the transition region between the ice-free ocean and the pack ice (Johannessen & Andersen, 2017), is a dynamic boundary that can shift by tens of kilometres in a day in response to winds, waves and currents. In the Arctic, the MIZ covers a growing portion of the total sea ice and may dominate the dynamics of sea ice

growth and decay, as it already does in the Southern Ocean. With less or no ice in future Arctic summers, navigating near and across the MIZ will require better data and deeper understanding (Stephenson *et al.*, 2011; Aksenov *et al.*, 2017).

Strong unstable current jets can form at the ice edge with velocities often exceeding 0.2 m/s (Manucharyan & Thompson, 2017). Strong currents can also flow along the ice edge, as in the southward East Greenland current that brings Arctic waters to the Atlantic along the shelf break (Figure 2.9). The proximity of ice means these important currents are hard to observe in situ and poorly resolved by satellite altimetry (Richter *et al.*, 2018). Ice drift can be estimated by cross-correlating ice features in consecutive SAR images (Howell *et al.*, 2013) but the method generally fails in the MIZ due to the rapid deformation of ice features, particularly in summer (Ricker *et al.*, 2018). The method also implies temporal and spatial averaging that makes it unable to detect rapid changes in ice motion within complex regions. Together with currents, winds and waves, Seastar's instantaneous sea ice velocity data will resolve small-scale rapid ice motions including ice convergence and divergence to bring deeper understanding of sea ice dynamics and sea ice interactions with the atmosphere and the ocean.
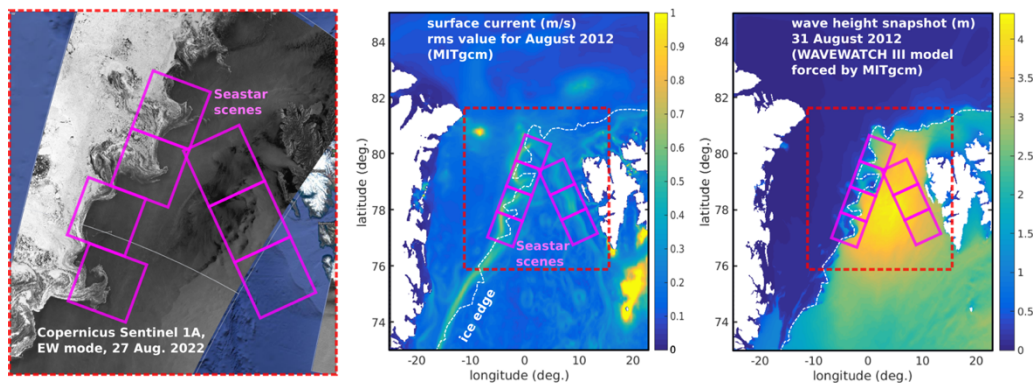
Figure 2.9: [Left] Sentinel-1A EW image over Fram Strait between Greenland and Svalbard showing a typical complex sea ice edge. Pink boxes outline the minimum size of Seastar images (100 km x 100 km) placed over the sea ice edge, East Greenland current, shelf break and the West Svalbard current. [Middle] Surface current variability from MITgcm model. [Right] Typical Significant Wave Height conditions at the sea ice edge from the WAVEWATCH III model [Credits: Ifremer, F. Ardhuin]

Sea ice also strongly attenuates waves and is a barrier to air-sea fluxes (e.g., heat). Within a few kilometres from the ice edge, ocean waves are strongly attenuated, giving up their momentum to the ice and producing localised patterns of ice drift, compaction and break-up. This process is highly heterogeneous however and thought to depend on ice type, floe size, thickness and horizontal compaction (e.g., Ardhuin *et al.*, 2020). Currents near the ice edge may also influence the wave field and thus ice edge properties (Dai *et al.*, 2019). Knowledge of these processes is very limited due to the lack of data. Field experiments rely on remote sensing to provide complementary data and spatial coverage. Waves are in practice easier to measure with SAR within sea ice than in the open ocean, due to the lack of azimuth cut-off (Ardhuin *et al.*, 2017). However, Sentinel-1 EW images in the Arctic are generally too coarse to allow wave detection, and analyses of wave transformation across the ice edge depend on rare Sentinel-1 IW or Wave Mode data near the ice edge, but none that can provide continuous tracking of wave fields over distances larger than 20 km (Stopa *et al.*, 2018). Seastar's multi-azimuth SAR imaging of the sea ice edge would bring new light on these processes.

2.4.2. Small-scale processes in Southern Ocean ice margins

Lastly, Seastar would provide unique and much needed data in the Southern Ocean, specifically around the Antarctic marginal ice zones, where extreme sea ice conditions signal that major changes are afoot (Siegert *et al.*, 2023; Figure 2.10). These transitional regions are where warm waters from the deep

ocean can bring heat towards the Antarctic ice sheets and shelves to melt the ice (Garabato *et al.*, 2017); where the pycnocline (rapid change in density with depth) of all Southern Hemisphere oceans is formed (Klocker *et al.*, 2023); and where coastal polynyas (semipermanent areas of open water in sea ice) produce dense Antarctic Bottom Water, the densest ocean water mass which fills most of the global abyssal ocean, and provide nutrients to the abundant marine life around Antarctica (Labrousse *et al.*, 2018). However, the small scales and rapid evolution of some processes, and the remoteness, inaccessibility and harsh conditions in these regions have resulted in limited *in situ* observations. Relying on *in situ* data almost invariably means measurements made in the austral summer, and the challenge of stitching together data from expeditions in different years. Numerical simulations are thus key to understanding the processes and changes in these regions (Dawson et al. 2023). Seastar's all-seasons wind, current and wave data over all Antarctic sea ice margins would bring valuable new information that complement in situ and model data to address many open questions.

Figure 2.10: Antarctic monthly mean sea ice concentration in February 2023 shown against the (red line) 1981–2010 median [Credits: ESA, 2023; Siegert *et al.*, 2023]

Like in the North Hemisphere, Seastar is relevant to air-ice-sea coupling in the Antarctic MIZ, where small scales impact the strength of air-sea fluxes and submesoscales may be responsible for equivalent heat fluxes of 240 W/m^2, large values that seem to be strongest in winter (Biddle & Swart, 2020). Within coastal polynyas, brine rejection from rapid sea-ice formation by katabatic winds (cold, dry air rushing off the continent) increases salinity and the density of shelf waters, which subsequently spill off the shelf to fill the abyssal ocean (forming the northward limb of the lower overturning circulation; Jacobs, 2004). Recent high-resolution modelling suggests that small-scale processes at ~20 km and daily/sub-daily scales may be coupling this dense water formation with on-shelf transport of warm waters (Morrison *et al.*, 2020), exchanges that Seastar may be able to observe and quantify.

Changes in Antarctic ice shelves suggest they are less stable than thought, and their collapse would release large quantities of freshwater from the Antarctic ice sheet that would accelerate sea level rise globally beyond the projections of current climate models (IPCC AR6, 2021). Since small-scale processes appear to govern the delivery of heat to Antarctic ice shelves (Naveira Garabato et al. 2017, Morrison et al. 2020), there is an urgent need to observe the strength and variability of ocean currents in these remote and challenging regions to set a baseline understanding of how the ocean contributes to Antarctic ice melt. Today's understanding is based on sparse in situ measurements, irregular sampling by tagged marine mammals, and high-resolution numerical simulations. Fast repeat, high resolution measurements of ocean surface currents, winds and waves would provide a new baseline from which to generate understanding about the role of these small-scale processes in modulating large-scale climate.

3. MISSION OBJECTIVES

This section presents the Science Goals (SG) and Mission Objectives (OBJ) of the Seastar mission derived from the scientific arguments presented in Chapter 2. The Science Goals (Section 3.1) are key strategic scientific issues addressed by the mission that relate to priorities identified in the ESA Earth Observation Science Strategy (ESA, 2015c, 2015b). The Seastar Mission Objectives (Section 3.2) relate to the mission itself and how its data will support the Science Goals outlined in Section 3.1.

3.1. Science Goals

The global ocean forms a central part of the climate system and communicates with other components of the climate system through exchanges at its interfaces in the coastal and shelf seas (with land), marginal ice zones (with the cryosphere) and the ocean surface (with the atmosphere). These interfaces are characterised by fast-evolving dynamic processes on multiple spatial scales that are predicted by state-of-the-art numerical models but are poorly constrained by observations. The observational challenges of measuring fast-evolving small-scale dynamics at the boundaries of the global ocean means our knowledge of how the ocean interacts with other parts of the climate system is incomplete. Seastar would provide new observations to quantify and reduce uncertainties about the representation in models and forecasts of fast-evolving surface processes, and about the contributions in the Earth system of coastal, shelf and marginal ice zones.

Together with these scientific ambitions, improved knowledge of surface dynamics in coastal, shelf and sea ice regions would benefit applied research and many applications of direct value to society. Seastar' unprecedented high-resolution high-accuracy description of current, wind and wave fields in these environmentally and economically strategic areas would result in the first comprehensive assessment from space of marine energy hotspots, marine hazards and dangerous seas. This new knowledge would serve to highlight opportunities, vulnerabilities and the impacts of human intervention on the natural environment, to promote the development and implementation of appropriate adaptation and mitigation strategies, build climate resilience and support the ambitions of the UN Ocean Decade and Sustainable Development Goals (oceandecade.org).

In light of this, the science goals identified by Seastar are to:

SG-1 Understand the role of fast-evolving small-scale ocean dynamics in mediating exchanges between land, the cryosphere, the atmosphere, the marine biosphere and the deep ocean. *This science goal contributes to the ESA Living Planet Ocean Challenge O2, Ocean Challenge O4, Land Surface Challenge L2 and Cryosphere Challenge C1.*

SG-2 Determine the ocean circulation and dominant transport pathways in the global coastal, shelf and marginal ice zones. *This science goal contributes to the ESA Living Planet Ocean Challenge O1 and Ocean Challenge O3.*

SG-3 Reduce uncertainties on the estimated contributions by coastal, shelf and marginal ice zones in the global climate system. *This science goal contributes to the ESA Living Planet Ocean Challenge O4 and Land Surface Challenge L2.*

3.2. Mission Objectives

Objectives	ID/Priority
SG-1 Understand the role of fast-evolving small-scale ocean dynamics in mediating exchanges between land, the cryosphere, the atmosphere, the marine biosphere and the deep ocean.	
Quantify the short-term temporal variability of ocean surface dynamics on all scales relevant to ocean energy cascades from 100km to 1 km and finer, to improve estimates of air-sea fluxes in open waters and in the vicinity of land and sea ice.	PRI-OBJ-1
Investigate the relations between fast-evolving small-scale ocean surface dynamics, air-sea interactions, lateral transport, vertical processes and marine productivity using synergy with high-resolution satellite data from optical, thermal and microwave sensors.	PRI-OBJ-2
Observe the instantaneous dynamic response of sea ice and ice floes to short-term small-scale forcing by currents, winds and waves, and its relationship with sea ice properties.	SEC-OBJ-1
SG-2 Determine the ocean circulation and dominant transport pathways in the global coastal, shelf and marginal ice zones.	
Deliver the first comprehensive high-resolution description of ocean surface currents, winds and directional waves in the global coastal ocean, shelf seas and marginal ice zones, quantifying the magnitude, variability and dominant ocean transport pathways across seasons and multiple years.	PRI-OBJ-3
Identify energy hotspots and interactions contributing to marine hazards and dangerous seas in the global coastal ocean, shelf seas and marginal ice zones, including impacts of human interventions on the natural environment.	PRI-OBJ-4
Examine ocean surface current and wind vector fields close to major estuaries to investigate the dispersion pathways of major river plumes in coastal zones, and the fate of terrestrial input to the ocean including nutrients and pollutants like marine plastic.	SEC-OBJ-2
Investigate Seastar's very-high resolution Single-Look Complex images in three azimuth directions to develop new experimental products for directional ocean wave spectra and localised surface phenomena, including fronts, wave breaking and Langmuir circulation.	SEC-OBJ-3
SG-3 Improve understanding of coastal, shelf and marginal ice zones contributions to the global climate system.	
Evaluate the representation of fast-varying small-scale processes in models, forecasts, reanalyses, Earth System Models and climate models, and support the development of new parameterisations to reduce uncertainties in estimated fluxes and transports.	PRI-OBJ-5
Assess the contributions of coastal, shelf seas and marginal ice zones in Earth System and climate models and how to improve their representation in forecasts and projections	PRI-OBJ-6

4. MISSION REQUIREMENTS

This section presents the mission requirements through a quantitative description and justification of the geophysical and observation requirements that would allow to fulfil the mission objectives. Measurement requirements are elaborated, including the level of priority.

4.1. Science and Geophysical Needs

Seastar is dedicated to observing fast-evolving small-scale ocean surface dynamics and to describe the ocean circulation in ocean boundaries in order to answer questions about exchanges of carbon, water, energy, gases and nutrients between land, the cryosphere, the atmosphere, the marine biosphere and the deep ocean.

Spatial Coverage –The objective to better understand how the ocean communicates with land and the cryosphere brings a natural focus to observing the ocean circulation at key interfaces of the Earth System in coastal seas, shelf seas and marginal ice zones. The ambition to deliver the first complete high-resolution description of the ocean circulation at these interfaces implies systematic and repeated observations of these regions. Spatial coverage should be sufficient to sample all transitions from the coast or ice edge to the open ocean, including the critically important continental shelf break regions.

Interactions and exchanges between the ocean and the atmosphere are relevant throughout these regions. It is a key objective of Seastar to evaluate how fast-evolving small-scale ocean surface processes affect air-sea fluxes close to land and ice as well as open waters. The latter can be achieved by considering air-sea exchanges in shelf seas but the mission should retain the flexibility to acquire data also over selected open ocean sites, for example to observe specific environmental phenomena, or to collocate with in situ monitoring infrastructure or validation campaigns.

Geophysical parameters – The geophysical parameters associated with fast-evolving small-scale ocean surface dynamics are the Total Surface Current Vector (TSCV), the Ocean Surface Vector Wind (OSVW) and the Directional Ocean Wave Spectrum (DOWS).

The Total Surface Current Vector (TSCV) is a vectorial quantity that represents the horizontal displacement of water at the ocean surface. Total Surface Current Vectors (TSCVs) comprise both geostrophic currents (classically derived from satellite altimeter sea surface height gradients) and ageostrophic currents (that arise from tides, wind-induced Ekman currents, wave-induced Stokes drift, inertial oscillations, internal waves, etc…). The science case in Chapter 2 clearly articulates the need to observe ageostrophic currents which play important roles in ocean surface dynamics e.g., in coastal regions or sub-mesoscale processes (e.g., Section 2.2.1, Section 2.3.1).

The Ocean Surface Vector Wind (OSVW) is a vectorial quantity that represents the motion of the atmosphere relative to the ocean surface. OSVWs are commonly expressed as 10-m height stress-equivalent winds, a metric developed and used by the satellite wind scatterometer community (Section 2.2.2). Scatterometers derive OSVW from microwave radar backscatter from the ocean surface, which is depends on ocean surface roughness, which in turn relates to surface wind stress. As demonstrated in Chapter 2, OSVWs are a key determinant of air-sea interactions and fluxes, with major effects on climate by mediating transfers of heat, moisture and radiatively-active gases (Section 2.2.2, Section 0). Observing OSVWs forms a central part of Seastar's objective of evaluating how fast-evolving small-scale ocean surface processes affect air-sea fluxes in open waters and close to land and ice.

The Directional Ocean Wave Spectrum (DOWS) represents the spectral density of ocean surface wave energy in wave number (or frequency) and direction. DOWS summarise the different contributions to

local wave energy made by swell from distant storms and by locally wind-generated waves. Integral wave properties like Significant Wave Height (SWH), Zero-crossing Period (T0) or Dominant Wave Direction (DWD) serve to summarise wave conditions and are traditionally derived from DOWS spectral moments (Tucker & Pitt, 2001) or directly from SAR images using Machine Learning (Quach et al., 2020; Pleskachevsky et al., 2022). The position of ocean surface waves at the air-sea interface gives them a central role to play in atmosphere-ocean interactions, but they make strong contributions also to ageostrophic transport (Stokes drift; Section 2.3.3) and sub-mesoscale processes (Section 2.3.1).

The importance of current-wind-wave interactions in coastal waters (Section 2.2.3) and sea ice margins (Section 2.4.1) adds to the rapid development of high-resolution coupled forecasting (Section 2.3.4) and point to the need for DOWS data that coincide with TSCV and OSVW in both time and space.

Spatial resolution and extent – A fine km-scale spatial resolution for TSCV and OSVW is mandated by the critical length scales of submesoscales and processes in coastal, shelf and marginal ice zones. For submesoscales, numerical models highlight a clear dynamical transition as ocean model resolution reaches 1 km or less (Section 2.3.1). In coastal, shelf and marginal ice zones, the grid spacing of forecasting models is typically of the order of 800 metres to 1.5 km (Section 2.3.3, Section 2.3.4). Likewise, many satellite products are provided routinely at 1 km resolution. These indicate a strict requirement for a spatial resolution of 1 km or finer for Seastar.

Theory and models hypothesise complex direct and inverse energy cascades at scales between 1 and 100 km (Section 2.3.1) that are yet to be confirmed with observations. High-resolution satellite images confirm the presence of intricate ocean structures at multiple scales (e.g., Figure 2.1, Figure 2.5, Figure 2.6) and draw attention to the need to observe the two-dimensional mesoscale context in order to interpret small scale features at 1 km and below. This imposes a requirement for Seastar to measure all spatial scales relevant to ocean energy cascades between mesoscale and submesoscale, implying 2D imaging at 1 km resolution (or finer) over one continuous 100 km swath (or wider).

Measurement uncertainty – Scientific arguments in Chapter 2 highlight the need for Seastar to achieve TSCV levels of uncertainty of 0.1 m/s or less at 1 km resolution to support coastal applications (Section 2.2.4), regional models and coupled forecasting systems (Section 2.3.3, Section 2.3.4) amongst others. Results in Figure 2.8 are a compelling demonstration of the large representation errors committed when TSCV uncertainty is worse than 0.1 m/s at 1 km resolution. The requirements for Seastar to deliver TSCV at 1 km resolution with errors at or below 0.1 m/s are fully aligned with the WMO requirements for ocean surface currents (WMO, 2018).

OSVW uncertainty levels are less rigidly prescribed, partly due to the lack of knowledge about wind variability at small scales. For Seastar, OSVW should achieve similar or better levels of uncertainty as is currently possible with scatterometers.

Gradients, Divergence, Vorticity – Properties like gradients, divergence and vorticity (i.e., the curl of the velocity field) are derivative measurements of vector fields that are used extensively by sea-going oceanographers and modellers to explore the relations between ocean sub-mesoscale/mesoscale circulation, air-sea fluxes and vertical exchanges (Section 2.3.1). Accordingly, Seastar is required to produce two-dimensional maps of gradient, vorticity and divergence for TSCV and OSVW to allow direct comparison with diagnostic tools used by the community. These first- and second-order derivatives are highly sensitive to the spatial resolution and errors of TSCV and OSVW fields. We show in Chapter 7 that the spatial resolution and uncertainty requirements for Seastar (above) will deliver information about these ocean dynamic properties with much greater accuracy and detail than any existing or planned mission.

Temporal Sampling and Orbit choice – Sequences of high-resolution satellite images and theoretical understanding indicate that small-scale ocean dynamics evolve rapidly, over hours to a few days. Inspired by SWOT's 1-day exact repeat in its first 90 days in orbit, Seastar targets 1-day revisit time to observe the evolution of fast-evolving small-scale processes with a temporal frequency not achievable by other missions, which would also have the added benefit of creating greater opportunities for synergy with daily products from optical and thermal sensors.

The requirement to observe fast-evolving small-scale processes needs to be balanced with the need to deliver the first complete description of the ocean circulation in global coastal, shelf and sea ice margins. Seastar should aim to observe those regions sufficiently often to resolve seasonal and inter-annual variability. Seastar should have the ability to shift between exact-repeat and slow-drifting orbits to achieve flexible temporal sampling and deliver maximum scientific benefit over the mission lifetime.

With interest growing in understanding sub-daily variability in ocean surface dynamics and marine ecosystems, for example in response to diurnal warming or sea breezes, Seastar should take advantage of opportunities to sample ocean surface dynamics at temporal scales shorter than 24 hours (e.g., at crossovers), but without making it a mission driver.

4.2. Observation requirements and traceability

The observation requirements for the Seastar mission are succinctly gathered in the table hereafter, specifying the needed geophysical parameters, resolution and uncertainty, coverage and temporal sampling and mission lifetime to meet the mission objectives described in Chapter 3.

Observation Requirement	ID
Geophysical Parameters Key Observational Requirements	
Seastar shall provide collocated two-dimensional (2D) images of TSCV and OSVW over one continuous swath. *Note 1: The 2D images of TSCV and OSVW are obtained from acquisitions taken over the same time period and the same spatial domain.* *Note 2: The dimension of the 2D images in range correspond to the swath width of the instrument.*	MR-OBS-01
Level 2 TSCV and OSVW images shall be provided at a resolution and posting rate ≤1 km. *Note 1: The 1 km posting rate is the spatial resolution of the L2 TSCV and OSVW images.* *Note 2: The spatial resolution of L1B images (backscatter, coherence, radial velocities) is much finer than 1 km to enable multi-looking and incoherent averaging and satisfy the Level 2 TSCV uncertainty requirement at 1 km.* *Note 3: This is a key requirement of the mission.*	MR-OBS-02
Seastar shall provide 2D images of high-order derivative products, including vorticity, strain and divergence. *Note 1: The high-order derivative products derive from the 1 km resolution products available at Level 2.*	MR-OBS-03
Seastar shall provide directional wave spectra for wavelengths above 50 metres, with a goal of 40 metres.	MR-OBS-04

Total Surface Current Vectors	
The magnitude of the vectorial uncertainty on Level 2 TSCV shall be ≤ 0.1 m/s or 10%, whichever is greater, at 1 km resolution. *Note 1: Vectorial uncertainty includes the uncertainty in the two cartesian components.* *Note 2: The Level 2 TSCV uncertainty requirement at 1 km implies stricter requirements at L1B on radial velocity measurements.* *Note 3: It is assumed that this requirement will be achieved after data driven calibration with static on-ground targets to account for residual systematic errors in the surface radial velocities.*	MR-OBS-05
Ocean Surface Vector Winds	
The magnitude of the vectorial uncertainty on Level 2 OSVW shall be ≤ 1 m/s or 10%, whichever is greater, at 5 km resolution. *Note 1: Vectorial uncertainty includes the uncertainty in the two cartesian components.* *Note 2: The coarser resolution of the Level 2 OSVW uncertainty requirement relates to the technical challenge of validating OSVW against other independent observations given the large space-time variability of coastal surface winds at small scales.* *Note 3: TSCV and OSVW are retrieved in a collocated manner by inversion of the same L1B data.* *Note 4: It is assumed that this requirement will be achieved after data driven calibration with static on-ground targets to account for residual systematic errors in the surface radial velocities.*	MR-OBS-06
Coverage and Revisit Requirements	
Seastar shall provide measurements over Coastal seas, Shelf seas and Marginal Ice Zones (CoSMIZ) and selected Ocean Regions of Special Scientific Interest (ORSSI). *Note 1: The CoSMIZ is defined by the Seastar mask provided as an input to the Phase 0 Industry study at KO. The CoSMIZ covers all ocean areas within 80km of the Coastline Boundary (CB), within 80km of the Sea Ice Boundary on the ocean side and over Shelf Seas (corresponding to areas where bathymetric depth ≤ 1000 metres). The resulting mask can be seen below in Figure 4.1.* *Note 2: The Coastline Boundary (CB) and the Sea Ice Boundary (SIB) are defined in SeaSTAR MATER (2023). The sea ice edge is defined as 5% sea ice concentration in the SIB. The SIB will be updated fortnightly (every 2 weeks) in line with best practice from other missions (e.g., CRISTAL).* *Note 3: The ORSSI are located in the open ocean and correspond to long-term monitoring stations or scientific campaigns. The number of ORSSI will not exceed 20 sites (TBC) that correspond to 20 (TBC) full swath scenes. Seastar system shall be able to update the ORSSI scenes location on the fortnightly basis. An indicative list of ORSSI locations will be provided as input to the Phase 0 Industry study at MTR.* *Note 4: Flexible and re-programmable data acquisitions is essential.*	MR-OBS-07
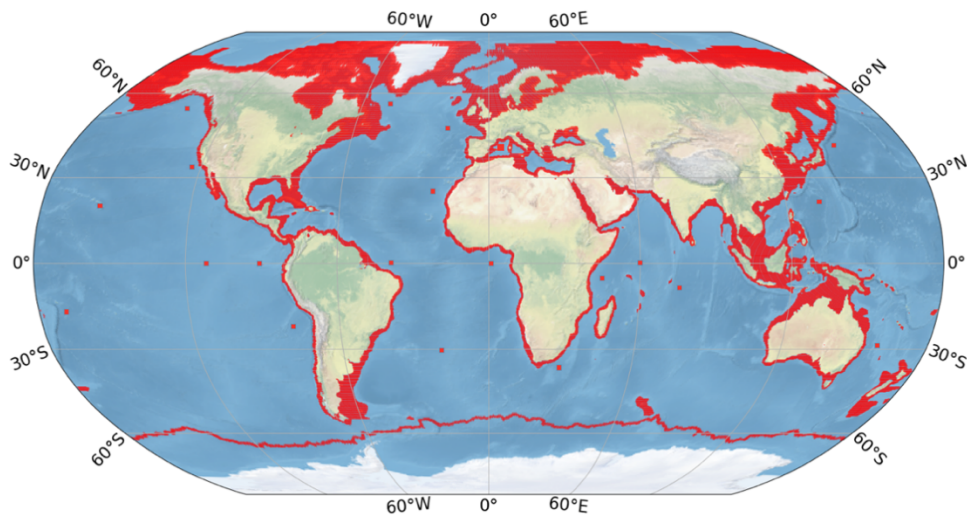
Figure 4.1: Seastar CoSMIZ acquisition mask during Phase 0

The L2 TSCV and OSVW images shall be obtained for a swath ≥ 100 km (Goal for swath: ≥150 km) over which uncertainty requirements for TSCV and OSVW are satisfied. *Note 1: This minimum swath width is needed to observe the wider mesoscale, coastal or MIZ context to support the interpretation of the high-resolution observations.* *Note 2: The instrument has to satisfy L1B uncertainty requirements on radial velocity and backscatter at VV polarisation over the full range of the swath.* *Note 3: The width of the swath over which the uncertainty requirement can be satisfied should be maximised and will be used as a key performance indicator to differentiate different concepts.*	MR-OBS-08
Seastar shall have a nominal operational lifetime of 5 years (Threshold of 3 years and with a goal of 7 years).	MR-OBS-09
The Seastar mission shall have a drifting orbit phase to achieve a seasonal repeat cycle (at least once over the lifetime) over all CoSMIZ and selected ORSSI for, at least, 3 years. *Note 1: A 91±5 or 271±5 days repeat cycle may be considered during the mission. Worst case between 91±5 and 271±5 days shall be considered for the mission performance analysis.*	MR-OBS-10
During the drifting phase, Seastar shall revisit all locations in the CoSMIZ during at least 3 days (threshold) to 5 days (goal) consecutive (goal) or alternate (threshold) days. In the same way, Seastar shall provide sub-daily observations of certain areas of interest. *Note 1: This requirement is essential to observe the temporal evolution of small ocean features. The sub-daily observations may be achieved over orbit crossovers, the location of which are determined by the orbit selection but could be tuned with the appropriate selection of specific orbit and instrument parameters.* *Note 2: "Consecutive" refers to a revisit time of 1 day; "alternate" refers to a revisit time of 2 days.*	MR-OBS-11

4.2.1. Traceability to Mission Objectives and EE11 Proposal

The traceability from the Science Goals and Mission Objectives to the observational requirements at Level-2 is illustrated in the diagram in Figure 4.2. It is worth noting here that the Seastar observational requirements from the original EE11 proposal have been fully maintained at the end of Phase-0.
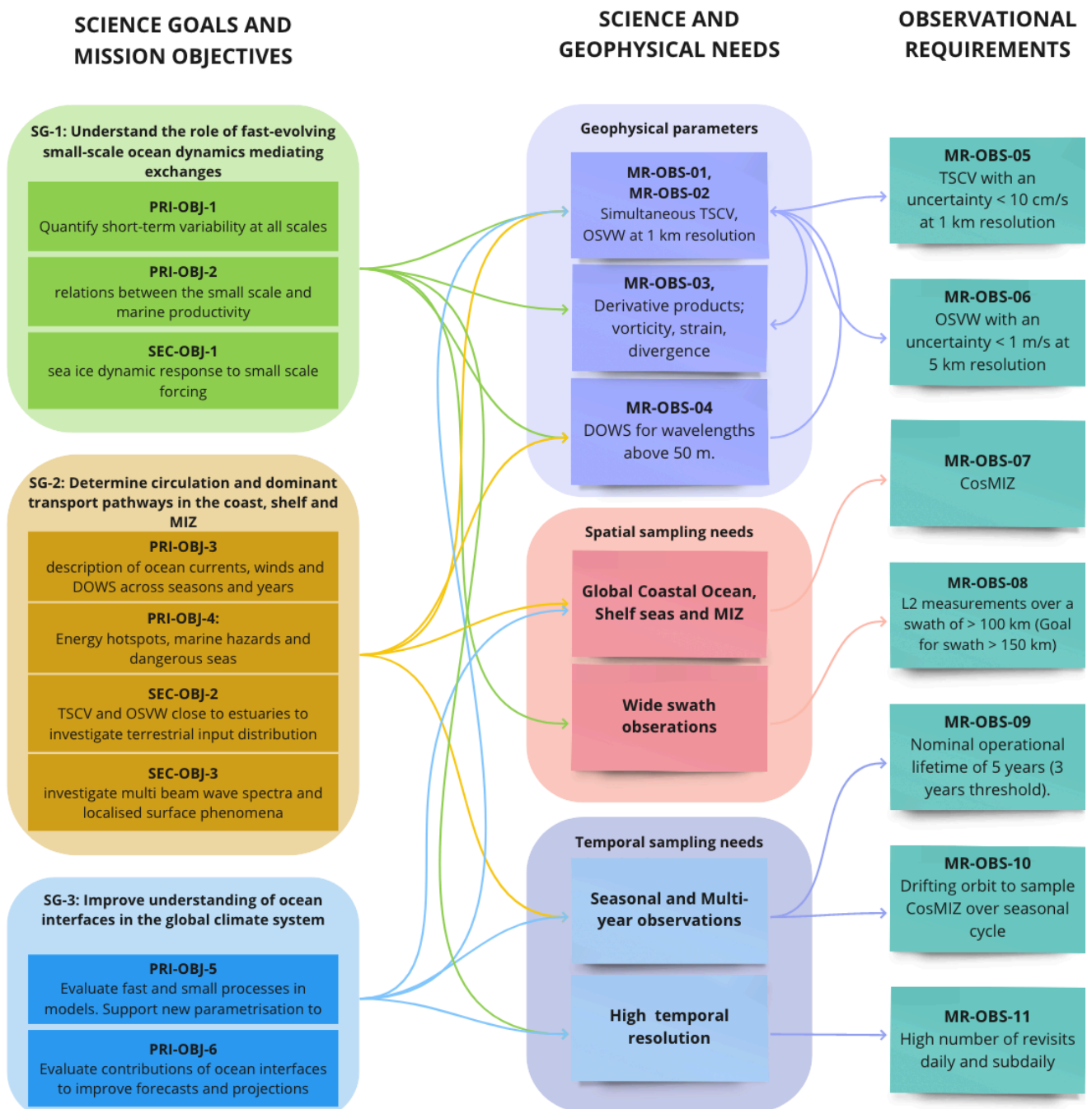

Figure 4.2: Seastar requirements traceability diagram showing full traceability between the observational level-2 requirements and the overarching science goals and mission objectives.

4.2.2. Comparison of Seastar with EE10 Harmony mission objectives

Despite some apparent similarities between Seastar and Harmony, it is important to note that the Science Goals and Mission Objectives of the two missions are distinctively different and complementary. Key differences are outlined here and further elaborated in Section 8.1.5:

- Seastar sets out to observe the temporal evolution of fast-evolving small-scale processes, calling for systematic sampling of the same area for extended periods with daily to sub-daily revisit times. In contrast, the space-time sampling of Harmony is tied to the Sentinel-1 orbit and its data acquisition plan (e.g., Sentinel-1 SAR operation modes), resulting in a revisit of multiple days at the equator. It follows that Harmony cannot satisfy the Seastar Mission Objectives identified under SG1 (Understand the role of fast-evolving small-scale ocean dynamics in mediating exchanges between land, the cryosphere, the atmosphere, the marine biosphere and the deep ocean; Section 3.2).

- Seastar seeks to observe the global ocean margins defined as the global coastal, shelf and marginal ice zones. The requirement stems from Seastar's Mission Objectives under SG-2 (Determine the ocean circulation and dominant transport pathways in the global coastal, shelf and marginal ice zones) and SG3 (Improve understanding of coastal, shelf and marginal ice zones contributions to the global climate system). Harmony's data acquisition strategy for Ocean and Air-Sea Interactions focuses mainly on global sampling of fine scale features using Sentinel-1 Wave Mode and in defined regions of interest (RoI) in Imaging Mode. Since these RoI do not correspond with Seastar's requirements, Harmony cannot achieve the Seastar's mission objectives under SG2 and SG3.

- Seastar imposes strict requirements for the spatial resolution (1 km or finer) and uncertainty (0.1 m/s or better) for Level 2 Total Surface Current Vectors. As shown in Section 2.3.3 (and also Section 7.2.1.2 and 7.2.1.3), observing Total Surface Current Vectors with coarser resolution and/or higher uncertainty will conceal critical information about small-scale ocean dynamics that underpins all of Seastar's mission objectives.

4.3. Observing principle and measurement technique requirements

Seastar's stringent requirements for fine resolution and high accuracy call for the use of single-pass squinted Along-Track Interferometry (ATI) Synthetic Aperture Radar (SAR) instrument. Seastar would embark the first multi-beam high-squint along-track interferometer SAR instrument in space, the first instrument and mission of its kind.

Standard ATI systems measure the ocean surface motion in the broadside line-of-sight (across-track) from which currents in the satellite across-track direction can be estimated. The Doppler shifts that allow to measure surface motion are computed between two SAR images of the same scene, acquired by two separate antenna apertures within a short time lapse (a few milliseconds depending on radar frequency, coherence and sea state). Alongside numerous airborne demonstrations (Goldstein & Zebker, 1987; Goldstein *et al.*, 1989; Romeiser, 2005), ATI showed promising results also from space, for example onboard the space shuttle, TerraSAR-X (divided-antenna) and TanDEM-X (Romeiser *et al.*, 2010; López-Dekker *et al.*, 2011; Romeiser *et al.*, 2014; Elyouncha *et al.*, 2019).

Squinted ATI is an extension of the well-established SAR ATI method, in which the beams are directed in the fore- and aft- flying direction, from which the radial component of the surface motion direction can

be retrieved. With a high enough angular diversity in the squint angle, it is possible to combine both fore- and aft- observations to recover both vectorial components of the surface velocity.

Up until now, extensions of ATI to measure two vectorial components of surface currents have been limited to airborne systems (Lyzenga *et al.*, 1982; Shemer *et al.*, 1993; Graber *et al.*, 1996), including the Dual Beam along-track Interferometer (DBI) proposed by Frasier & Camps (2001), which uses two pairs of antennas squinting respectively forward and backward with respect to broadside (Farquharson *et al.*, 2004; Toporkov *et al.*, 2005). The DBI concepts use very high incidence angles (>60-70◦) that give very good sensitivity to currents. Unfortunately, high incidence angles make it incompatible with spaceborne implementation due to power considerations.

Seastar is an evolution of the DBI (Frasier & Camps, 2001; Farquharson *et al.*, 2004; Toporkov *et al.*, 2005) building also on past ESA and UK-funded studies of the Wavemill (Buck, 2005) and the Ocean Surface Current Mission (OSCM) concepts (Donlon, 2013). Seastar's key innovations are:

1. an adjustment from DBI towards lower incidence angles to make it amenable to implementation in space whilst retaining high sensitivity to ocean currents.

2. large angular separation between fore- and aft- squint beams to achieve good azimuth diversity.

3. the addition of a third line-of-sight in the broadside direction to give Seastar the combined benefits of a scatterometer-type three-look sensitivity to wind vectors (Stoffelen & Portabella, 2006) with the fine spatial resolution of SAR imagers.

It is noted that the broadside beam needs no interferometric capability: the main purpose of the broadside beam is to provide backscatter data (NRCS) in the third azimuth direction to disentangle the contributions by the wind and current vectors during geophysical inversion. Standard SAR Doppler Centroid Anomaly (DCA) data can also be obtained, Chapron *et al.*, 2005, although no broadside Doppler data is currently used for Level 2 inversion (Martin *et al.*, 2023).

In addition to TSCV and OSVW, Seastar will provide collocated high-resolution SAR images of the ocean surface in three different look directions (azimuth), which can be used to estimate directional ocean wave spectra and integral wave parameters (e.g., Significant wave height, wave period) derived with Machine Learning (Quach *et al.*, 2020; Pleskachevsky *et al.*, 2022). Further details about Seastar data products are provided in Section 6.1.

Figure 4.3 provides a conceptual representation of the Seastar measurement principle. In the diagram, the fore and aft interferometric squinted beams are shown, together with the broadside beam. These beams overlap on-ground in order to form the instrument swath. The squinted and broadside beams are acquired quasi-simultaneously by the SAR instrument in order to ensure a continuous measurement of the swath. Because of Seastar's observation geometry the fore-, aft- and broadside beam SAR images for a particular location on-ground are acquired at different moments in time. The Doppler signals measured in all three azimuth look directions are converted into a velocity component in the slant range, which is subsequently combined with observations in the other azimuth directions to retrieve total current and wind vectors as part of the Level-2 inversion.
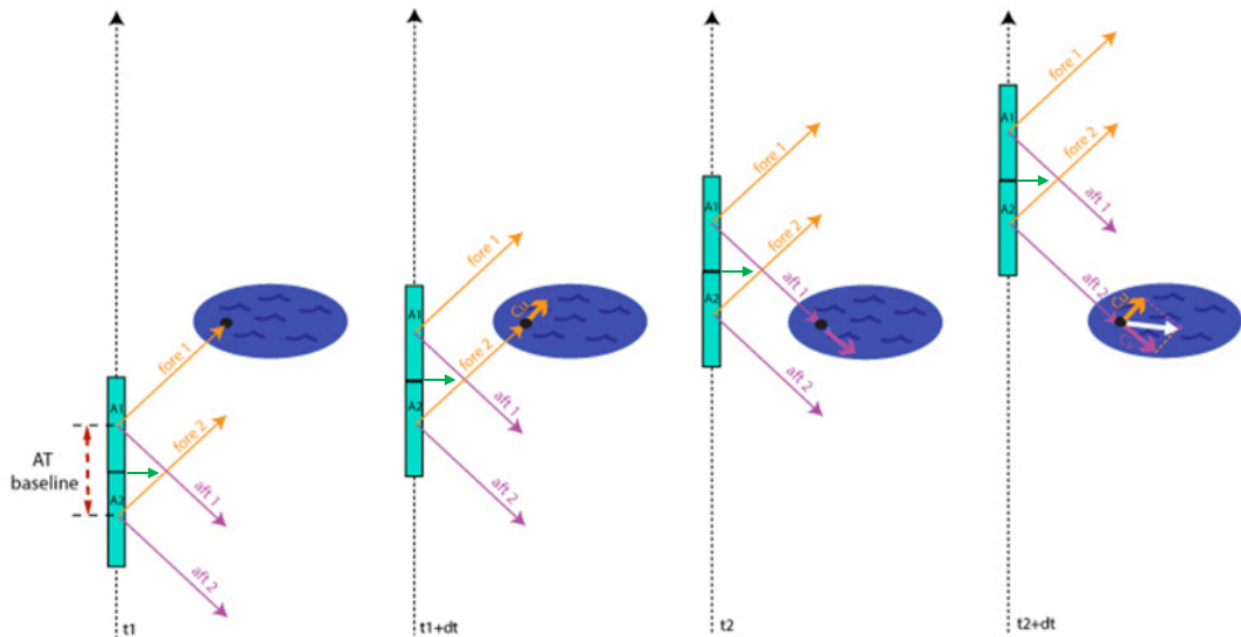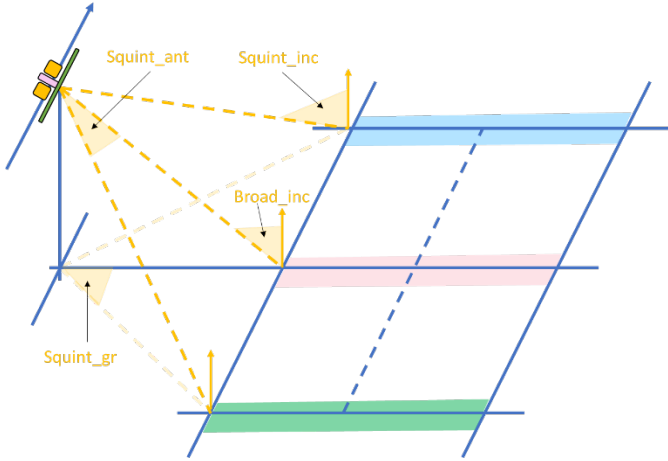
Figure 4.3: Measurement principle of high-squint Along-Track Interferometry as implemented on Seastar. The fore and aft squinted beams are represented in orange and purple colours respectively, and the broadside beam in green.

The Seastar measurement principle is similar to that used by EE10 Harmony mission, which achieves dual beam interferometry from two passive SAR systems as bistatic observations with Sentinel-1. The bistatic configuration limits the observations azimuth diversity. However, Seastar's stringent requirements on spatial resolution and uncertainties -imposed by its mission objectives- mean that the dual-beam interferometry must be implemented on a single platform. The Seastar solution provides optimal angular diversity that delivers quasi-orthogonality (~ 90 degrees) between the two squinted look directions.

The Seastar along-track interferometric measurements will be sensitive to any instrumental, geometrical or geophysical phenomena that affect the interferometric phase. The major contributions to the error budget are: baseline deformations; platform attitude errors; instrument performance (driven by coherence and signal-to-noise ratio) and external phase calibration. In order to retrieve accurate TSCV and OSVW measurements, a data-driven calibration method is introduced to correct for any systematic errors in the retrieval process. This is further discussed in Section 5.3.

4.4. Measurements requirements

Measurement Requirements	ID
Level-1 observation requirements	
Seastar shall provide calibrated measurements of normalised radar cross section and radial velocity in two squinted directions, fore and aft of broadside, using squinted SAR along-track interferometry (ATI). *Note 1: Fore and aft azimuth directions should be 90 degrees apart to measure two orthogonal components of the ocean surface motion.* *Note 2: For best performance, the squint angle should be greater than 30 degrees and smaller than 60 degrees (TBC; Frasier & Camps, 2001).* 	MR-MEA-01
Seastar shall provide calibrated measurements of normalised radar cross section in the broadside direction. *Note 1: Collocated retrieval of TSCV and OSVW requires at least three azimuth looks of the same ground area to achieve good azimuth diversity.* *Note 2: As goal, Seastar will provide L1B radial surface velocity measurements in the broadside direction with standard deviation ≤ 0.4 m/s (TBC).*	MR-MEA-02
The instrument shall operate at Ku-band. *Note 1: Ku-band ensures good sensitivity to ocean currents Doppler with a reduced payload.* *Note 2: Ku-band guarantees an availability of 90% or higher at any geographical location due to the different atmospheric losses.*	MR-MEA-03
The instrument shall operate in VV polarisation in the squinted directions. *Note 1: VV gives the best SNR and Coherence over the swath, especially in low wind conditions.* *Note 2: If the squint is achieved with electronic beam steering, the polarisation vector at the surface will rotate across the swath. The requirement calls for polarisation at the surface to be close to VV at the mid-point of the minimum swath. See e.g., Frasier & Camps, 2001.*	MR-MEA-04

The instrument shall operate in VV (Goal: VV and HH) in the broadside direction. *Note 1: VV and HH data would be obtained for the same scenes but acquisitions in the two polarisations do not need to be exactly simultaneous.* *Note 2: The acquisition of both polarisations would be desirable for the estimation of the wave Doppler bias, however, it is not strictly necessary for the fulfilment of the mission requirements.*	MR-MEA-05
All incidence angles shall be > 20° from nadir. *Note 1: Incidence angles above 20° bring multiple benefits including greater sensitivity to horizontal motions, reduced Doppler wave bias errors and greater benefit of dual-pol. It profits from high SRL for NRCS and OSVW due to scatterometer heritage.* *Note 2: This requirement sets the minimum incidence angle of the near-range edge of the broadside swath. By geometry, all other incidence angles will be greater.*	MR-MEA-05

Level-1 Product Requirements

Seastar Level-1 products shall consist of Single Look Complex (SLC) images of amplitude and phase for fore-master, fore-slave, aft-master, aft-slave and broadside.	MR-MEA-06
Seastar Level-1 SLC images shall have a point target resolution of at least 20 m (range) x 30 m (azimuth), at least, for one of the look directions (squint or broadside). (Goal: 20 m (range) x 30 m (azimuth) resolution in both look directions). *Note 1: The spatial resolution of L1B images is the same as for L1. This will serve to identify and remove contaminations from unwanted targets and artefacts (e.g., ships, wind turbines, sand banks,…) in the higher-resolution products prior to inversion to 1 km products at Level 2 and to enable the retrieval of wave spectra using the squinted beam.* *Note 2: The effective spatial azimuth resolution over ocean may not be to achieve this requirement because of the loss of coherence in high wind condition (High wind conditions considered as 15m/s).* *Note 3: The spatial resolution of L1 SLC images in the squinted directions is a trade-off between having a large number of fine-resolution pixels (beneficial to improve uncertainty at 1 km through incoherent averaging) and medium resolution that avoids registration errors linked to the velocities of ocean surface waves affecting the SAR imaging.* *Note 4: The primary purpose of the L1 SLC images in the broadside direction is to measure NRCS in a third azimuth direction.* *Note 5: The spatial resolution and specifications of the broadside beam could be similar to those of Envisat ASAR to benefit from high SRL, in the case the broadside beam is used for the wave spectra retrieval.* *Note 6: The image resolution in the broadside direction is a trade-off between the need to satisfy the required performance (noise) and the need to fit within the PRF and switching constraints imposed by the squinted beams.*	MR-MEA-07
Seastar Level-1B products shall consist of 2D images of calibrated Normalised Radar Cross Section, Coherence and Interferograms for fore and aft squinted directions, and 2D images of calibrated Normalised Radar Cross Section for the broadside direction.	MR-MEA-08
The instrument shall provide L1B radial surface velocity measurements in the squinted line-of-sights with a standard deviation ≤ 0.07 m/s (Goal ≤ 0.05 m/s) at 1 km resolution after calibration.	MR-MEA-09

Note 1: The radial surface velocity (u_rs) is the radial velocity on the ocean surface. It is related to the radial velocity measured by the system in the line-of-sight (u_r) by: $u_r = u_{rs} \cdot \sin(\theta)$ with theta the incidence angle. *Note 2: At Ku-band (13.5 GHz) and 30 degrees incidence, this requirement is equivalent to a standard deviation ≤ 2Hz on calibrated Doppler shifts for the squinted beams at 1 km resolution.* *Note 3: The Doppler frequency (f_d) is related to the radial surface velocity, u_rs by: $f_d = 2 \cdot u_{rs} \cdot \sin(\theta)/\lambda$ with λ the radar wavelength.* *Note 4: The 0.05 m/s error budget includes all non-geophysical errors affecting Doppler frequency measurements including instrument noise, and errors linked to platform attitude, baseline knowledge and antenna deformation.* *Note 5: The standard deviation of the radial surface velocity is related to the coherence (Gamma) and the number of independent looks (N) by (Wollstadt et al., 2017):* $du_{rsv} = 1/\sin(\theta) \cdot \lambda/4\pi \cdot \sqrt{[(1 - \text{Gamma}^2)/(2N \text{ Gamma}^2)]} \cdot B\_AT/(2.Vp)$ *with B_AT the along track interferometric baseline and Vp the platform velocity.* *Note 6: The reference NRCS for the performance calculation shall be the mean value between the NRCS at 5m/s upwind and the NRCS at 5m/s cross wind.*	
The instrument will provide calibrated NRCS in the squinted directions with a relative radiometric resolution Kp $\leq$ 3% (TBC). *Note 1: Kp is related to the Noise Equivalent Sigma Zero (NESZ) and the Signal to Noise Ratio according to the definitions in Appendix A* *Note 2: Kp is related to the coherence due to noise, Gamma_SNR, and the number of independent looks by: $\text{Gamma\_SNR} = 1/(1 + 1/\text{SNR})) = 1/(Kp.\sqrt{N})$* *Note 3: The reference NRCS for the Kp calculation shall be the mean value between the NRCS at 5m/s upwind and the NRCS at 5 m/s cross wind.* *Note 4: This requirement is not a driver for Seastar mission.*	MR-MEA-10
The instrument shall provide calibrated NRCS in the broadside direction with a relative radiometric resolution Kp $\leq$ 4% in 5 km cells. *Note 1: The reference NRCS for the Kp calculation shall be the mean value between the NRCS at 5 m/s upwind and the NRCS at 5 m/s cross wind.*	MR-MEA-11
The instrument shall use observations over coastal land and islands to calibrate the interferometric baseline and correct antenna thermoelastic deformation effects. *Note 1: Most Seastar scenes will image coastal land or islands that can be used to calibrate the radial velocity measurements.*	MR-MEA-12

4.5. Proof of Measurement Concept

The squinted ATI principles of Seastar were successfully demonstrated experimentally and scientifically with airborne data from the two-beam Wavemill demonstrator during the Irish Sea proof-of-concept campaign in October 2011 (Márquez *et al.*, 2010; Yague-Martinez *et al.*, 2012; Martin *et al.*, 2016). Level-0 data were processed to produce Level-1 interferograms (correcting large aircraft navigation/attitude variations) and retrieve Level 2 TSCV (Figure 4.4).

At 1.5 km resolution, the Wavemill TSCV RMS Error against HF radar was better than 0.1 m/s and 10 degrees. The experiment also revealed the system's ability to detect fine-scale current intensification close to land associated with underwater bathymetry channels.

Wavemill's two-beam configuration and the lack of NRCS calibration prevented OSVW retrieval. Both three-beam and Ku-band (VV and HH) OSVW retrieval from stable, but uncalibrated, NRCS are at high SRL in wind scatterometry (e.g., Vogelzang & Stoffelen, 2022).

The measurement concept has since been further demonstrated and validated with the experimental campaigns performed within the frame of the Seastar Phase-0 contracts. An overview of these flight campaigns and their main outcomes and results are detailed in Section 7.3.
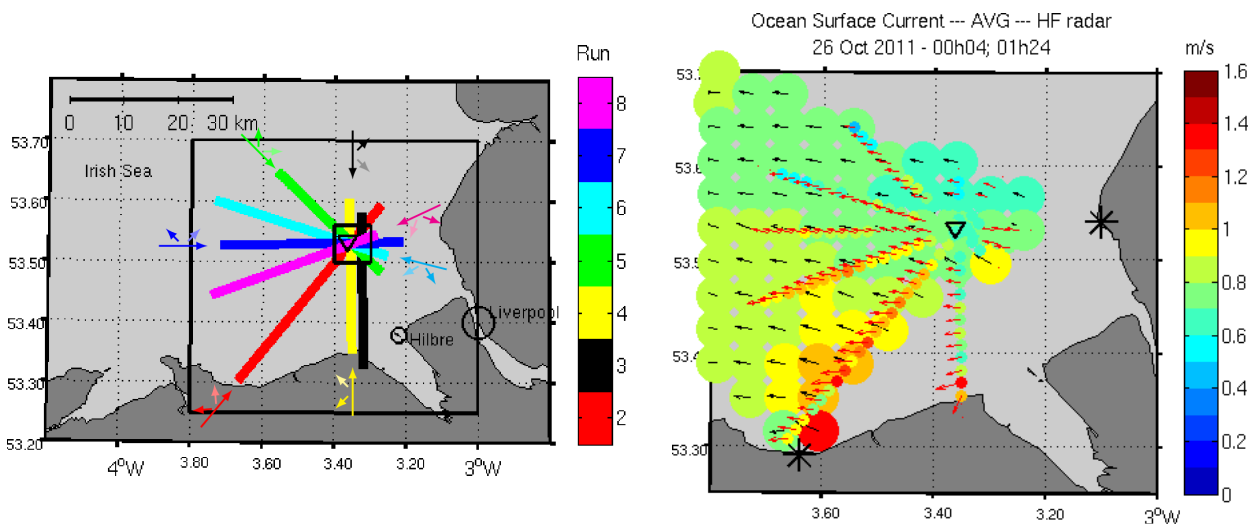
Figure 4.4: Wavemill airborne proof-of-concept campaign in Irish Sea in October 2011. (left) Location of the flight star pattern over the Acoustic Doppler Current Profiler (inverted triangle). (right) Measured Total Surface Current Vectors: colours indicate TSCV magnitude. Large circles and black arrows show TSCV from HF radar (4 km resolution). Small, coloured circles and red arrows show TSCV from Wavemill (1.5 km resolution). Two black stars onshore indicate the HF radar antennas (Source: Martin & Gommenginger, 2017)

5. PRELIMINARY MISSION CONCEPTS

This chapter provides a concise technical description of the Seastar mission. Whenever relevant, two implementation concepts (Concepts A and B) are described to present the different implementation options and their expected performance at Level 1.

These concepts were developed in two parallel Phase 0 system studies by two industrial consortia led by Airbus Defence and Space – GmbH (Concept A) and OHB Systems AG (Concept B), respectively. The Airbus Defence and Space – GmbH consortium includes Airbus Defence and Space Ltd as payload prime, while OHB Systems AG include Thales Alenia Space Italy as payload prime. The figures below are courtesy of the respective industrial consortia unless otherwise mentioned at the foot of the picture.

5.1. Mission Overview

5.1.1. Mission architecture

The main architectural elements of the Seastar mission are shown in Figure 5.1 for both consortia, the overall architecture is the same. It includes the following elements:

- The **Launch Segment**, designed to be compatible with a launch on Vega-C.

- The **Space Segment,** consisting of single spacecraft carrying a Ku-band Interferometric SAR, operating in Low-Earth-Orbit (LEO) based on a heritage platform.

- The **Ground Segment**, based on the Earth Explorer ground segment infrastructure and is composed of the Flight Operational Segment (FOS) and the Payload Data Ground Segment (PDGS).

Figure 5.1: Seastar mission architecture elements

5.1.2. Observation Concept

As briefly introduced in Section 4.3, the space segment consists of one single platform carrying a SAR instrument capable of providing measurements in three different look directions as described in Figure 5.2. Along-Track Interferometry (ATI) is performed in two directions by means of two pairs of ant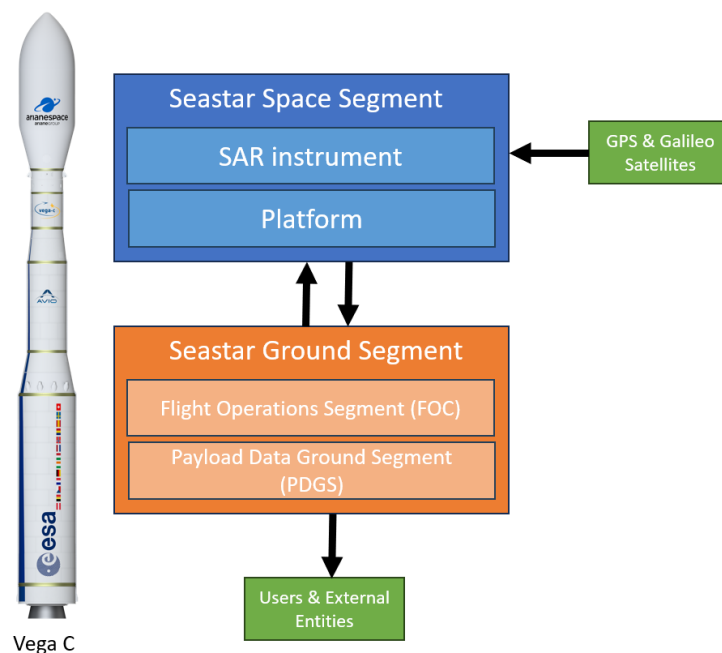ennas squinted 45 degrees forward and backward with respect to boresight. A third beam is implemented pointing broadside.

The Seastar imaging geometry is unique because the system cycles through beams in different along-track positions. To generate a valid TSCV image of a patch of ocean, Seastar will image this same area with all three look directions. This means that this patch of ocean needs to be illuminated by the fore, aft, and broadside antenna beams.

In the discussion of measurement modes, the following abbreviated terms are used:

- **FORE**: The transmit antenna which is squinted in the fore (positive along-track) is transmitting, and the two fore-squinted Rx antennas are receiving. The two fore-squinted Rx antennas are separated by an ATI baseline.

- **AFT**: The transmit antenna which is squinted in the aft (negative along-track) is transmitting, and the two aft-squinted Rx antennas are receiving. The two aft-squinted Rx antennas are separated by an ATI baseline.

- **BROADSIDE**: The transmit-receive antenna which is side facing is active.

5.1.3. Driving Requirements

Seastar Level-1B products consists of 2D images of calibrated Normalised Radar Cross Section, Coherence and Interferograms for fore (VV) and aft (VV) squinted directions, and 2D images of calibrated Normalised Radar Cross Section for the broadside direction. Table 5.1 lists the main instrument observational requirements which drive the design of Seastar payload and satellite configuration.

Table 5.1: Seastar summary of the key instrument requirements.

| Parameter/Req. ID	Requirement
Swath Width *MR-OBS-08*	≥ 100 km (Goal for swath: ≥150 km)
Repeat cycle *MR-OBS-10*	Seasonal (~91 or ~271 days)
Minimum revisit time and number of alternate or consecutive observations. *MR-OBS-11*	Revisit all CoSMIZ locations during at least 3 (threshold) to 5 (goal) consecutive (goal) or alternate (threshold) days, and sub-daily observations of certain areas of interest.
Minimum Incidence Angle *MR-MEA-05*	> 20° from nadir
Surface Radial Velocity Standard Deviation *MR-MEA-09*	≤ 0.07 m/s at 1km resolution after calibration
Relative radiometric resolution (Kp) in the broadside direction *MR-MEA-11*	≤ 4% in 5 km cells
Swath Width *MR-OBS-08*	≥ 100 km (Goal for swath: ≥150 km)
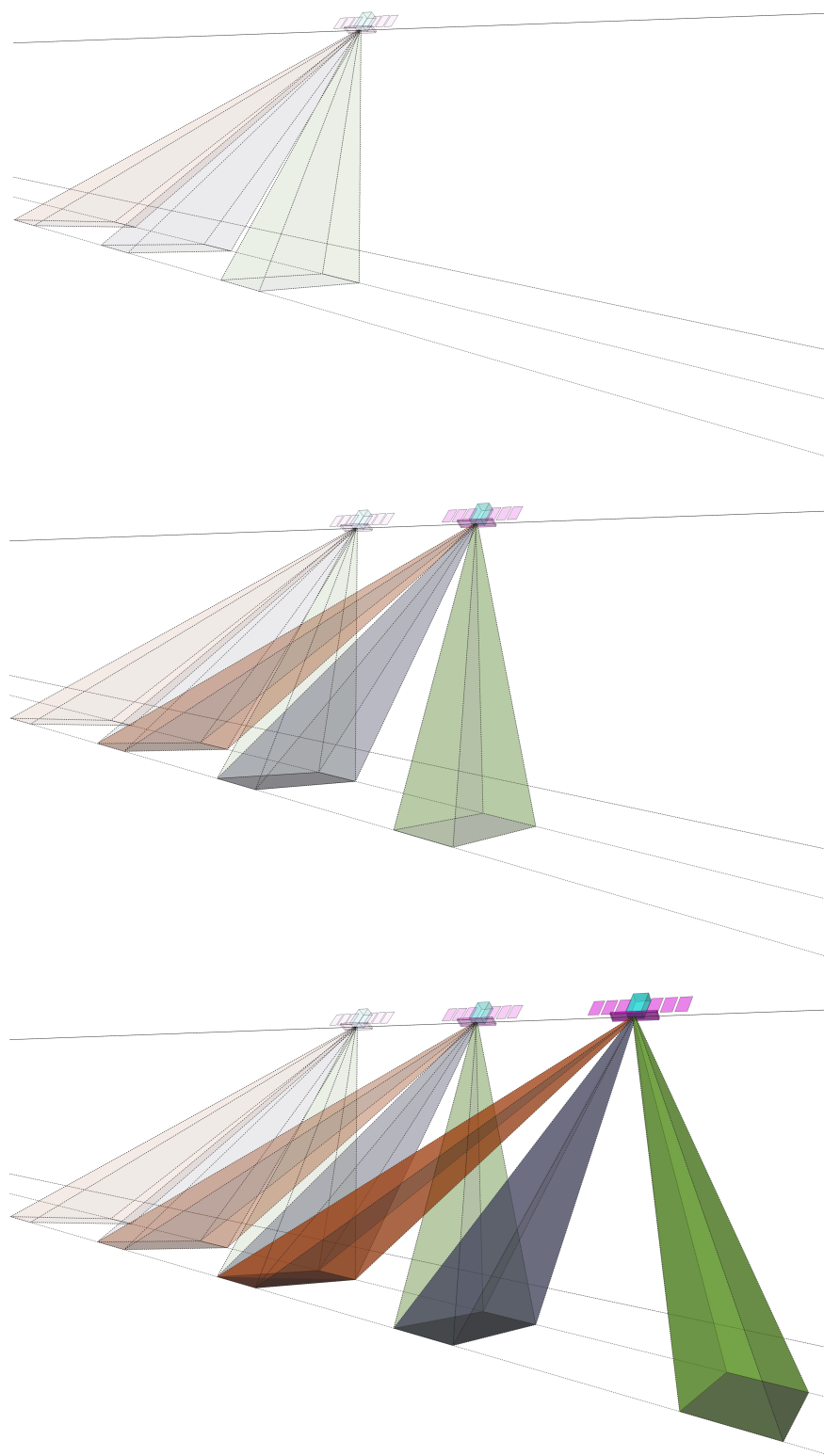
Figure 5.2 Seastar acquisitions at three different times to illustrate the three looks geometry and AFT, FORE and BROADSIDE beam overlapping. FORE and AFT beams are formed by two antenna pairs separated along-track.

A brief explanation of the parameters and their associated requirements in Table 5.1 is provided next:

- **Swath Width:** The instrument must satisfy L1 uncertainty requirements on radial velocity and backscatter at VV polarisation over the full range of the swath. A wider swath will increase the overlapping for consecutive/alternate days. Maximising the number of consecutive/alternate observations will result in the orbit selection and could impact the acquisition strategy. Performance at far range for a large swath could be limited by the instrument signal-to-noise ratio (SNR). Swath width has a direct impact in the instrument SAR mode, timing, resolution, and overall instrument complexity. In addition, to achieve the 100 km swath as the overlapping product of FORE, BROAD and AFT beam, a continuous yaw steering attitude control law is implemented.

- **Required Coverage:** Seastar will provide measurements over Coastal seas, Shelf seas and Marginal Ice Zones (CoSMIZ) and selected Ocean Regions of Special Scientific Interest (ORSSI). The Seastar mission will have a drifting orbit phase to achieve a seasonal repeat cycle (~91 or ~271 days repeat cycle). The coverage together with the repeat cycle and the revisit time (1 (goal) or 2 (threshold) days sub-cycle) will also drive the orbit selection together with the swath width described previously. Coverage mask will also define the orbit duty cycle of the instrument and the consequent sizing of the power sub-system, memory, and data downlink sub-system. The orbit duty cycle could also set technological limits for elements such the RF power amplifiers.

- **Revisit Time:** The drifting phase will provide swath overlap between alternate days (Goal: consecutive days) of, at least, 65%. This, together with the swath width and the required coverage will have an impact in the orbit selection.

- **Minimum Incidence Angle:** Incidence angles above 20° bring multiple benefits including greater sensitivity to horizontal motions and reduced Doppler wave bias errors. This requirement is defined for broadside and squinted beams. The incidence angle requirement is having an overall impact in the beam SNR which is related to instrument transmit power level need and the reference Normalised Radar Cross-Section (NRCS) from the sea surface.

- **Radial Velocity Standard Deviation:** This requirement sets the boundary of the allowed ATI phase errors. These are mainly driven by interferometric phase noise, coming from limited SNR and ambiguity rejection, and by the interferometer sensitivity given by squinted view antenna phase centre separation. For a given SNR, this requirement drives the ATI baseline selection. The selection of the SNR and ATI baseline will impose certain restrictions in terms of short-term errors such as, but not limited to, pointing error, wind antenna vibration from appendage dynamics and internal calibration phase accuracy. Systematic errors are not captured in this requirement.

- **Relative Radiometric Resolution (Kp):** Relative radiometric resolution is related to the number of multi-looks and SNR. This requirement mainly impacts the design of the broadside beam where resolution and SNR is driven by the Kp parameter. This requirement will drive the antenna size and transmit power level.

5.2. Mission analysis

5.2.1. Orbit selection and orbit description

The primary driving requirement for selecting an orbit is the specified seasonal repeat cycle described in MR-OBS-10, which is either ~91 or ~271 days, combined with the minimum overlapping requirement on alternate or consecutive days derived from MR-OBS-11. Both concepts have chosen a sun-synchronous dusk/dawn orbit which is a heritage orbit for SAR satellites as there are long periods of

continuous solar illumination with eclipses restricted to the eclipse seasons occurring around one of the solstice periods. In this way solar array area and battery sizing are minimised. The summary of the selected orbits is presented in Table 5.2.

Table 5.2: Orbit Information and lifetime.

Element	Concept A	Concept B
Orbit	SSO Dawn/Dusk	SSO Dawn/Dusk
Altitude (km)	560	412
Sub-cycle (days)	1 day	2 days
Lifetime (years)	7.5	3.5
Orbit	SSO Dawn/Dusk	SSO Dawn/Dusk

For Concept A, two orbits capable to meet the two seasonal repeat cycle options are proposed. In both cases the mean altitude orbit height is ~560 km which provides a 1-day sub-cycle.

Concept B also proposes two orbits capable to meet the two seasonal repeat cycle options. In both cases the mean altitude orbit height is ~412 km which provides a 2-day sub-cycle operation. The chosen orbit is driven by instrument performance (mainly SNR and day sub-cycle), although it incurs a higher penalty for orbit maintenance with a large impact on the delta-V budget and consequently a reduction in the mission lifetime down to the minimum as stated in the Seastar MR-OBS-09, MR-OBS-10 and MR-OBS-11.

The proposed orbits by the two consortia fulfil the requirements of coverage, repeat cycle, and day sub-cycle. Seastar is a fully flexible mission in terms of repeat cycle selection. Although not part of the baseline mission, Seastar can be operated in a repeat cycle of ~91 or ~271 days, with the ability to transition between the two of repeat cycle options at minimal delta-V cost. The delta-V requirement for such a manoeuvre is relatively small, in the order of 1 m/s, and several transitions could be completed between the 2 repeat cycles over the course of the mission with negligible impact on the mission lifetime.

Additionally, near the baseline orbit for Concept A, exact 1-day repeat orbits can be found, offering a set of fixed orbits (15 in this case) that repeat daily. In case of Concept B, 2-days exact repeat orbit can also be found. The same conclusions regarding the required delta-V also apply.

5.2.2. Coverage and revisit

The orbit selection flexibility described in previous section impacts the coverage and revisit time. Two examples are provided for illustration regarding the ~271 days and the ~91 days cases.

The coverage analysis is performed considering only one pass, either ascending or descending. Coverage, repeat cycle and revisit time requirements are met by both consortia under any of the prescribed seasonal revisit times (~271 days and the ~91 days).

Figure 5.3 presents the number of consecutive days within a repeat cycle of ~271 days for Concept A. Full coverage of the requested mask is achieved providing a revisit time which is related to the repeat cycle. Currently, Concept A and B will provide, at least, 10 revisits in consecutive (Concept A) or alternate (Concept B) days for a ~271-days repeat cycle.

The number of alternatives during a full repeat cycle of ~91 days for Concept A is presented in Figure 5.4. The number of consecutive days is minimum at the equator and increases with the latitude. Currently, Concept A and B will provide, at least, 3 revisits in consecutive (Concept A) or alternate (Concept B) days for a 91-days repeat cycle.
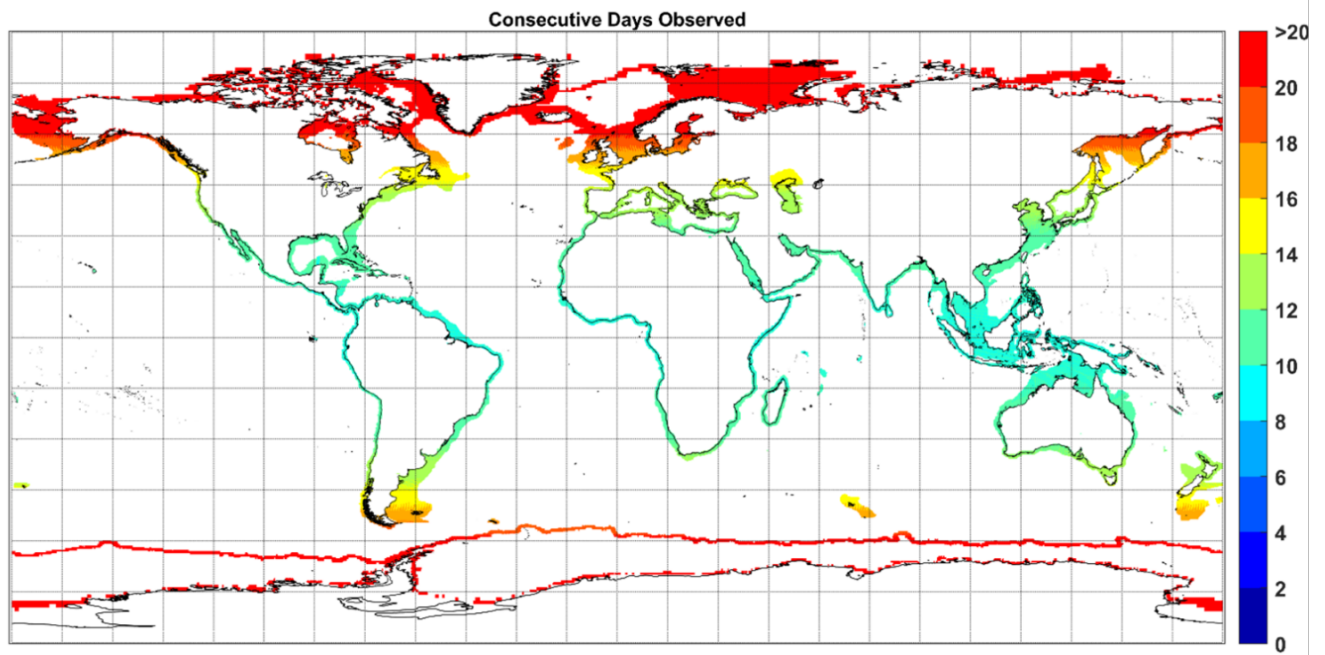

Figure 5.3: Number of consecutive days being observed for orbit 15+1/271 with the full swath achieving a 7cm/s surface radial velocity standard deviation (Concept A).
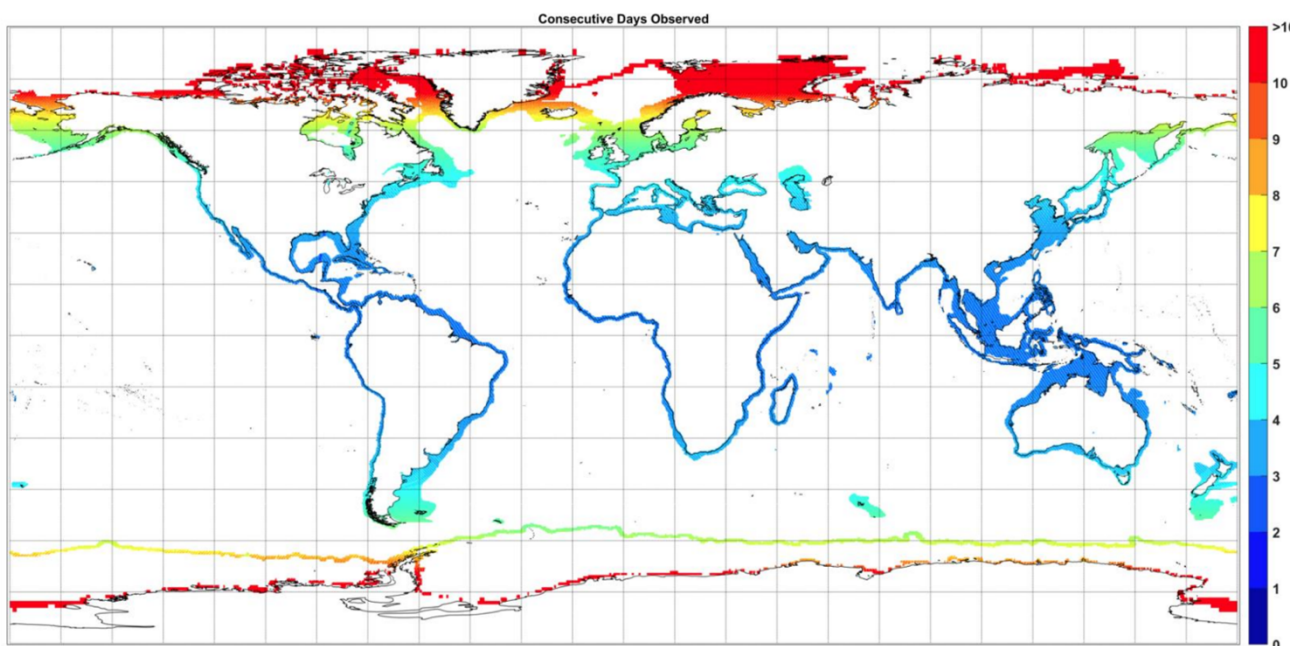
Figure 5.4: Number of consecutive days being observed for orbit 15+1/91 with the full swath achieving a 7cm/s surface radial velocity standard deviation (Concept A)

The sub-daily observations may be achieved over orbit crossover bands considering ascending and descending passes as illustrated in Figure 5.5. These crossover bands also offer additional opportunities for fast revisit observations beyond the coverage mask, e.g., ocean areas far from the coastal edges. The percentage of the crossover bands is dictated by the margins in the memory, data downlink and power sub-system capabilities. Both consortia can provide observations in large portion of these crossovers over sea areas with the current designs. Optimisation of the current mask and areas of interest within the cross-over are possible.
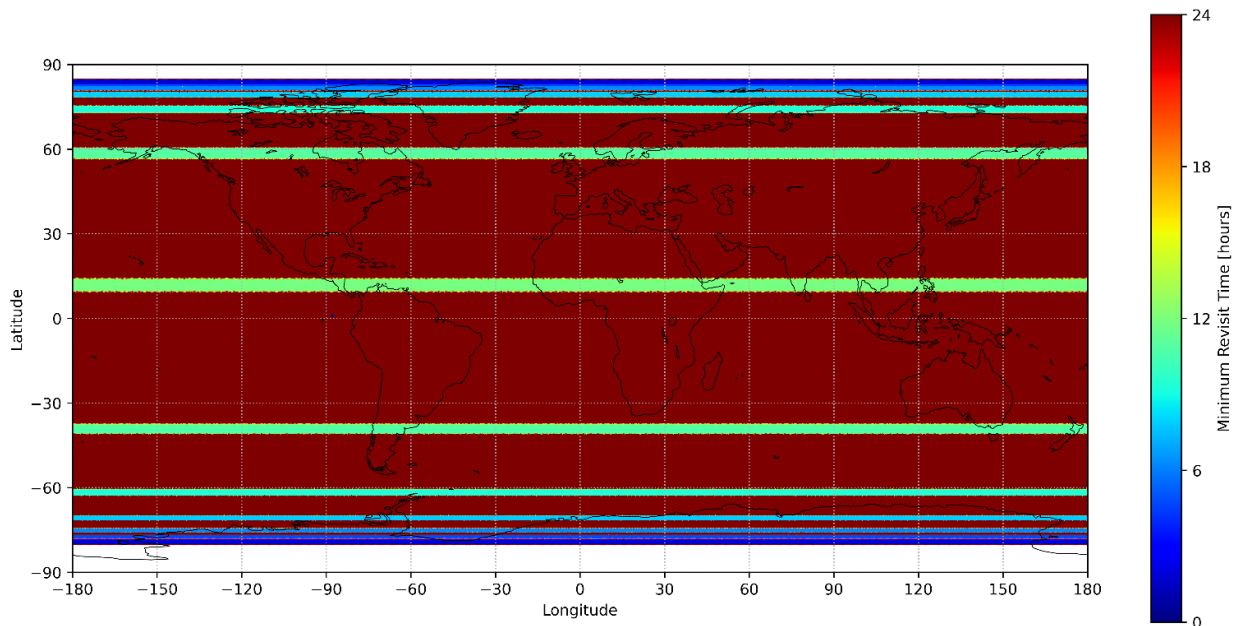
Figure 5.5: Crossover analysis using ascending and descending - for illustration

5.3. Space segment

5.3.1. SAR Payload

The Seastar baseline payload is an Along-Track Interferometry (ATI) SAR payload which operates with a carrier frequency of 13.5 GHz at Ku-band. The system is designed to perform an ATI velocity measurement of the sea surface in both a fore and aft looking direction. In order to perform ATI, the SAR payload requires two phase centres which are offset in the along-track direction. As the ATI performance is related to the separation of these phase centres, the SAR antenna is longer than many typical SAR payloads in the along-track (azimuth) direction.

Monostatic and bistatic topologies, illustrated in Figure 5.6, where traded-off during the Phase 0 studies. A monostatic solution results in reduction of the physical baseline while maintaining the ATI baseline. However, this improvement comes at the price of:

- Higher PRF, with the potential degradation of range ambiguities.
- Increase in the number of number of beams of the ScanSAR operation, resulting in degradation of the azimuth resolution.
- For the same peak power output and duty cycle, power consumption and the Tx duty cycle are both doubled.
- The complexity and mass are increased with respect to the Bistatic configuration.
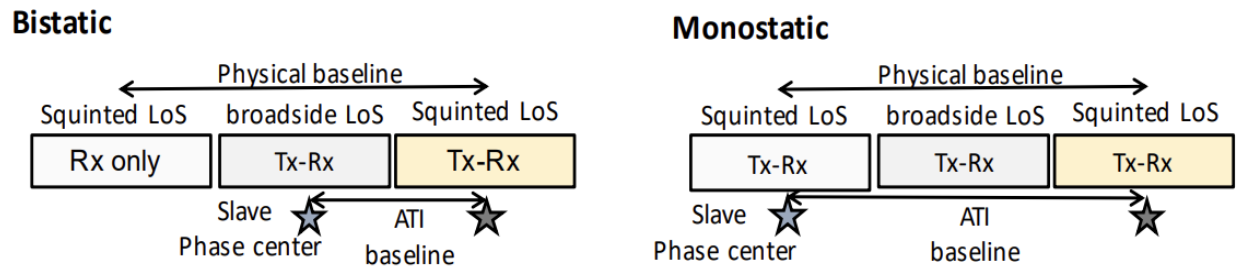
Figure 5.6: Comparison of monostatic and bistatic and configurations to provide ATI operation. (Concept A)

Although the monostatic configuration is preferred in terms of mechanical accommodation, the bistatic configuration has been selected by both consortia as the reduction in mass, power and complexity for a similar payload performance is considered a better overall solution to achieve both the technical and programmatic requirements of the mission.

The antenna will need to be folded to fit within the fairing, a trade-off has been completed to look at the length of each folded section and the subsequent impact the stowed antenna has on the width of the satellite. The dimensions on each section are driven by the following constraints, long sections require a tall structure to mount Hold Down and Release Mechanisms (HDRMs) to ensure that the stowed antenna survives the rigors of launch, and a tall structure is restricted by CoG requirements of the launch vehicle. The number of antenna sections that can be folded on top of each other is limited by the width of the fairing and also the increase in complexity of the deployment mechanism associated with each additional section.

For both concepts the optimum design for the payload antenna is to be split into 2 wings with each wing comprised of 3 sections, this reduces the overall width of the Satellite whilst also minimising the height of the platform and the complexity of the deployment system.

The lateral SAR antennas in both concepts will be exposed to the Sun, and thus the backside must be covered by MLI to ensure a constant thermal environment. Depending on the antenna design, the effects from Thermo-Elastic Distortion (TED) may cause slow variations in the antenna pattern over timescales of an orbital period. An initial analysis of the TED of the proposed antenna designs has been completed by each consortium and these results have been assessed in terms of the impact on the proposed mission concept.

The payload implementation of the 2 concepts is slightly different with a centralised power amplifier for concept A resulting in a largely passive antenna versus a distributed solution with the high power amplifiers mounted on the antenna panels of one of the wings for concept B. This difference in architecture results in differences in the thermal environment of the antenna such that the criticality of the Thermo-Elastic Distortion (TED) on the antenna and resulting antenna pattern are different between the 2 concepts.

For both concepts a thermal model of the complete antenna has been created and a number of thermal cases have been assessed to determine the worst case in terms of TED. The results of the thermal model have then been mapped to a Finite Element Model (FEM) of the antenna in order to complete this initial assessment of the TED.

For both concepts, an initial TED analysis has been completed, no major issues have been noted with the current implementations, but this aspect will be revisited in greater detail during future phases as the antenna design is matured.

Details regarding the analysis for each concept are included in the corresponding sub-section.

5.3.2. SAR Instrument Concept A

For Concept A, the Tx squinted (FORE and AFT) and Tx broadside panels are placed in the centre of the antenna with the goal to reduce the RF distribution loss and implement a symmetrical configuration, leading to a better thermal management and potential easier management of the antenna/baseline deformations.

The payload diagram is shown in Figure 5.7 and is composed of the following key components:

- A centralised <u>High-Power Amplifier</u> (HPA) based on an Extended Interaction Klystron (EIK). The selection of the technology is based on the capability to deliver high peak power. EIK are capable to provide better thermal management than alternative technologies such as helix Travelling Wave Tubes (TWTs).

- A dedicated <u>Electronic Power Conditioner</u> (EPC) for the centralised EIK.

- A <u>switching network</u> to make connections from the HPA to the antennas. The switching network unit oversees routing the transmitted chirp from the EIK to the antennas (FORE, AFT and broadside).

- The <u>antenna sub-system</u> is presented in Figure 5.8. Squinted beams are achieved by means of the use of leaky wave technology which provide a natural squint avoiding the need for azimuth mechanical/electronic steering. This results in a flat antenna radiating panel which simplifies the antenna accommodation and deployment. The Broadside antenna is implemented using slotted waveguide. The antenna sub-system is composed of:
    - A 13-meters **Tx antenna squinted** in the **fore** direction (Squint Tx-Fore-V pol).
    - Two 3-meters **Rx antennas** squinted in the **fore** direction, separated in the along-track direction by 16-meter baseline (Rx-Fore-V pol).
    - A 13-meters **Tx antenna squinted** in the **aft** direction (Squint Tx-Aft-V pol).
    - Two 3-meters **Rx antennas squinted** in the **aft** direction, separated in the along-track direction by 16-meter baseline (Rx – Aft - V pol).
    - A 13-meters **Tx-Rx antenna** facing **broadside** (Broadside TxRx - V pol).

- A <u>backend</u> taking heritage from the ROSE-L mission, including the use of Universal Processing Modules (UPM).

- A <u>digital backend</u> which can implement Scan-On-Receive (SCORE) for the squinted Rx antennas.

- A <u>harness and signal distribution network</u> which is designed to be lightweight and minimise RF feed losses.

- An <u>internal RF calibration network</u> capable of characterising all the active components.

Redundancy is implemented in all critical elements such as HPA and UPM. For the distributed receivers located in the Rx squinted antennas, the instrument performance impact due to the failure of a number of LNAs has been analysed, resulting graceful degradation while keeping the instrument fully operative.
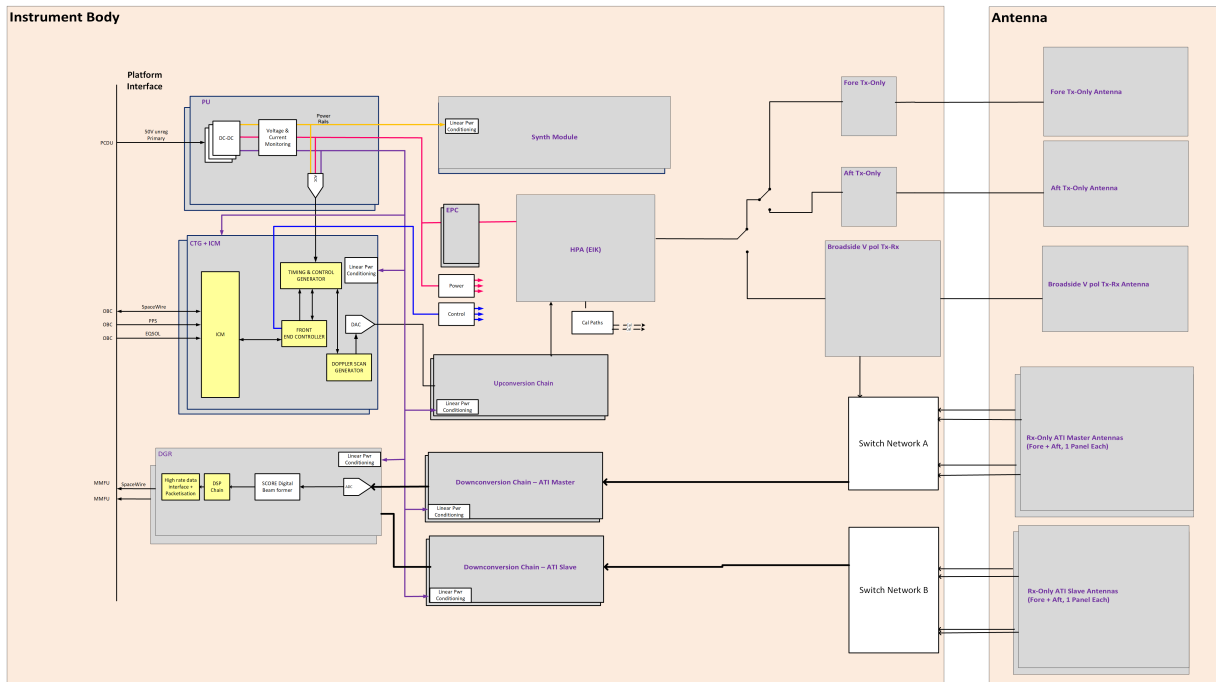
Figure 5.7: SAR block diagram. (Concept A)
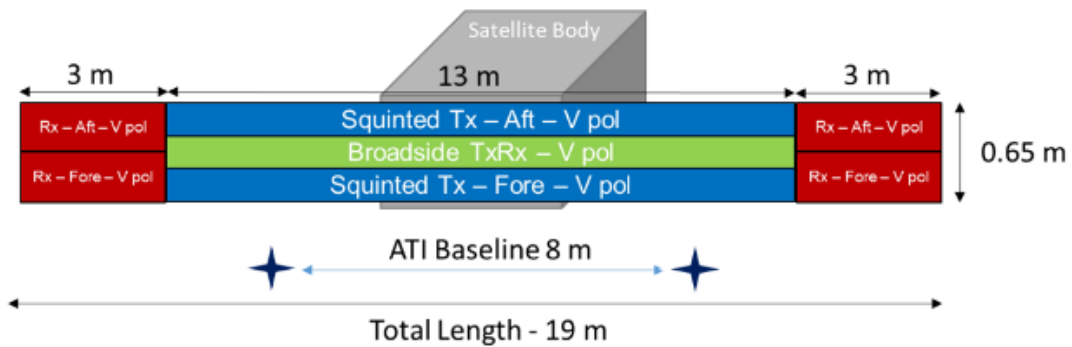
Figure 5.8: Illustration of the Seastar baseline instrument configuration. Not to scale. (Concept A)

For Concept A the SAR antenna, shown in Figure 5.8, has an overall length of 19 m. The squinted Rx antennas in each wing have a separation of 16 m between their phase centres.

The Tx squint antennas are built-up of 9 sub-arrays in azimuth and multiple leaky way rows in elevation. An azimuth and elevation beamforming network are also included to connect the radiating panels and the switch matrix. The baseline FORE and AFT antenna are built in separated panels and implement a vertical polarisation. Slot inclination is implemented to improve the amount of power contained in the direction of propagation.

The Rx squint antennas are built-up of 1 single array and rows are grouped in elevation to form the SCORE channels. The SCORE channels are connected to the frequency converters and UPMs by means of a low power switch network. For illustrative purposes, a simplified payload architecture highlighting the key hardware element is shown in Figure 5.9.

The Tx/Rx broadside antenna is built-up of 18 sub-arrays in azimuth and multiple slotted waveguides rows in elevation. Azimuth and elevation beamforming network is also included to connect the radiating panels and the switch matrix.
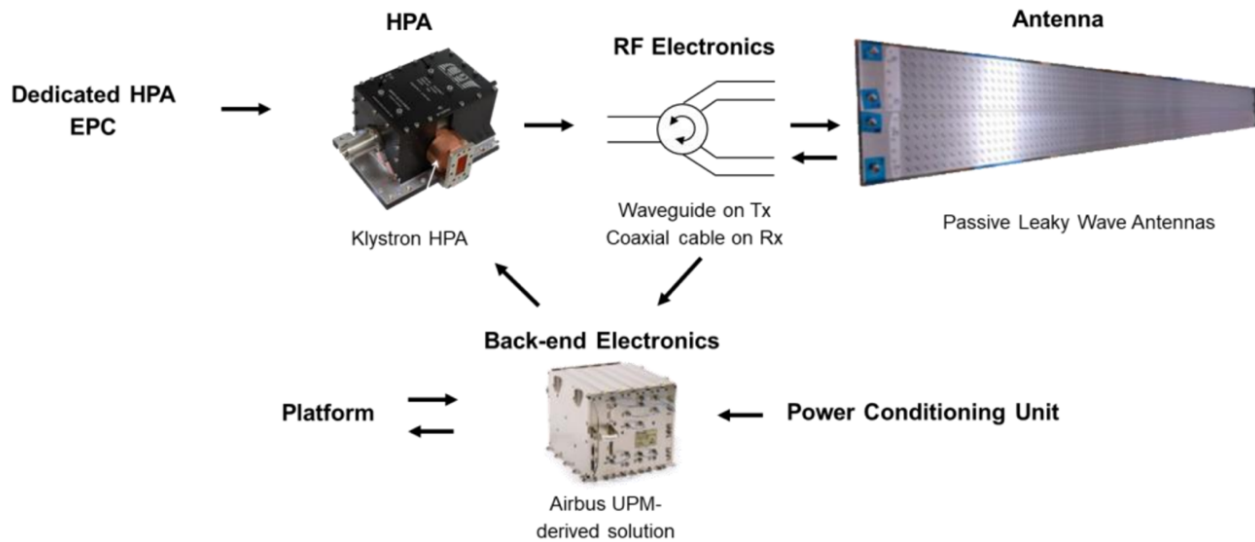
Figure 5.9: Key subsystems of the Seastar Payload. (Concept A)

The Seastar mask contains coastal areas and as a result majority of the acquisitions (>80%) of the mask will also acquire land areas. These land acquisitions can be used to perform system calibrations and result in a simplification of the satellite design as no on-board metrology system is required.

For Concept A, the initial TED analysis has been completed looking at the impact of different times of the year on the thermal environment in order to determine the worst case. The worst-case environment has then been used to determine the TED and it has been concluded that any deformations of the antenna will be symmetric and, that the impact on the antenna pattern for both transmit and receive is negligible, also for the interferometric products. At this time no changes need to be made to the current concept with respect to TED.

A strategy for the calibration of systematic errors has been developed. The idea is to use land acquisitions to calibrate the baselines components. Estimated precision in calibrating baselines is presented in Figure 5.10. The onboard-metrology system is deemed not necessary because of the current coverage mask and the calibration strategy using land which provides a good baseline estimation.
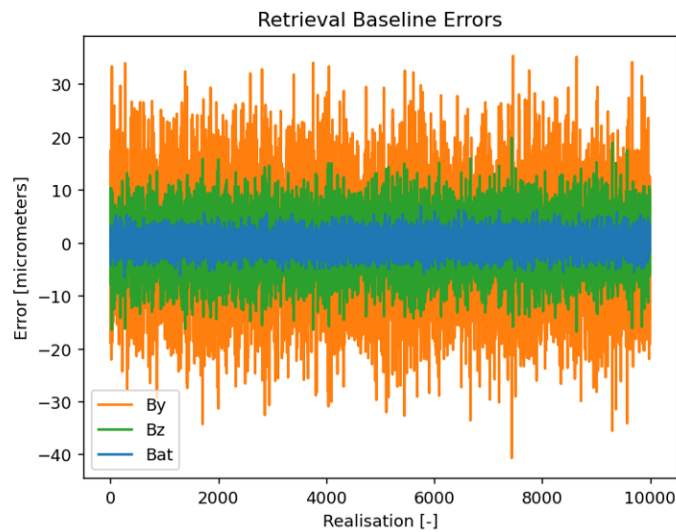
Figure 5.10: Error in the estimation of the baseline [micrometers] for 1 million Montecarlo runs.
Simulations with 4.5mm baseline 1-σ error in [Bat, By, Bz] and 0.000170º. in [Yaw, Pitch, Roll] 1-σ error (Concept A)

5.3.3. SAR Instrument Concept B

For Concept B the Tx/Rx antennas for squinted (FORE and AFT) and broadside directions are placed on one of the antenna arms while the opposite arm implements only squinted Rx beam.

The payload diagram is shown in Figure 5.11 and is composed of the following key components:

- **S**AR **A**ntenna **S**ub-system **(SAS)** is devoted to providing the following functions:

  o radiation of RF signals at vertical polarisation in Ku-band, in aft and fore squinted directions.

  o radiation of RF signals at vertical polarisation in Ku-band, in the broadside direction.

  o simultaneous reception of RF signals at vertical polarisation in Ku-band through two antennas forming an along track interferometer looking in aft and fore squinted directions.

  o reception of RF signals at vertical polarisation in Ku-band, through one/two antennas forming an along track interferometer or exploiting DCA technique for the broadside measurement.

  o actuation of the ScanSAR functionality through the dynamical handling of multiple beams.

  Squinted beams are achieved by means of the use of leaky wave technology which provide a natural squint avoiding the need for azimuth mechanical/electronic steering. This results in a flat antenna radiating panel which simplifies the antenna accommodation and deployment. Broadside antenna is implemented using slotted waveguide.

- The **S**AR **F**ront-**E**nd **E**lectronic **S**ub-system **(SFEES)** consists of the active elements (e.g., Electronic Front-Ends - EFEs) and splitters/combiners to distribute the signal from platform to

the different EFEs separating Rx and Tx path considering the number of EFEs input and output ports. The updated approach foresees to use the same EFEs for Squint and Broad beam antennas.

High Power Amplifier (HPAs), Low Noise Amplifiers (LNAs), phase shifters, and variable attenuators are distributed on each antenna row and column, moreover each antenna is able to steer electronically the beam towards all the needed directions (i.e., fore, broadside, or aft and steering in elevation).

- The **S**AR **E**lectronics **S**ubsystem **(SES)** manages all the radar functions of the Instrument such as generation of chirp pulses, amplification and filtering, frequency conversion, digitisation, IQ demodulation, compression and formatting of radar data, generation of frequency references, command, control and monitoring of the Instrument, generation of timing signals, antenna beam dynamic control and switching to implement the ScanSAR functionality.

Redundancy is implemented in all critical elements such as SES. For the distributed receivers located in the antennas, the instrument performance impact due to the failure of a number of TRMs or RMs has been analysed, resulting graceful degradation while keeping the instrument fully operative.
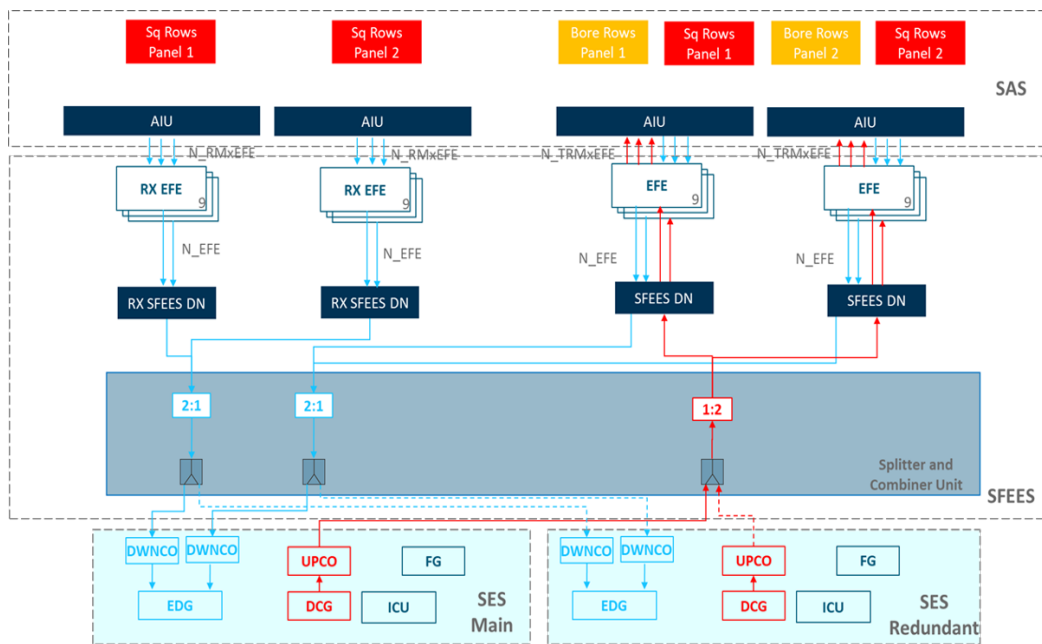
Figure 5.11: SAR block diagram. (Concept B)
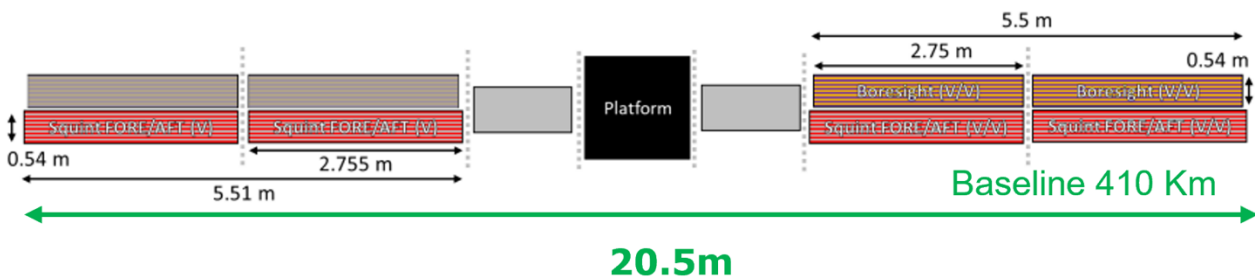
Figure 5.12: Illustration of the Seastar baseline instrument configuration. Not to scale. (Concept B)

For Concept B, the SAR antenna, presented in Figure 5.12, has an overall length of 20.5 m. The squinted Rx antennas in each wing have a separation of 15 m between their phase centres.

The Tx/Rx squint antennas are built-up of 2 sub-arrays in azimuth and multiple leaky way rows in elevation. Azimuth beamforming network is included to connect the different panels. Baseline FORE and AFT antennas are built in interleave panel and implement a vertical polarisation. Slot inclination is implemented to improve the amount of power contained in the direction of propagation. Each panel is equipped with a number of Transmit and Receive modules (TRMs) being used for FORE, broadside and AFT beams. Similar implementation is done for the Rx-only squinted antenna where the TRMs are replaced by only Receive Modules (RMs).

The Tx/Rx broadside antenna is built-up of 2 sub-arrays in azimuth and multiple slotted waveguides rows in elevation. Azimuth and elevation beamforming network is also included to connect the radiating panels and the switch matrix.

For Concept B, the initial TED analysis has been completed and several key points have been noted. Firstly, the payload solution for concept B is asymmetric with the transmitter hardware located only the right wing (see Figure 5.12) of the antenna, therefore the power dissipation of the right antenna wing is larger than that of the left and consequently the displacement caused by the TED is greater for the right wing. This results in an asymmetric distortion across the full antenna that has been anticipated by Concept B with the baseline including a mechanism that will be used to correct the gross displacement once at the start of the mission. The residual distortion has been assessed with a negligible impact on the payload performance.

A strategy for the calibration of systematic errors has been developed. The approach is to use land acquisitions to calibrate the baselines components. The estimated precision in calibrating the normal (left panel) and parallel (right) baselines is presented in Figure 5.13. The onboard-metrology system is deemed not necessary because of the current coverage mask and the calibration strategy using land which provides a good baseline estimation.
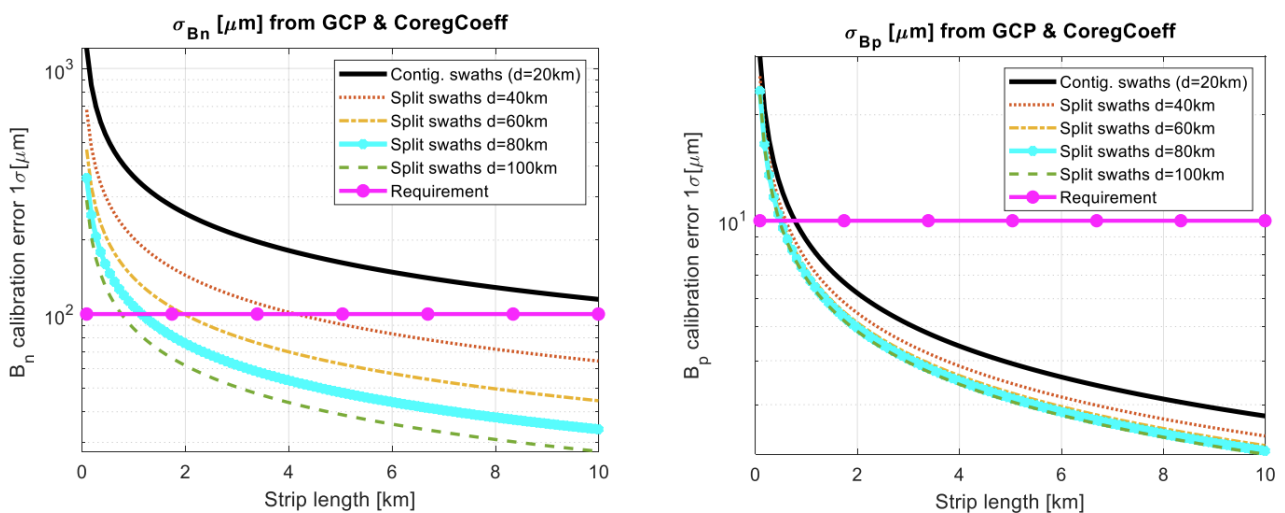
Figure 5.13: Achievable precision in the calibration of normal (left) and parallel (right) baselines. (Concept B)

5.3.4. Platform architecture

For both concepts the baseline approach has been to reuse existing hardware and platform designs starting with a heritage platform that is then adapted to fit the Seastar mission. The approach that has been followed by both consortia is to reuse the avionics from the current generation of EO platforms but mounted on a structure that is able to accommodate the large payload antenna.

For Concept A the Seastar platform avionics is based on the Airbus standard EO platform called AstroBus. The current baseline for the Seastar platform equipment is LSTM with some adaptations where necessary.

For Concept B, the platform avionics baseline is based on a new platform from the OHB EOS Standard platform with heritage from the C02M mission, again with adaptations as required to meet the Seastar requirements.

5.3.4.1. Structure and mechanisms

For both concepts the primary structure from heritage missions is not appropriate for Seastar and an alternative primary structure has been selected as a baseline that can then be adapted to meet the mission needs.

In terms of accommodation the two main drivers on the primary structure are the payload antenna and the accommodation of the propellant tanks required to perform the controlled re-entry at the End of Life (EOL). For these reasons the concept selected has a Central Thrust Tube (CTT) with the propellant tanks mounted in the centre of the CTT. The CTT is interfaced to the launch adaptor providing an efficient load bearing path from the launch adaptor up to the payload antenna mounted at the top of the structure.

The dimensions of the primary structure are driven by several competing requirements, the overall width of the satellite is driven by the size of the propellant tanks, the accommodation of the stowed payload antenna and the available volume within the Vega-C fairing. The key driver is the stowed antenna.

A secondary structure provides mounting locations for the platform avionics and payload electronics, with the payload electronics mounted close to the payload antenna to reduce losses. There is a significant amount of space to accommodate this equipment within the structure as the main drivers on the configuration are the payload antenna and the propellant tanks.

The Solar arrays in both concepts are also stowed for launch and require HDRMs, the mounting interface to the primary structure is with a simple hinge as no Solar Array Drive Mechanisms (SADM) are foreseen.

5.3.4.2. Thermal Control

The main function of the thermal control subsystem is to guarantee the operating and non-operating temperature ranges for all the satellite components. Seastar is flying in a dusk-dawn Sun Synchronous Orbit (SSO) orbit, with one side of the satellite always facing towards the sun which results in a stable thermal environment with a hot and cold side to the satellite.

The exception is during the eclipses season which lasts for 3 months, when the satellite will experience relatively brief eclipses that linearly increase over the eclipse season with a peak of 21 minutes for the 560 km orbit and 24 minutes for the 412 km orbit.

Both concepts include a completely passive thermal architecture relying on Multi-Layer Insulation (MLI), radiators, heatpipes, and heaters for temperature control.

Concept A also includes the option to make use of Phase Change Material (PCM) in order to reduce the overall mass of the required thermal hardware, this will be studied further in a future phase.

Thermal analysis related to the antenna is described in described in the respective SAR Instrument Concepts.

5.3.4.3. Power and Energy Storage

The baseline electrical power subsystem will use a standard approach for the generation, storage and management of the spacecraft's power. The solar array in concept A is based on a single deployable fixed solar array of 9.5 m^2, whereas the concept B has 2 deployable fixed solar arrays giving a combined area of 24 m^2. In both concepts the solar arrays are optimised in regard to the orbit and the attitude law to assure efficient power generation throughout the mission. The use of fixed solar arrays also removes any risk of coupling into the dynamic modes of the large antenna that could occur from the use of a rotating solar array, this simplifies the engineering challenges with managing antenna and the associated impact on other subsystems such as the AOCS.

For both solutions, minor adaptations are required for the Power Conditioning and Distribution Unit (PCDU) to in order to manage the high Power required for the payload.

Concept A has an unregulated main bus with a 22V to 37V, in comparison concept B also has a dual bus architecture with a primary bus 40V to 65.5V unregulated and a secondary regulated 28V bus.

5.3.4.4. Payload Data Handling and Transmission (PDHT)

In order to transfer the payload data volume to ground (see Table 5.7), both concepts foresee a single-channel X-band system with an isoflux antenna and TWTA power amplifier. The X-band solution requires more access time than available from using a single ground station, for both concepts two ground stations have been identified that provide complementary access time.

Concept A is capable of delivering up to 1300 Mbps to Svalbard and Inuvik. Concept B includes a Variable Coding and Modulation (VCM) scheme with a data-rate up to 1.210 Gbps (depending on the elevation angle) to Svalbard and Troll. The size of the mass memory required to meet the mission requirements is 4 Tbit for both Concept A and Concept B.

5.3.4.5. Telemetry, Tracking and Command (TT&C)

The TT&C subsystem for concept A uses an X-band transponder which combines the TT&C functionality and the PDHT into a single unit that provides the X-band communication capabilities between the satellite and ground stations. The X-band TT&C data rates are an uplink data rate of up to 64 kbit/s and a downlink data rate of 152 kbit/s for the low rate and 2667 kbit/s for the high rate. This unit is currently under development and will be available for the Seastar mission.

For concept B are more standard arrangement with a separate S-band unit that provides the S-Band communication capabilities between the satellite and the ground station. This is a flight proven heritage unit with an uplink data rate of up to 64 kbit/s and a downlink data rate of 2048 kbit/s.

The TT&C will be used to establish communications with the Seastar spacecraft in each mission phase, from Launch and Early Orbit Phase (LEOP) to End of Life (EOL).

5.3.4.6. Attitude and Orbit Control (AOCS)

The AOCS is a key sub-system for Seastar as the spacecraft pointing directly effects the payload performance that can be achieved, the effect is shown in the performance section, section 0.

In order to identify a suitable baseline solution for the AOCS sub-system a pointing budget has been constructed by both consortia to inform their respective AOCS trade-offs. All the contributors to the pointing budget have been identified and initial allocations made for each contributor. For both concepts the performance of the heritage baseline has been assessed against the pointing budget and adaptations have been made to the AOCS baseline to achieve the required performance.

For both concepts a standard 3-axis stabilised attitude control system has been defined with a continuous yaw steering attitude control law being envisaged for the Seastar satellite, using a standard actuator and sensor suite including, reactions wheels, magnetorquer rods, magnetometer, sun sensors (Coarse Earth & Sun Sensor for concept A), GNSS receiver, star trackers and Gyroscopes.

The mission instrument performance requirements lead to a particularly challenging pointing needs and, in that sense, both concepts have addressed this in more detail.

For Concept A, the allocation has been done for Relative Knowledge Error (RKE) while for Concept B an allocation has been made for a Relative Performance Error (RPE).

In both cases, this led to the need of a mid-to-high performance Gyroscope, coupled with a high precision star tracker, ensuring that over the full swath the relative error is kept well within the allocation. According to the preliminary analysis, the usage of a mid-to-high performance Gyroscope allows the existence of a margin versus the instrument performance requirement, leaving an opportunity that deeper analysis in the next phases might prove sufficient the usage of only a medium performance Gyroscope.

5.3.4.7. Propulsion

A conventional monopropellant hydrazine system is proposed for both Concept A and B, with a pressurised tank of 331 l (Concept A) and 2 tanks both with a capacity of 198 l (Concept B). Concept A includes 8x 20 N thrusters and a one-shot pressurisation system to ensure a suitable inlet pressure for the final re-entry manoeuvre. Concept B includes 8x 20N Orbit Control System (OCS) thrusters for orbit control as well as an additional 8x 1N Reaction Control System (RCS) thrusters for attitude control.

5.3.5. Satellite configuration and budgets

The satellite physical configurations are shown in Figure 5.14 for Concept A and Figure 5.15 for Concept B. Both concepts have a similar configuration with a central thrust tube housing the propellant tanks and using the 1194 mm launch adaptor ring. The main antenna is stowed on the +/-Y facets of the spacecraft and it is the main driver for the spacecraft volume and the amount of clearance with the fairing.

The central thrust tube extends along the full height in concept A providing a large internal volume for placement of the platform and payload hardware, the lower section being kept exclusively for payload hardware in order to minimise cable lengths and the associated losses.

For concept B, in order to increase the height of the spacecraft for safe stowage of the antenna, the grey cylinder (red arrow) has been included in the design. This gives a mass efficient increase in the height without a large mass penalty as would occur if the structure was simply extended.
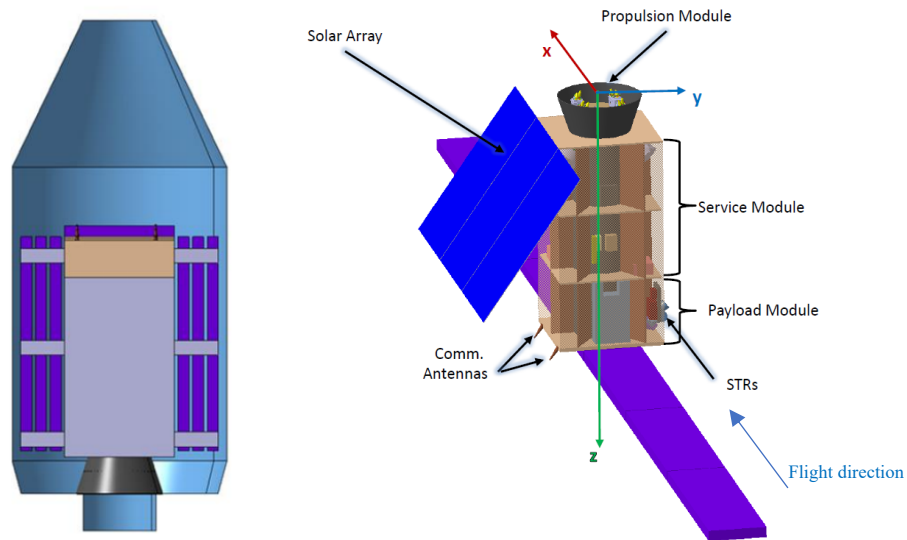
Figure 5.14: Seastar satellite stowed inside the fairing and deployed. (Concept A)
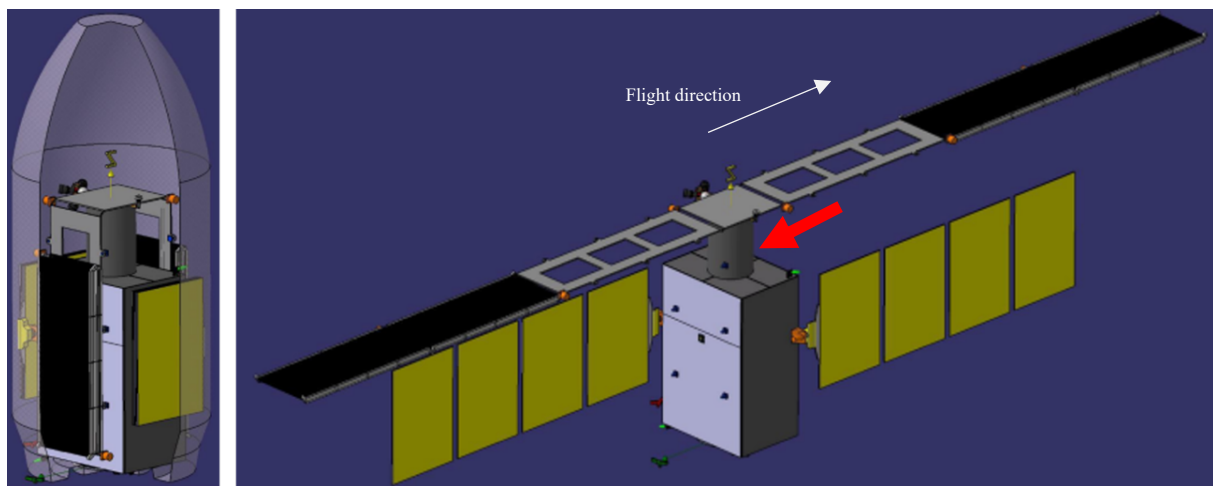
Figure 5.15: Seastar satellite stowed inside the fairing and deployed. (Concept B)

5.3.5.1. Mass budget and Volume margin

The mass budget shown in Table 5.3 highlights a number of key points of both concepts. The limiting factor for concept A is the launch mass with a current margin of 2.6% on top of the 20 % system margin.

Concept B has a 5.6% margin on top of the 20% system margin, however the main limiting factor is not the launch mass but the volume within the Vega-C fairing. The volume of concept B is driven by the size of the propellant tanks and the stowed volume of the antenna that leaves very little margin or scope to increase the propellant that can be carried, which limits the operational lifetime in line with MR-OBS-09.

The margin between the satellite and the dynamic envelope of the fairing is shown in Figure 5.16 for both concepts. The current margin for concept A is 57 mm and concept B the margin is 37 mm.

Table 5.3: Satellite mass budget

Element	Mass (Kg) – A (560 km)	Mass (Kg) – B (412 km)
Platform	956	815.8
Payload - Antenna + Front End	483	640.4
Payload – Back End	189	62.6
Payload Total	672	702.7
Dry Total	1628	1518.5
Dry including (20%) system margin	1954	1822.2
Propellant (in line with proposed concept lifetime)	275	367.2
Total satellite	2229	2189.4
Launch Vehicle Adaptor	95	95
Total Launch Mass	2324	2284.4
Launcher capabilities to target orbit	2385	2420
Additional margin with respect to launch capabilities (%)	2.6	5.6
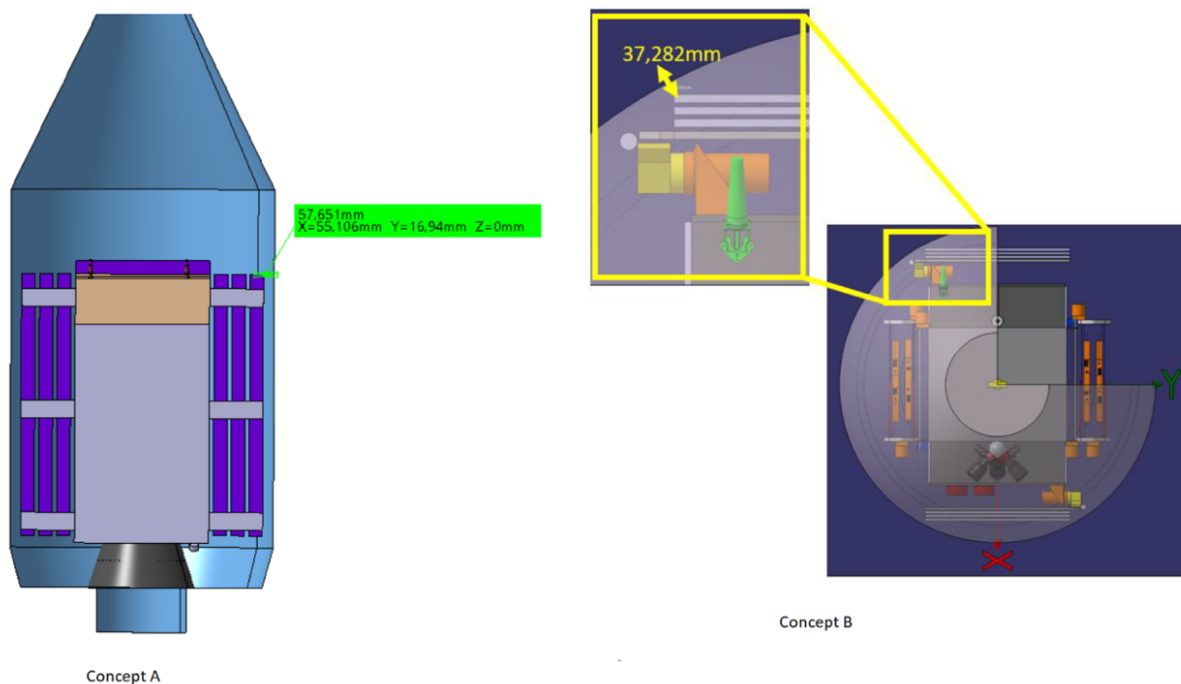
Concept A

Concept B

Figure 5.16: Volume margin to the Vega-C fairing for both concepts

5.3.5.2. Power budget

A summary of the power budget is shown in Table 5.4 for the peak power during an observation with all margins included. The main power requirement for Seastar is as expected dominated by the SAR payload, the power required by the platform being approximately 10% of the total for concept A. The platform power for concept B is slightly higher at 16% of the total. The payload power for concept B is slightly higher than for concept A. The high power requirements for both concepts are key drivers for the sizing of the required solar array area and PCDU design.

Table 5.4: Satellite power consumption budget

Element	Power (W) - A	Power (W) - B
Platform	326	584
Payload	2269	2402
Total including system margins	3114	3652

5.3.5.3. Delta-v and propellant budget

The delta-v and propellant budgets are shown in Table 5.5 highlighting the key difference between the 2 selected orbits and the corresponding impact on the required propellant. The lower orbit of concept B benefits from a lower delta-v required for de-orbit and from the higher launch capability of the Vega-C but this is somewhat offset by the higher station keeping delta-v of 207 m/s compared to the 43.73 m/s for concept A. The available tankage is 331 litres and 396 litres for concept A and B respectively, comparable to the total propellant requirement of 276 litres and 368 litres.

Table 5.5: Satellite delta-V and propellant budget

Mission Phase	Delta-V (m/s) - A 7.5 years	Propellant (kg) - A 7.5 years	Delta-V (m/s) - B 3.5 years	Propellant (kg) - B 3.5 years
Launcher Injection Error	33.04	34.2	24.81	28.18
Station Keeping	43.73	50.7	207.12	223.63
Collision Avoidance	0.31	0.3	0.04	0.05
Controlled re-entry	193.23	182.8	131.48	115.37
Residuals	-	7.5	-	
Total	270.31	275.5	363.45	367.23

5.4. System performance

To link the design to achievable performance, detailed error trees, analysis performance tools and error budgets have been developed. In this section, the performance evaluation against the main performance requirements is reported for both concepts. Because the fore and aft measurement are identical but mirrored in the positive-negative along-track direction, the fore and aft performance are considered as a single "squinted" performance calculation.

Surface radial velocity standard deviation in squinted direction is achieved using along-track interferometry as requested by MR-MEA-01. Incidence angles selection is driven by the minimum

incidence angle with respect to nadir (20 degrees) and the required overlapping between the three looks (FORE, AFT and BROADSIDE). The reference NRCS for the Kp calculation is the mean value between the NRCS at 5 m/s upwind and the NRCS at 5 m/s cross wind as defined in the MR-MEA-09. A summary of the compliance status for the main instrument requirements is provided in Table 5.6.

Table 5.6: Summary of main requirement for both Concepts

Parameter	Concept A	Concept B
Frequency of Operation	13.5 GHz	13.5 GHz
Swath	>100 km	>100 km
Spatial resolution (range x azimuth)	6 x 26 m	20 x 18 m
Surface Radial Velocity Standard Deviation	< 7cm/s	< 7cm/s
Relative radiometric resolution (Kp)	< 1%	< 1%

Figure 5.17 and Figure 5.19 provide the performance for both Concepts for the squinted beams. The driving requirement is the surface radial velocity standard deviation where the compliance is shown for the 7cm/s (threshold) and the 5cm/s (goal) requirements. Both Concepts meet the threshold of 7cm/s. SNR is provided for information.

Due to the use of leaky-wave antenna technology to implement squinted beams, the pointing slightly changes with the operational bandwidth. This frequency dispersion has been considered for the instrument performance assessment together with other processing losses such as scalloping due to the ScanSAR acquisition operation.

Concept A, implementing SCORE, results in a continuous swath across-track while the electronic steering in elevation, implemented by Consortium B, results in 5 sub-swaths in order to cover the 100 km across-track swath required in Seastar MR-OBS-08.

The error contributors considered during Phase 0 are: interferometric phase errors (due to coherence loss because of limited SNR, limited quantization, co-registration or volume/temporal decorrelation, ambiguities), antenna vibration, internal calibration phase error, instrument electronic mis-pointing, platform pointing and position/velocity error, platform vibration, topography errors and baseline errors.

Systematic errors, which are not part of the L1b requirement for surface radial velocity standard deviation, have also been considered for the performance analysis and the design of a preliminary external calibration strategy using land data. Particular attention is drawn to the pointing errors budget. As described in section 5.3.4.6, the platform is equipped with Star trackers and Gyroscopes which, in conjunction with the other AOCS units, is able to provide the required knowledge of the pointing. This, together with the external calibration strategies described in 5.3.2 and 5.3.3, enable the achievement of the surface radial velocity standard deviation requirement. Thanks to this performance, there is no need for on-board metrology system.

Figure 5.18 and Figure 5.20 provide the performance for both Concepts with respect to the broadside beam. The performance and plotted together with the required SNR related to the specify Kp value. Both consortia meet the threshold for the Kp in the broadside beam. The spatial resolution of L1B images will serve to identify and remove contaminations from unwanted targets and artefacts (e.g., ships, wind turbines, sand banks...) in the higher-resolution products prior to inversion to 1 km products at Level 2 and to enable the retrieval of wave spectra using the broadside or squinted beam.
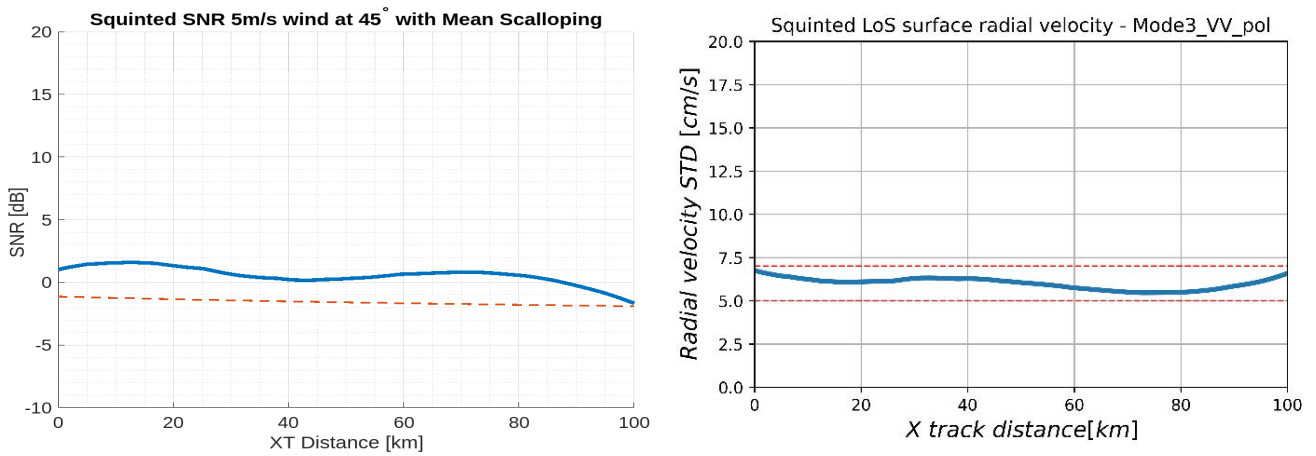
Figure 5.17: Seastar Squinted beam performance: SNR together with the Kp requirement (left) and Radial Velocity Standard Deviations with the 7cm/s and 5cm/s reference line (right) (Concept A)
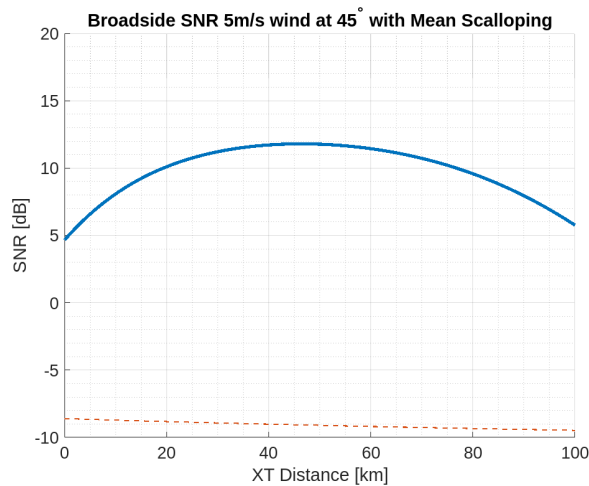
Figure 5.18: Seastar Broadside beam SNR performance (blue) and Seastar SNR requirement -equivalent to Kp for 5 km cell- (red) - Concept A
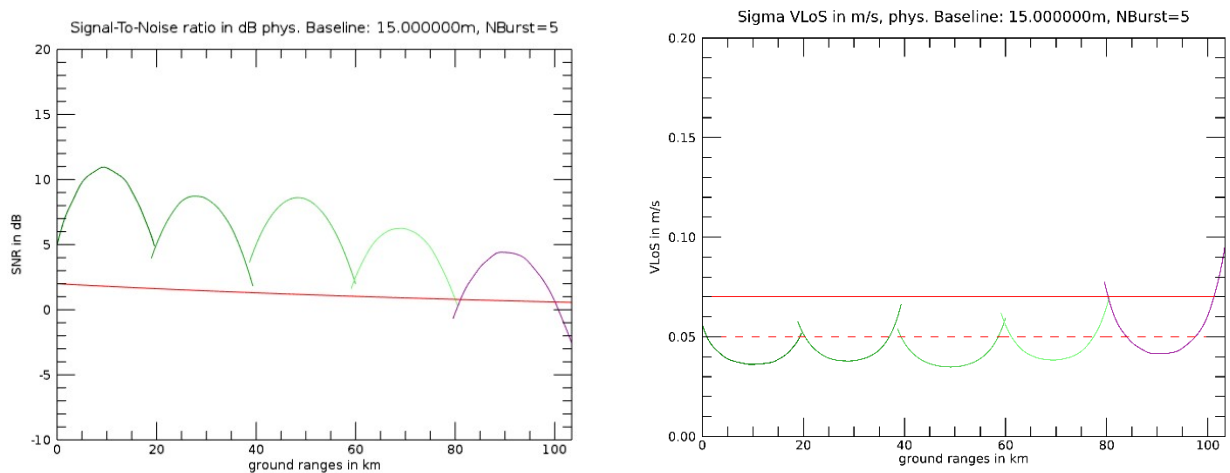
Figure 5.19: Seastar Squinted beam performance: SNR (left) and Radial Velocity Standard Deviations (right) (Concept B)
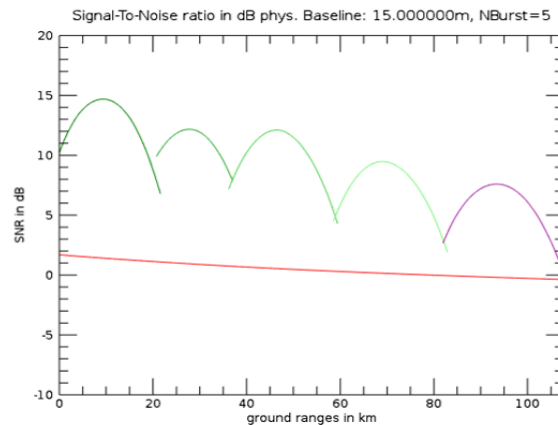
Figure 5.20: Seastar Broadside beam SNR performance (5 sub-swaths) and Seastar SNR requirement -equivalent to Kp for 1 km cell- (red) - Concept B

Fine spatial resolution will positively translate in higher number of pixels to be used when applying multi-look. However, too small pixels can also translate in registration errors. It is worth to mention that current spatial resolution in MR-MEA-07is defined for point target. The effective spatial azimuth resolution over the ocean, may be affected by the loss of coherence due to surface motion. The estimated point target spatial resolution meets the required one of 20 x 30 m (range x azimuth) for both Concepts.

Current instrument performance has been calculated considering a continuous operation, meaning that the instrument is continuously switching between the different look directions, resulting in long scenes. However, instrument performance can be improved by continuously operating in one look direction (e.g., FORE) until the BROADSIDE beam reaches the already observed areas by the FORE beam and the BROADSIDE beam is then operated. This acquisition strategy results in lower scalloping losses and improved performance. The operation in this mode brings some limitations in terms of scene length, distance between scenes and, potentially, may affect the coverage. The instrument acquisition strategy can be modified in orbit with the possibility to perform enhanced observations in specific areas of interest at the expenses of potential coverage gaps. This will be further optimised in next study phases.

5.5. Ground Segment and Operations

A typical Earth Explorer Ground Segment (G/S) uses generic components configured or adapted to each mission. Following this approach, the Seastar G/S consists of two main components, the Flight Operations Segment (FOS) and the Payload Data Ground Segment (PDGS). The FOS includes the S-band (concept B) or X-band (concept A) Telemetry Tracking and Command (TT&C) ground stations and the Flight Operations Control Centre (FOCC) in ESOC.

The function of the PDGS is to receive the science data from the satellite via dedicated ground stations, the application of the processing algorithms and the delivery of data products to the users.

5.5.1. FOS

The FOS is responsible for the spacecraft operations control and monitoring during all mission phases. Operations control and monitoring activities include housekeeping telemetry, performance monitoring, telecommanding of all activities, orbit control, constellation monitoring and control, reaction to space debris conjunction warnings, on board software maintenance and mission planning. The Seastar FOS is based on existing ESA hardware and software, no major changes foreseen given the operational approach of Seastar.

5.5.2. PDGS

Seastar will use the generic, but configurable, PDGS components developed for previous Earth Explorers. Thus, a standardised PDGS provides all necessary functions, including payload data acquisition and ingestion for downlink of science data telemetry, processing and reprocessing, archiving, user services and dissemination, mission planning, calibration and validation, and instrument performance and monitoring.

5.5.3. Data Downlink Strategy

Table 5.7 shows the data volumes produced by the payload over one orbit, for both concepts. The downlink strategy for both concepts is largely identical with the use of an X-band Tx and two ground stations in order to retrieve all of the payload data, note that there is no timeliness requirement for the Seastar payload data. For concept A, the combination of Svalbard and Inuvik has been considered. For concept B, Svalbard and Troll have been considered.

Table 5.7: SAR Payload Data Volume

Concept A			Concept B		
Data Rate (Mbps)	Operation/orbit (mins)	Data vol/orbit (Tbit)	Data Rate (Mbps)	Operation/orbit (mins)	Data vol/orbit (Tbit)
510	Ave: 15.9, Peak: 32.5	Ave: 0.487, Peak: 0.995	403.73	Ave: 15.2, Peak: 27.8	Ave: 0.368, Peak: 0.673

5.5.4. Mission Timeline and Compliance with Debris Policy

The baseline for both concepts is direct injection by the Vega-C launcher into their desired orbit, for Concept A this is the 560 km orbit and for Concept B this is the 412 km one. For both concepts a typical period of 6 months has been assumed for LEOP and commissioning, that is deemed sufficient to complete all of the activities in order to be ready to use the SAR payload during the scientific phase.

Both concepts achieve the minimum operational lifetime of 3 years with concept A able to extend the mission lifetime to 7 years. The lifetime for concept B is limited by the amount of propellant that can be carried as the delta-v requirements for station keeping in the 412 km orbit makes up more than 50% of the budget. In comparison the delta-v requirement for station keeping for concept A is only 15% of the total budget. During the scientific phase, the baseline scenario is to operate in the slow drifting orbit (~91 or ~271 day) for the full minimum lifetime of 3 years. Although not part of the baseline mission, space segment allows for the operational orbit to be swapped between the ~91 and the ~271 day repeat, and also an exact repeat orbit with minimum impact on delta-V and mission lifetime.

Both concepts have baselined a controlled re-entry for the End of Life (EOL) phase of the mission, as an uncontrolled re-entry is considered highly likely to exceed the casualty risk threshold. For the controlled re-entry, the satellite will firstly be lowered by 20 km where the orbit will be circularised. The perigee will then be progressively lowered down by subsequent manoeuvres to 250 km ready for the final manoeuvre at which point the perigee will be lowered down to 50 km. This final manoeuvre is planned in order to assure that the re-entry trajectory is over the South Pacific.

Both satellite concepts are based on the product lines developed for Sentinel Expansion missions, which adhere to the space debris mitigation requirements concerning health monitoring and passivation.

6. DATA PRODUCTS AND USAGE

6.1. Data Products

6.1.1. Seastar Level 2 Primary Products

The geophysical variables in the Seastar Level-2 primary products are the Total Surface Current Vectors (TSCV), Ocean Surface Vector Winds (OSVW), Higher Order Derivatives (HOD) and the Directional Ocean Wave Spectrum (DOWS). Table 6.1 provides a concise summary of the main products to be delivered by the Seastar PDGS.

Both TSCV and OSVW are provided at the critical resolution of 1 km or finer over a swath of 100km or more. 'Total' Surface Current Vectors signifies all surface velocities that contribute to horizontal water mass transport (e.g., tides, inertial oscillations, Stokes drift, wind…) after correcting for Doppler wind-wave bias (Martin *et al.*, 2016). Unlike altimetry, tidal currents are sensed directly, so there are no special constraints regarding orbital sampling of tides. Because the relation between microwave scattering and ocean winds is multifaceted, OSVW are typically obtained with a Geophysical Model Function (GMF) derived empirically from large matchups of scatterometer data with buoy and Numerical weather prediction (NWP) model 10-m height stress-equivalent winds (de Kloe *et al.*, 2017). The OSVW GMF is one of the components of the Seastar Level 2 inversion baseline algorithm adopted to retrieve TSCV and OSVW simultaneously (Section 7.1; Martin *et al.*, 2018; Martin *et al.*, 2023).

The Higher Order Derivatives Products (HODP) are two-dimensional fields of TSCV and OSVW higher derivatives like gradients, vorticity, divergence and strain, provided on the same geocoded swath as TSCV and OSVW. The scientific interest in resolving the fine details of 2D current and wind vector fields and their higher order derivatives calls for high accuracy at 1 km resolution that should be no worse than 0.1 m/s for TSCV and 1 m/s wind vector accuracy across the swath. As demonstrated in Chapter 7 (Figure 7.7), the ability to recover high-derivative information with 2D TSCV fields is jeopardised if the spatial resolution or the measurement uncertainty do not satisfy these requirements, leading to unusable maps of divergence and vorticity where scientific information has been lost. These requirements are also fully aligned with the needs identified by WMO (WMO, 2018).

The Directional Ocean Wave Spectrum (DOWS) products are obtained from broadside beam data using high SRL algorithms developed for side-looking SAR missions (Engen & Johnsen, 1995; Collard *et al.*, 2005). DOWS also includes integral directional wave properties like Significant Wave Height (SWH), Zero-crossing Period (T0) or Dominant Wave Direction (DWD) derived from the moments of the wave spectrum and from the SAR images directly using Machine Learning methods (Quach *et al.*, 2020; Pleskachevsky *et al.*, 2022).

6.1.2. Seastar Level 2 Secondary Products

Seastar Secondary Products relate to experimental products for sea ice and coastal applications. Sea Ice Drift Vectors (SIDV) will provide instantaneous sea ice drift vector components in two line-of-sights with high accuracy, extending and advancing existing capability with Sentinel-1 Doppler Centroid Anomaly or Tandem-X interferometry (Dammann *et al.*, 2019; Wang *et al.*, 2023). Full Directional Wave Spectra (FDWS) are experimental products to better resolve short ocean waves based on exploiting the Seastar data in three azimuth lines-of-sight, building on capabilities being developed for Harmony but with greater azimuth diversity (Kleinherenbrink *et al.*, 2021). And lastly, Estuarine River Flow (ERF) products will seek to estimate water velocities over large estuaries. As secondary mission objectives, SIDV, FDWS and ERF are not mission drivers.

Product Level			Description
L0			Decompressed, reconstructed, unprocessed Instrument Source Packets (ISPs) after restoration of the chronological data sequence for the instrument with all supplementary information to be used in subsequent processing (e.g., orbital data, health, time conversion, etc.) appended, after removal of all communication artefacts (e.g., synchronisation frames, communications headers, duplicated data, compression coding...). Level 0 data are time-tagged. The precision and accuracy of the time-tag shall be such that the measurement data can be geo-located to an accuracy compatible with the mission requirements.
L1A			Single look complex (SLC) images for the master and slave antennas for both fore and aft squinted beams, as well as the boresight beam in the instrument native resolution. Each image pixel is represented by a complex (I and Q) value and therefore contains both amplitude and phase information. The processing for all SLC products results in a single look in each dimension using the full available signal bandwidth in both range and azimuth. The data is radiometrically calibrated and synchronisation errors have been corrected.
L1B			Co-registered SLC images for fore, aft, (master/slave) and broadside beams at the instrument native resolution.
			Intermediate products for fore, aft (master and slave images) and broadside beams, including Normalised Radar Cross Section (NRCS) and coherence.
			Complex interferograms for fore and aft beams at instrument native resolution.
L1C			Calibrated radial surface velocity images resulting from the combination of fore and aft beams, after data driven calibration of systematic errors, including Thermoelastic Distortions, platform attitude and interferometric baseline errors, for both fore and aft beams. Residual uncertainties are provided in the product.
L2	Primary	TSCV	Total Surface Current Vectors provided in geolocated pixels at 1km x 1km resolution
		OSCW	Ocean Surface Vector Winds provided in geolocated pixels at 1km x 1km resolution
		HODP	Higher Order Derivative Products (gradients, vorticity, strain, divergence) on the same grid and swath as TSCV and OSVW
		DOWS	Directional Ocean Wave Spectrum products, including integral directional wave properties (e.g., SWH)
	Secondary	SIDV	Sea Ice Drift Vectors in the Marginal Ice Zone in geolocated pixels at 1km x 1km resolution
		FDWS	Full Directional Wave Spectra including shorter ocean waves in three-look directions
		ERF	Estuarine River Flow in geolocated pixels at 1km x 1km resolution

6.2. Data Processing

The diagram in Figure 6.1 illustrates the various data processing and calibration steps required by the mission up to L2.
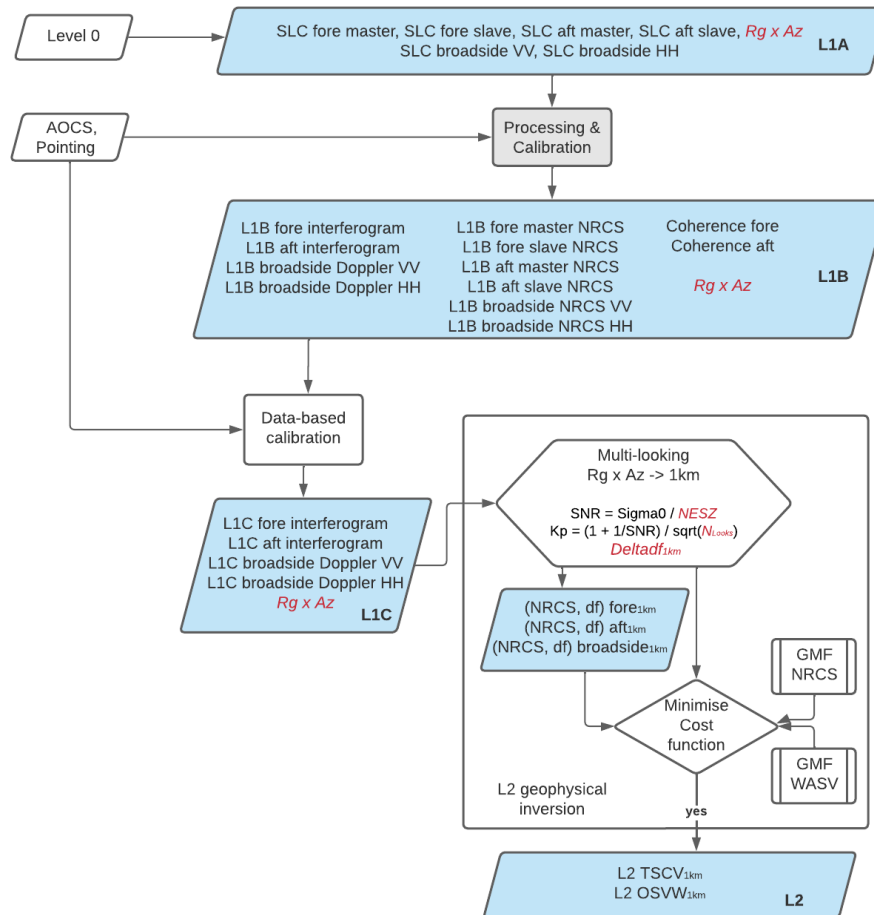
Figure 6.1: Data processing and calibration steps flow to be implemented in the Seastar PDGS up to L2. Blue boxes show the different level products. Text in red italics indicate system parameters that drive performance of L2 primary products.

- L0 processing is responsible for the processing of the instrument packets, e.g., sorting out the transmit or receive events, identification of corrupted echoes, and extraction of the different polarisations.

- L1A processing involves SAR processing and radiometric calibration, based on onboard platform measurements, to mitigate signatures and errors in L1 measurements linked to system and platform navigation and fluctuations (e.g., power, navigation, attitude, pointing). System calibration relies on standard practice for SAR and SARIn systems and is part of the work in the Seastar Phase 0/A System studies.

- L1b processing entails phase synchronisation and co-registration of the interferometric pairs, i.e., the fore and aft master and slave images, the computation of Normalised Radar Cross Section (NRCS) images, coherence, and interferograms geocoded to a reference Earth Ellipsoid, such as WGS84, or over a reference DEM.

- An additional data-based vicarious calibration after L1B to remove residual biases in the interferograms along the orbit, based on interferometric phase measurements over land. Data driven calibration methods have been demonstrated in recent studies (e.g., Want et al., 2021; Martin *et al.*, 2022). The rationale behind the data-driven calibration method for Seastar relies on using land imaged in the SAR scenes as static targets on land from which systematic errors around the orbit, linked to platform attitude errors, antenna thermoelastic distortions and interferometric baseline error can be estimated and removed from radial surface velocity data.

- The L2 processing entails the inversion approach used as baseline for Seastar, consisting of simultaneous retrieval of TSCV and OSVW (Martin *et al.*, 2018; Martin *et al.*, 2023). The inversion uses least-square fit to minimise a cost function that combines up to 8 L1C inputs to solve for 4 unknowns (TSCVx,y, OSVWx,y). Simultaneous inversion makes it possible to account for the coupling between the wind and current vectors at the surface (relative wind) and to spread uncertainties consistently according to the cost function's strongest dependencies (particularly wind direction). Further details of the retrieval approach are provided in Section 7.1.

6.3. Data exploitation and user communities

Seastar L2 products are expected to be a real breakthrough for a wide range of stakeholders with interest in the coastal, shelf and marginal ice zone domains. Better understanding of fast-evolving ocean surface dynamic properties and submesoscales are of global interest. A non-exhaustive list of stakeholders includes:

1. Weather Forecasting Agencies: Meteorological agencies can utilise Seastar's high-resolution current, wind and wave data to verify and improve weather, ocean and coupled forecasting models (Section 2.3.3, Section 2.3.4), especially regarding improved representation of fast-evolving fine-scale events at air/sea, land/sea and ice/sea boundaries, e.g., tip jets, katabatic winds, rip currents, dangerous sea states.

2. Climate Research Institutions: Seastar provides crucial information to analyse exchanges and transports at the global ocean boundaries and reduce uncertainties about the contributions of coastal, shelf and marginal ice zones to global carbon, heat and water budgets. Climate research institutions can leverage Seastar data to develop improved parameterisations of small-scale ocean surface dynamics like submesoscales that influence marine ecosystems, transports and exchanges globally (Section 2.2.2, Section 2.3.1, Section 2.4), to improve projections of overall climate dynamics and the evolution of the Earth coupled climate system.

3. Oceanographic Research Institutes: Oceanographic research institutes can use Seastar data to complement their observations and refine their theoretical understanding of ocean surface processes, particularly at boundaries and remote locations where data are scarce (Section 0, Section 2.4.2. Specifically, the Seastar information will contribute to better understanding of the ocean's interactions with other parts of the Earth System, and of the impacts of future climate change on marine ecosystems, and transports of heat, water, nutrients, and pollutants.

4. Offshore wind farm and tidal energy farm developers and operators can utilise Seastar observations of currents, winds and waves to optimize the siting, design, operation and maintenance of renewable energy projects, and to anticipate and limit the environmental impacts of these installations (Section 2.2.4). Accurate information on surface currents, vector winds and directional waves will aid the industry to maximise green energy production in safe and environmentally sustainable ways, ultimately contributing to viable expansion of clean renewable energy production.

5. Marine and Coastal Management Authorities: Government agencies responsible for marine and coastal management can utilise the Seastar data to assess the impacts of surface currents, winds and waves on coastal erosion, pollutant dispersion, and the movement of marine species. This information supports coastal zone planning, pollution management, and conservation efforts (Section 2.2.1, Section 2.2.3, Section 2.2.5).

6. Fisheries and Aquaculture Industries: The fishing and aquaculture sectors can benefit from Seastar's accurate high-resolution data to improve fishing strategies, locate and manage fish stocks, assess water quality and pollution risks and optimize aquaculture operations (Section 2.2.1, Section 2.3.3, Section 2.4.1). This information aids in resource management and sustainable practices.

7. Maritime Industry: Shipping companies, port authorities, and maritime navigational services can exploit the Seastar data to enhance maritime safety and efficiency. Accurate surface current, vector wind and directional wave information helps optimize vessel routing close to land and ice, reduce fuel consumption, minimize transit times and identify unchartered underwater hazards and dangerous seas to limit maritime incidents (Section 2.2.3, Section 2.2.5.1).

8. Search and Rescue Organisations: Search and rescue organisations can use the data to assist in locating and tracking individuals or objects lost at sea. The knowledge of surface currents, vector winds and directional waves can aid in understanding drift patterns, improving search and rescue operations, and enhancing response times. Seastar data are particularly relevant in coastal regions where 80% of all Search and Rescue operations take place and where data are generally unavailable (Section 2.3.4).

7. MISSION PERFORMANCE

7.1. Retrieval approach: simultaneous inversion

Seastar proposes to deliver observations with a spatial resolution and accuracy unmatched by any other mission. The Seastar L2 retrieval algorithm follows the work of Martin *et al.* (2018) and retrieves TSCV and OSVW simultaneously, without the need for ancillary information. Seastar's objective is to provide products derived solely from its own measurements, without dependence on external input. Outside a few instrumented sites, there are generally no reliable wind or current data at the fine spatial resolution targeted by Seastar. Input from high-resolution ocean models or atmospheric models could be used, but suffers from a lack of validation, particularly in coastal, shelf seas and marginal ice zones.

The *simultaneous* retrieval of TSCV and OSVW is considered essential because the two variables are tightly intertwined for an accurate estimation of these two variables. The action of the atmosphere on the moving ocean is known as the relative wind, and accounts for the relative directions of the wind vector and the current vector. Winds and currents are closely coupled at the ocean surface and it is commonplace to observe that ocean surface roughness flattens (resp. raises) when currents flow with (resp. against) the wind.

The ocean roughness response to the relative wind will affect Bragg-type microwave scattering at moderate incidence angles. This phenomenon manifests frequently in SAR images as enhanced or reduced backscatter e.g., in regions of strong alternating tidal currents. Simultaneous retrieval of TSCV and OSVW makes it possible to account for this effect by correctly representing the response of the microwave signals to the ocean roughness generated by the relative wind.

7.1.1. Cost function minimisation

The Seastar L2 retrieval is an extension of the Bayesian method used by L2 algorithms in scatterometry to retrieve OSVW (Stoffelen, 1998; Stoffelen & Portabella, 2006; OSI SAF, 2022). A cost function is defined and subsequently minimised using least-square fitting to determine the wind and current vectors that are most consistent with the radar observables (i.e., Normalised Radar Cross Section and Radial Surface Velocity in different azimuth directions). The inversion seeks to find four unknowns, namely two components of the TSCV and two components of the OSVW. If more than four observations with Gaussian noise are available, these four unknowns can be estimated using a quadratic estimator as the objective function to determine TSCV and OSVW.

Based on Bayes' probability theorem, and following Martin *et al.* (2018) and Stoffelen & Portabella (2006), the Maximum Likelihood Estimator is represented by the cost function, J, defined as:

$$J(\overrightarrow{u_{10}}, \vec{c}) = \frac{1}{2N} \sum_{i=1}^{N} \left(\frac{KuMod(\overrightarrow{u_{10}} - \vec{c}) - \sigma_{obs,i}^0}{\Delta\sigma_i^0} \right)^2 \qquad (7.1)$$
$$+ \frac{1}{2N} \sum_{i=1}^{N} \left(\frac{KuDop(\overrightarrow{u_{10}} - \vec{c}) + c_{//i} - RSV_{obs,i}}{\Delta RSV_i} \right)^2$$

With

i	the azimuth beam number (1 = fore squint; 2 = broadside; 3 = aft squint)	1, 2 or 3
$\sigma_{obs,i}^0$	the observed Normalised Radar Cross Section (NRCS) in azimuth beam i	NRCS (linear)

$RSV_{obs,i}$	the observed Radial Surface Velocity (RSV) in azimuth beam i	m/s
KuMod	the predicted NRCS, $\sigma^0_{GMF,i}$ in azimuth beam i obtained with the chosen Geophysical Model Function for NRCS at Ku-band.	NRCS (linear)
KuDop	the predicted RSV, $RSV_{GMF,i}$ in azimuth beam i obtained with the chosen Geophysical Model Function for Wind-wave Artefact Surface Velocity at Ku-band.	m/s
$\overrightarrow{u_{10}}$	the stress-equivalent Ocean Surface Vector Wind (OSVW) at 10 metres height	m/s
$\vec{c}$	the Total Surface Current Vector (TSCV)	m/s
$\Delta\sigma^0_i$	the uncertainty (standard deviation) on the observed NRCS, $\sigma^0_{obs,i}$ in azimuth i	linear
ΔRSV_i	the uncertainty (standard deviation) on the observed RSV, $RSV_{obs,i}$ in azimuth i	Hz
$c_{//i}$	the component of the TSCV in azimuth beam i	m/s
N	the number of azimuth beam directions	1, 2 or 3

The cost function, J, is a unit-less function of 4 unknown variables ($\overrightarrow{u_{10}}$, $\vec{c}$). Minimising the cost function finds the values of TSCV ($\vec{c}$) and OSVW ($\overrightarrow{u_{10}}$) that best reduce the quadratic differences between the observables ($\sigma^0_{obs,i}$, $RSV_{obs,i}$) and the predicted quantities ($\sigma^0_{GMF,i}$, $RSV_{GMF,i}$). Here, the cost function is shown for a single polarisation configuration, a more general expression is given in Martin *et al.* (2023).

As in scatterometry, the minimisation returns up to four solutions (Portabella, 2002), leading to a well-known ambiguity problem. An ambiguity selection procedure is applied to find the most likely solution.

In scatterometry, calibration (e.g., Rivas *et al.*, 2017), QC for rain (Verhoef & Stoffelen, 2021), GMF (Wang *et al.*, 2017) and ambiguity removal (Vogelzang & Stoffelen, 2018) are operationally implemented in intercalibrated processing chains for C-band static fan-beam scatterometers, a rotating C- and Ku-band fan beam scatterometer (Li *et al.*, 2023) and for rotating pencil-beam scatterometers (Wang *et al.*, 2021) and well validated (Vogelzang & Stoffelen, 2022). These retrievals are hence of the highest scientific readiness level (SRL).

7.1.2. Wind-wave Artefact Surface Velocity

The Wind-wave Artefact Surface Velocity (WASV; Martin *et al.*, 2016; Martin *et al.*, 2022), also known as the Wave Doppler velocity, is a large velocity signal caused by the motion of the surface scatterers responsible for the microwave backscatter. The WASV needs to be removed from observed radial surface velocities in each azimuth direction before TSCV and OSVW can be correctly retrieved. The WASV is an artefact of the scattering and has no associated displacement of water mass (i.e., current).

The simultaneous inversion baselined for Seastar makes it possible to account directly for the Wind-wave Artefact Surface Velocity (also known as Wave Doppler velocity) through the choice of Geophysical Model Function (GMF) used to describe the dependence of the RSVs on incidence angle, azimuth and environmental conditions. There are currently three main GMFs published in the literature, including Mouche et al. (2012), Yurovsky et al. (2019) and Moiseev (2021). The three models offer different levels of complexity and skill.

At this stage, Yurovsky et al. (2019) is chosen as baseline for Seastar. Yurovsky et al. (2019) demonstrated the applicability and validity of its Ka-band formulation to a wide range of radar

observations at frequencies from C-band to Ka-band. Moreover, a recent study by Martin et al. (2022) confirmed that Yurovsky et al. (2019) was the most appropriate GMF to retrieve unbiased radial ocean surface currents from Sentinel-1 C-band Doppler data against HF radar data in the German Bight.

7.2. Performance estimation with simulated data

7.2.1. Performance estimation with simulated data

The numerical framework set up and used in Phase 0 to estimate the Seastar mission performance at Phase 0 is illustrated in Figure 7.1. The simulation tools make it possible to determine the Seastar performance at Level 2 for different instrument configurations, geometries, L1 performance specifications and ocean conditions. Ocean input conditions are represented by the Total Surface Current Vectors and Ocean Surface Vector Winds (Figure 7.1. top blue box). The red boxes indicate input parameters linked to system parameters, geometry and instrument configurations.
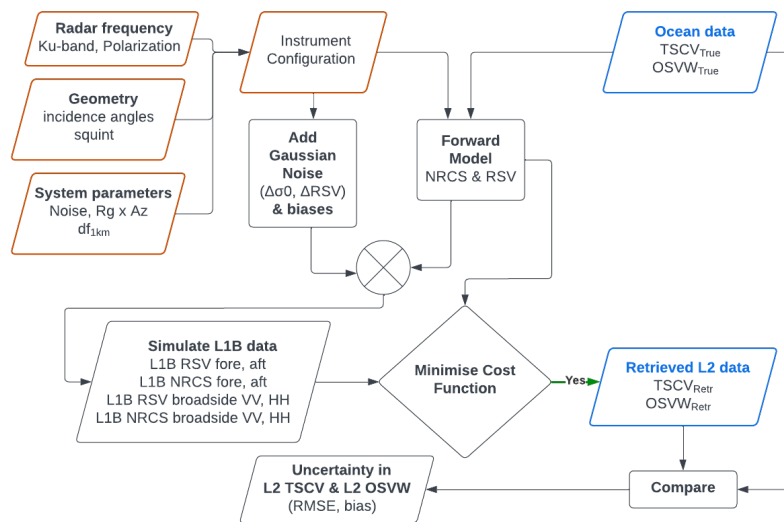
Figure 7.1: Numerical framework used to evaluate Seastar mission performance in Phase 0.

The ocean TSCV and OSVW serve as input to the Forward Models of the Normalised Radar Cross Section (NRCS) and Radial Surface Velocity (RSV) to produce noise-free observables. White Gaussian noise with standard deviations $\Delta\sigma^0$ and ΔRSV is added to NRCS and RSV respectively to produce simulated L1B observables (σ^0 and RSV) for each azimuth look direction and/or polarisation specified by the instrument configuration. The simulated L1B data are input to the cost function minimisation module which finds the best TSCV and OSVW solutions (Section 7.1). Mission performance is evaluated by comparing retrieved L2 TSCV and OSVW (Figure 7.1. bottom blue box) with 'true' TSCV and OSVW input (Figure 7.1. top blue box). The performance estimation was applied to simulated input data representing idealised current and wind fields (Section 7.2.1.1) and realistic TSCV and OSVW input fields obtained from high-resolution ocean models (Section 7.2.1.2).

7.2.1.1. Performance with simulated data for idealised current and wind fields

An example of idealised current and wind input fields is shown in Figure 7.2 wind field (5 m/s, from 270 degrees). Here, performance is estimated for the following configuration and L1 specifications: Ku-band (13.5 GHz); Satellite heading 0° North; Across track distance calculated perpendicular to the track, with 0 km and 150 km corresponding to near and far range respectively; Broadside pointing perpendicular

to the track, i.e., 90° azimuth from North; Broadside incidence angles from 20.0° (0 km) to 33.4° (150 km); Ground squint angle from 52.2° (near range, 0 km) to 37.8° (far range , 150 km) leading to azimuth angles (from North) for the Fore look of 37.8° (0 km) and 52.2° (150 km) and for the Aft look of 142.2° (0 km) and 127.8° (150 km); Squinted beams line-of-sight incidence angles from 31.5° (0 km) to 40.0° (150 km); Squinted beams VV polarisation; Broadside beam single-polarisation (VV); Squinted beams L1 RSV Noise = 0.07 m/s; Broadside beam L1 RSV Noise = 0.4 m/s. Squinted beams NRCS Noise (Kp) = 3%. Broadside NRCS Noise (Kp) = 5%; No bias on RSV or NRCS.

The L2 errors with this setup are presented in Figure 7.3 as a function of range inside the swath. Figure 7.3 left panel shows the RMSE of TSCV velocity for different wind directions depicted by different colour lines. The instrument three-beam orientation relative to wind vectors is shown in the wind rose inset. The thick black line represents the mean TSCV velocity RMSE averaged over all wind directions. The dashed red line is the Seastar 0.1 m/s L2 TSCV uncertainty requirement. Results confirm that the mean RMSE for TSCV velocity (averaged over wind directions) is compliant with L2 requirement across the full swath for U10 = 5 m/s. Performance is degraded however in some wind directions (when squinted beams align with wind).
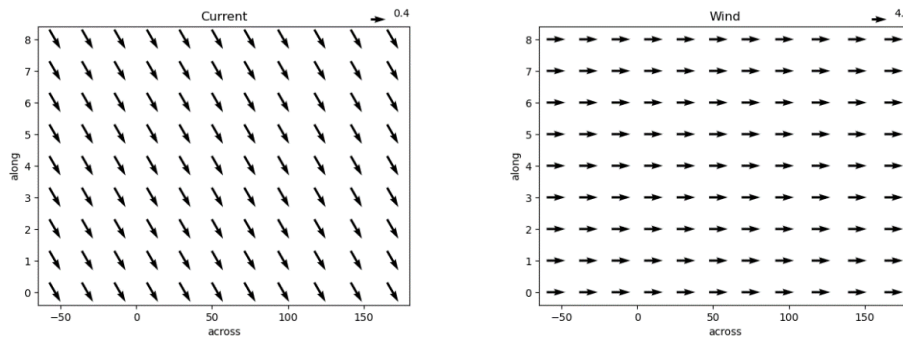
Figure 7.2: 2D TSCV and OSVW fields used as geophysical input. 'Across' represents the eleven 1km x 1km pixels subsampling the swath in range across-track; 'Along' represents the nine 1km x 1km pixels located along-track.
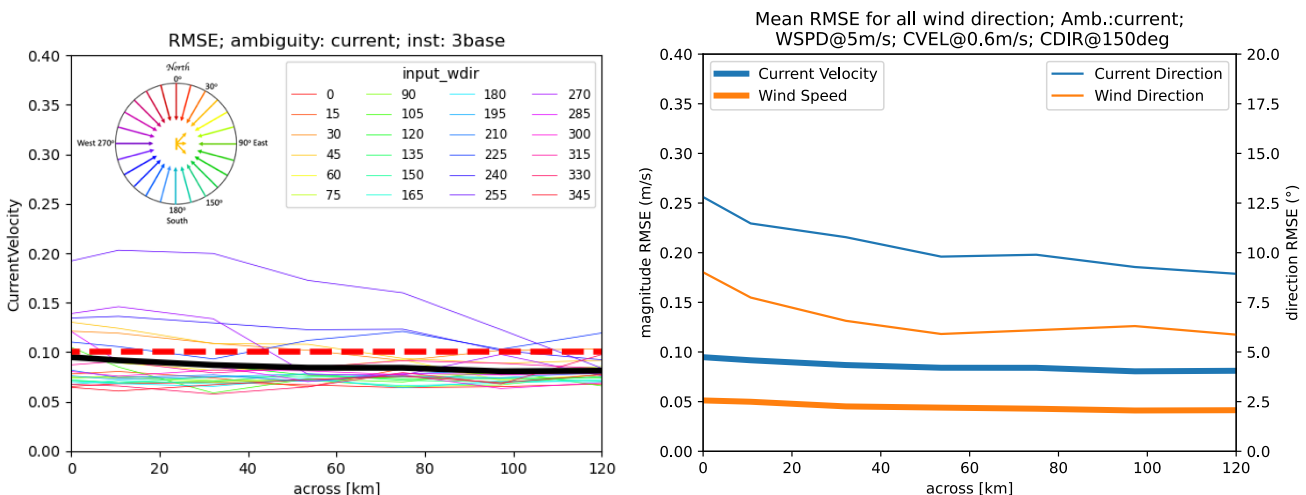
Figure 7.3: (Left) Seastar simulated performance for L2 TSCV at 1 km x 1km resolution shown as RMSE of TSCV velocity across the swath for all wind directions. The inset shows the Seastar three look directions relative to different wind vectors. The thick black line is the mean TSCV velocity RMSE averaged over all wind directions. The dotted red line indicates the L2 TSCV 0.1 m/s mission requirement. U10 = 5 m/s. L1 squinted RSV error is 0.07 m/s. (Right) Seastar simulated L2 performance for L2 TSCV and OSVW at 1 km x 1km resolution shown as the mean RMSE of TSCV and OSVW velocity and direction (averaged over all wind directions) across the swath. Blue thick (thin) lines represent current velocity (direction). Orange thick (thin) lines represent wind speed (direction). U10 = 5 m/s. L1 squinted RSV error is 0.07 m/s.

The right panel in Figure 7.3 shows the mean RMSE (averaged over all wind directions) for TSCV (velocity, direction) and OSVW (velocity, direction) as a function of range inside the swath. Thick lines refer to (left vertical axis) TSCV and OSVW velocities, thin lines refer to (right vertical axis) TSCV and OSVW directions. The thick blue line is the same data as the thick black line in the left panel. These results demonstrate that the L2 performance specified in the Seastar observational requirements for TSCV and OSVW can be met with the mission's threshold requirements on Level-1 radial velocities for both velocity and direction.

7.2.1.2. Performance with simulated realistic currents and winds in Ouessant

This first example uses TSCV and OSVW input from a high-resolution model over Ouessant, an island located a few kilometres west of Brittany (France; Figure 7.4). The area features strong tidal currents and current gradients through narrow gaps between islands and the mainland. This area was also observed during the OSCAR airborne campaign in Iroise Sea in May 2022 (Section 7.3).
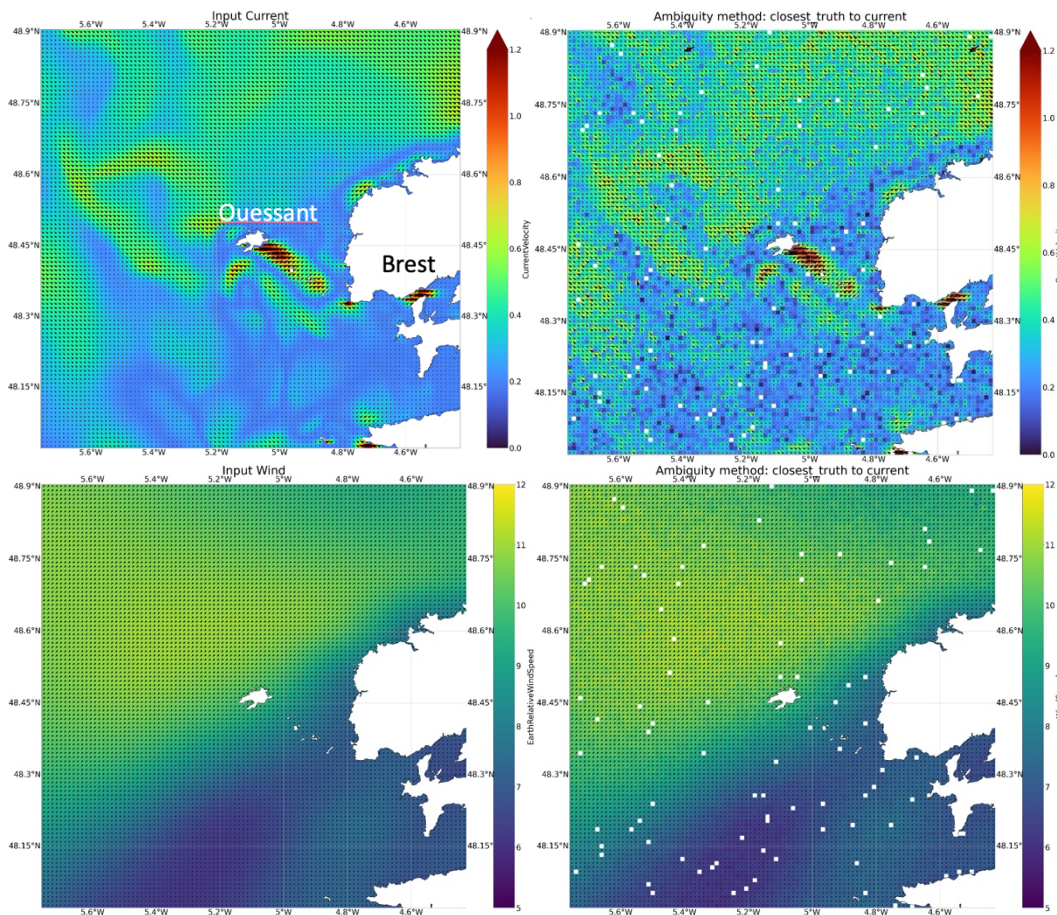
Figure 7.4: Seastar simulated L2 performance for realistic current and wind fields near Ouessant. (Left) Input TSCV and OSVW ("truth") from CROCO model on 1 km^2 grid. (Right) Retrieved TSCV and OSVW from Seastar simultaneous inversion. See text for instrument configuration and L1 specifications. [Credits: Noveltis, D. Andrievskaia, A.C. H. Martin]

The high-resolution TSCV and OSVW fields are from the CROCO model (Coastal and Regional Ocean Community model; https://www.croco-ocean.org) obtained via Ifremer. CROCO is an oceanic modelling system that aims to resolve very fine scales (especially in the coastal area) and their interactions with larger scales. The model provides hourly output on 1 km^2 grid cells. The hourly snapshot used here displays spatially variable TSCV (0.2 to 1.2 m/s, to North-East or North-West) and spatially

homogeneous OSVW, except for sharp south to north increase (~ 6m/s north-easterlies to 10 m/s north-easterlies). The 100x100 km^2 area shows the typical size of Seastar images.

The simulated L1 images of NRCS and Radial Surface Velocities were obtained for the fore, broadside and aft lines-of-sight (Figure 7.5) for the instrument configuration and specifications in Section 7.2.1.1. Bottom panels in Figure 7.4 show the retrieved L2 TSCV and OSVW obtained with the Seastar simultaneous inversion (Section 7.1.), revealing Seastar's extraordinary ability to recover the original TSCV and OSCV fields with great levels of detail and accuracy.
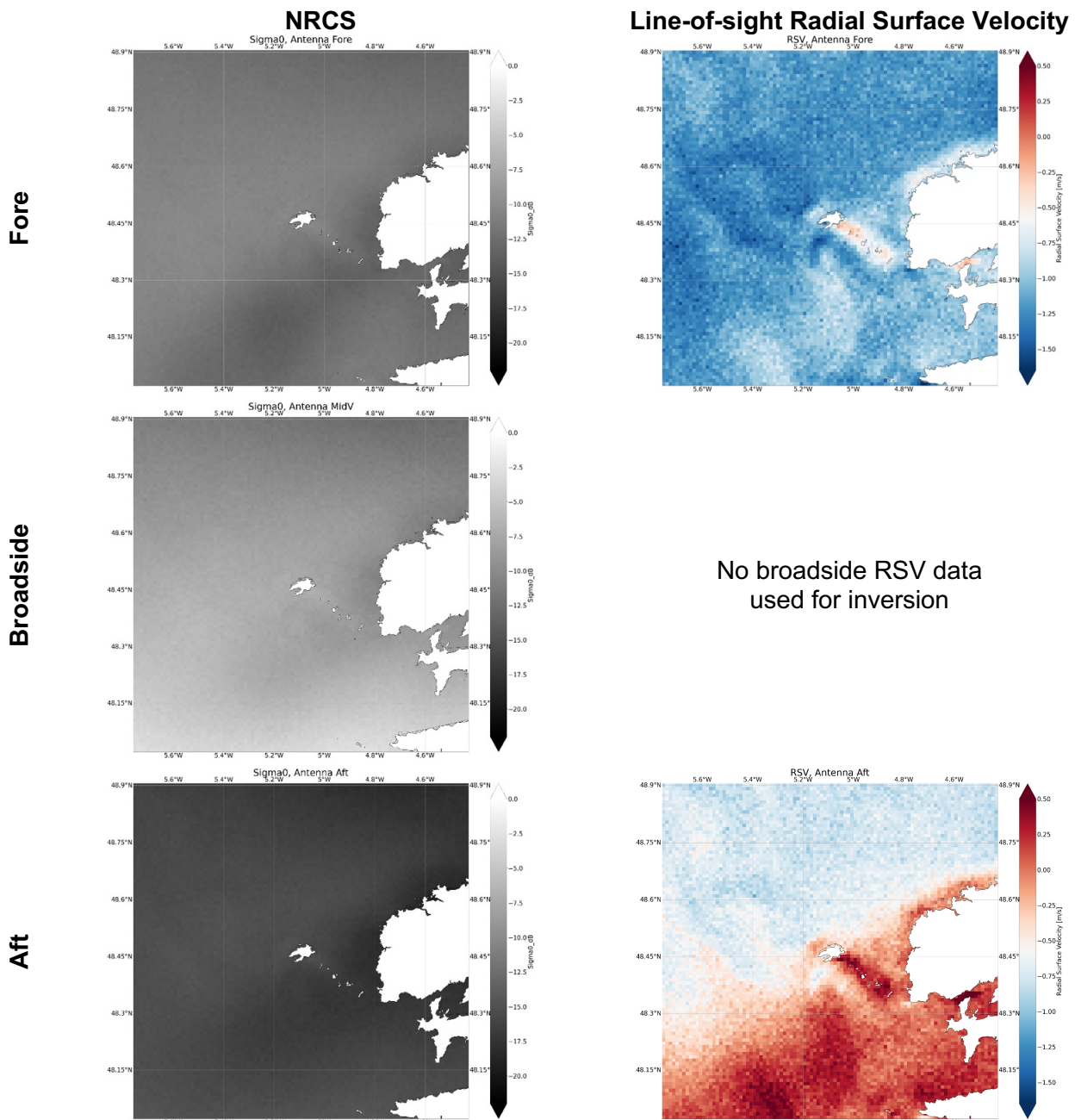
Figure 7.5: Seastar simulated L1 images for realistic currents and winds near Ouessant in (top) fore, (middle) broadside and (bottom) aft lines-of-sight (Left) Simulated L1 Normalised Radar Cross Section (Right) Simulated L1 Radial Surface Velocity. See text for instrument configuration and L1 specifications. [Credits: Noveltis, D. Andrievskaia, A.C. H. Martin]

7.2.1.3. Performance for simulated realistic currents and winds in California Current

The second example uses TSCV and OSVW input fields from a high-resolution coupled model over the California Coastal Current, an area famous for its coastal upwelling and rich sub-mesoscale dynamics. The model uses a 1 km grid spacing. As expected, TSCV (Figure 7.6, top left) reveals strong mesoscale and sub-mesoscale variability with current velocities from 0.0 to 1.0 m/s. The OSVW field is similarly dynamic, with winds from 7 to 15 m/s (not shown for brevity).

The top right panel in Figure 7.6 shows the TSCV velocity retrieved using an implementation of the Seastar simultaneous inversion algorithm on the OceanDataLab supercomputers, showing reconstructed TSCV velocity field with a 1 km^2 retrieval and ~0.1 m/s uncertainty. For comparison, the two bottom plots in Figure 7.6 show the reconstructed TSCV velocity for a 2 x 2 km^2 grid and 0.2 m/s uncertainty, and 5 x 5 km^2 and 0.5 m/s uncertainty; the former case corresponds to Harmony's L2 requirement when Sentinel-1 operates in IW mode and the latter to OdySea, (see Chapter 8). These results confirm that 1 km^2 spatial resolution and 0.1 m/s uncertainty on TSCV are absolute requisites to adequately observe the small scale highly dynamic processes targeted by the Seastar mission.
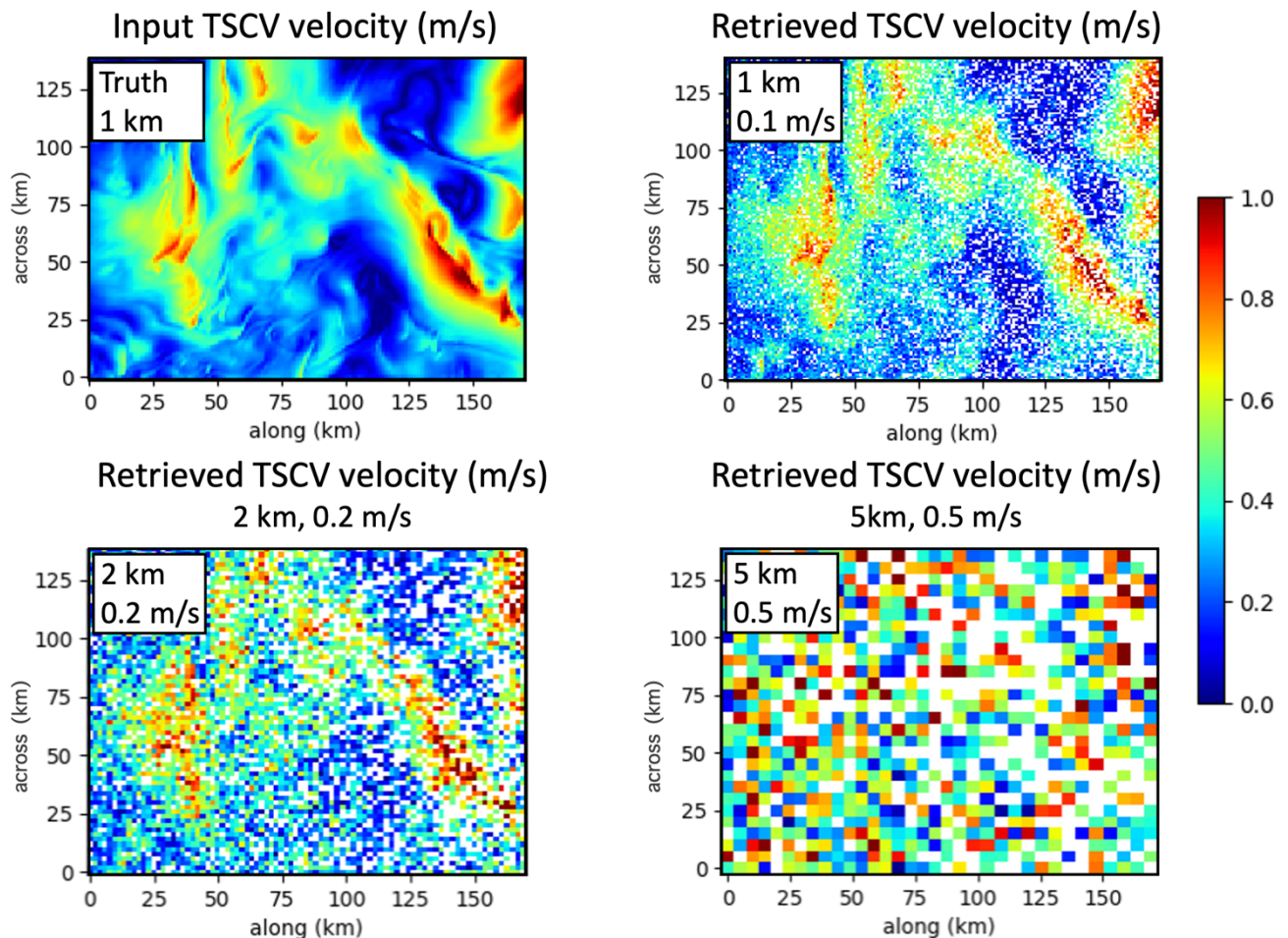
Figure 7.6: Simulated L2 TSCV performance for realistic current and wind fields in the California Coastal Current. (Top left) Input TSCV velocity ("truth") from the coupled model on 1 km^2 grid. (Top right) TSCV velocity retrieved with Seastar simultaneous inversion at 1 km^2 resolution and 0.1 m/s RMSE. (Bottom left) TSCV velocity for 2 x 2 km^2 resolution and 0.2 m/s RMSE. (Bottom right) TSCV velocity for 5 x 5 km^2 resolution and 0.5 m/s RMSE. See text for instrument configuration and L1 specifications. [Credits: Ocean Data Lab, L. Gaultier, F. Collard]

In Figure 7.7, we present further evidence of the importance of high resolution and low measurement uncertainty in TSCV, with reconstructed 2D divergence and vorticity fields obtained for different TSCV resolutions and uncertainties. It is shown clearly that the level of detail and fidelity to the truth (top row) quickly deteriorates as soon as resolution and uncertainties become larger than 1 km^2 and 0.1 m/s RMSE, consolidating further the strict requirements of the Seastar mission regarding L2 TSCV spatial resolution and uncertainty.
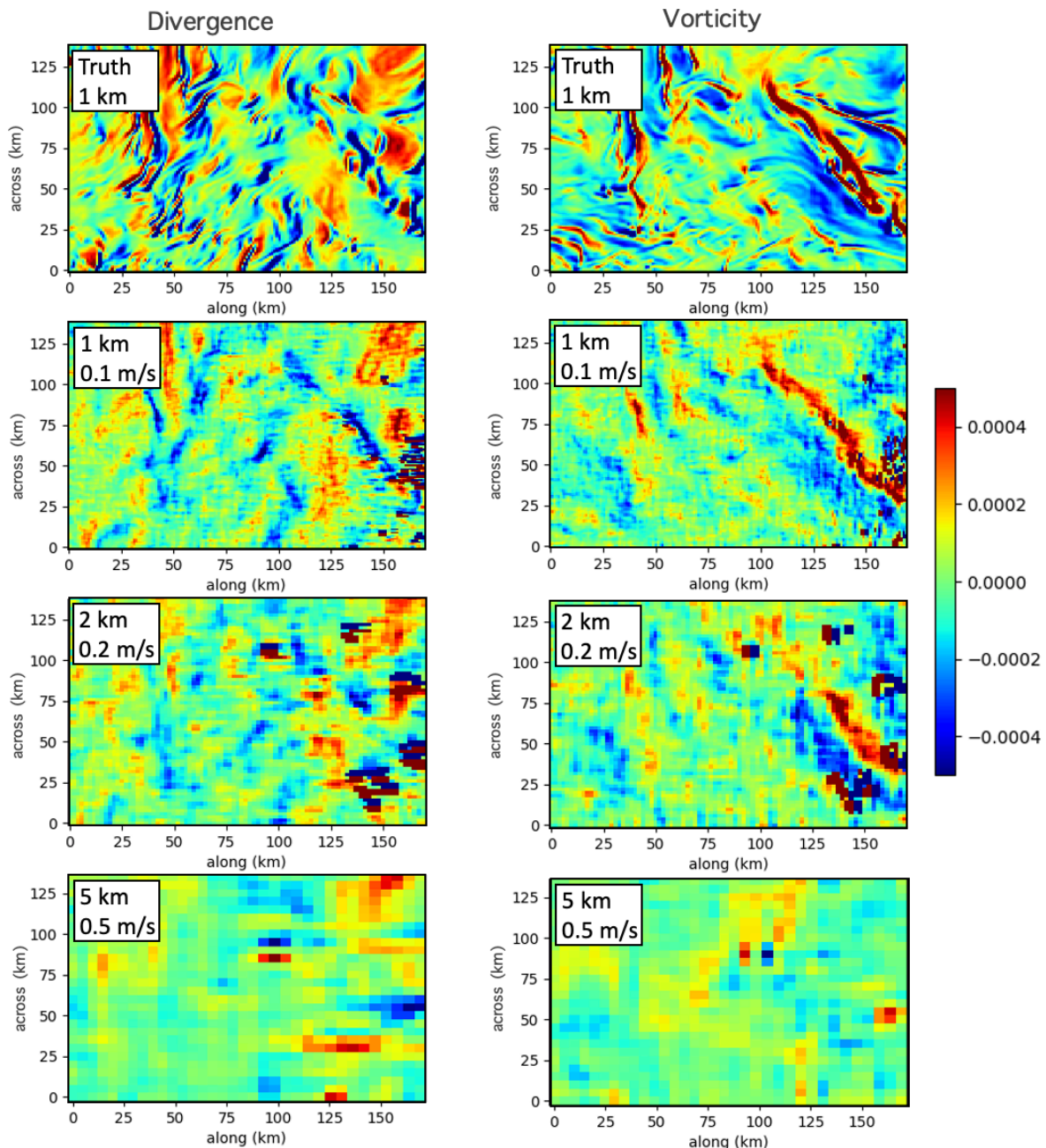
Figure 7.7: Simulated L2 performance for realistic current and wind fields in the California Coastal Current, showing 2D fields of divergence and vorticity calculated from: (top) Input TSCV velocity ("truth") from the coupled model on 1 km^2 grid. (Row 2) Retrieved Seastar TSCV at 1 km^2 resolution and 0.1 m/s RMSE. (Row 3) TSCV for 2 x 2 km^2 resolution and 0.2 m/s RMSE. (bottom) TSCV for 5 x 5 km^2 resolution and 0.5 m/s RMSE. See text for instrument configuration and L1 specifications. [Credits: Ocean Data Lab, L. Gaultier, F. Collard]

7.3. Performance Verification with Experimental Campaigns

7.3.1. Performance with OSCAR airborne campaign data in Iroise Sea

Following the Wavemill airborne proof-of-concept campaign (Section 0), a new airborne demonstrator known as OSCAR was developed for ESA to demonstrate squinted ATI with three-azimuth beams (Meta *et al.*, 2015; Gebert *et al.*, 2018; Trampuz *et al.*, 2018; Martin *et al.*, 2019). After several years delay (due to aircraft and radome procurement issues), OSCAR was finally flown in its first scientific campaign over the Iroise Sea, west of Brittany (France) in May 2022. The OSCAR airborne system has the same three-beam configuration as Seastar, with two pairs of interferometric antennas squinted 45 degrees forward and backward of broadside and a third beam pointing broadside.

The Iroise Sea campaign took place in the context of the ESA Seastarex activity. OSCAR flights took place between 17-26 May over two contrasting sites in the Iroise Sea (Figure 7.8) with strong tidal currents close to Ouessant island, and homogeneous currents and winds away from land over the Trefle mooring. Both sites provided opportunities for independent validation with ground-truth from HF radar, X-band radar or Acoustic Doppler Current Profiler (ADCP). Details of the subset of OSCAR flights shown here are given in Table 7.1. Results are shown first for the OSCAR flights on 22 May 2022 over homogeneous conditions at the Trefle mooring, and then for the flights over strong tidal currents near Ouessant on 17 May 2022.

Table 7.1: Details of Iroise Sea OSCAR flights presented in this report, showing also available ground-truth for different flights.

Date & time	Location	Expected ocean conditions			Ground-truth			Coincident satellite SAR
		Currents	Winds	Waves	X-band	HF radar	ADCP	NovaSAR-1
Tue 17 May 2022 09:30 UTC	Ouessant & La Jument lighthouse	0.5 m/s to NW	7 m/s from SE	Hs: 2.5 m	✅	❌	❌	✅
Sun 22 May 2022 06:20 UTC	Star flight pattern over Trefle mooring	0.6 m/s to N	5.7 m/s from NE	Hs: 1.1 m	❌	✅	✅	N/A

7.3.1.1. Results over homogeneous currents and winds at the Trefle mooring

Quantitative evaluation of TSCV and OSVW performance with OSCAR data was carried out over the Trefle mooring where homogeneous wind and current conditions were expected. Although OSCAR maps vectorial fields of TSCV and OSVW in each single-pass, the assessment considered all OSCAR tracks in the star pattern flight (Figure 7.8E) which made it possible to check the L1 measurements in different lines of-sights relative to current and wind vector fields.

TSCV and OSVW were retrieved at each pixel using simultaneous inversion (Section 7.1) applied to calibrated NRCS and Radial Surface Velocity data. This is the first time the simultaneous inversion was applied to real data and this represents a major step forward in terms of scientific maturity (SRL).

The TSCV and OSVW fields measured by OSCAR for tracks in the star pattern are shown side-by-side with output from state-of-the-art ocean and atmospheric models (Figure 7.9), demonstrating the excellent quality and consistency of TSCV and OSVW in both velocities and direction with expected conditions. The RMSE for TSCV and OSVW velocities and directions against moored ADCP ground-truth data (Table 7.2) confirms the exceptional quality of the OSCAR retrieved current and wind fields, with levels of uncertainty that are fully aligned with the scientific requirements of the Seastar mission.
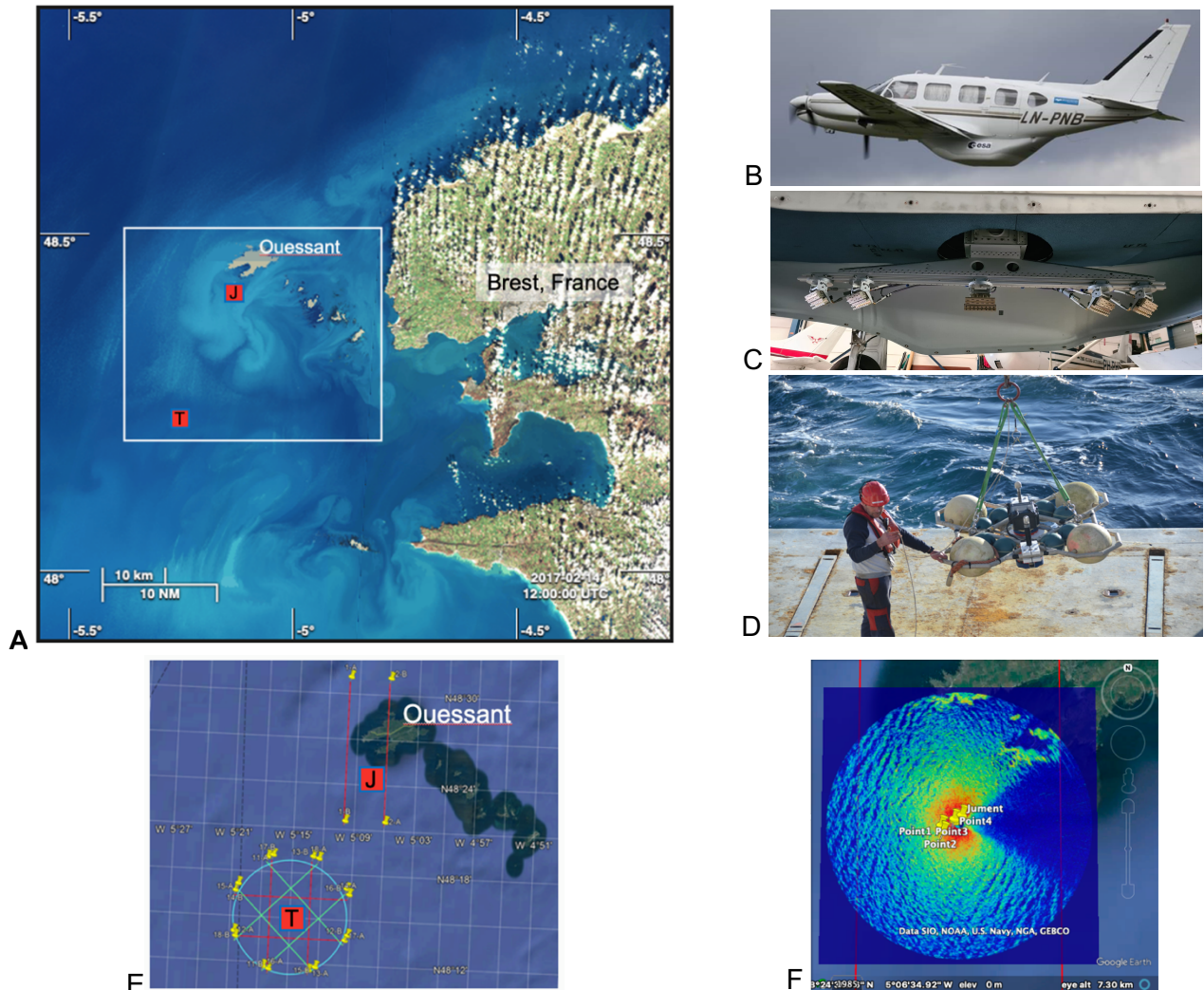
Figure 7.8: OSCAR airborne campaign in Iroise Sea on 17-26 May 2022. A) Sentinel-2 image of the campaign site west of Brittany, France. Red boxes marked 'J' and 'T' show the locations of the 'La Jument' lighthouse and the 'Trefle' mooring. B) The MetaSensing aircraft with OSCAR radome. C) The OSCAR instrument inside the radome. D) Deployment of the Trefle mooring to measure in situ ocean current profiles and directional wave spectra. E) OSCAR flight tracks over Ouessant and for the star pattern over Trefle. F) X-band radar image from 'La Jument' lighthouse to measure TSCV (Credits: National Oceanography Centre, D. McCann – MetaSensing, A. Meta – Ifremer, L. Marié – Hereon, R. Carrasco Alvarez).

Table 7.2: Performance of OSCAR TSCV and OSVW at 1km x 1km resolution against independent ground-truth data for the star pattern acquisitions at the Trefle mooring.

	TSCV velocity (m/s)	TSCV direction (degrees North)	OSVW velocity (m/s)	OSVW direction (degrees North)
OSCAR measured	0.64	14.4	5.54	49.1
Ground-truth ADCP	0.62	8.4	5.86	45.8
RMSE	**0.08**	**8.5**	**0.44**	**5.4**
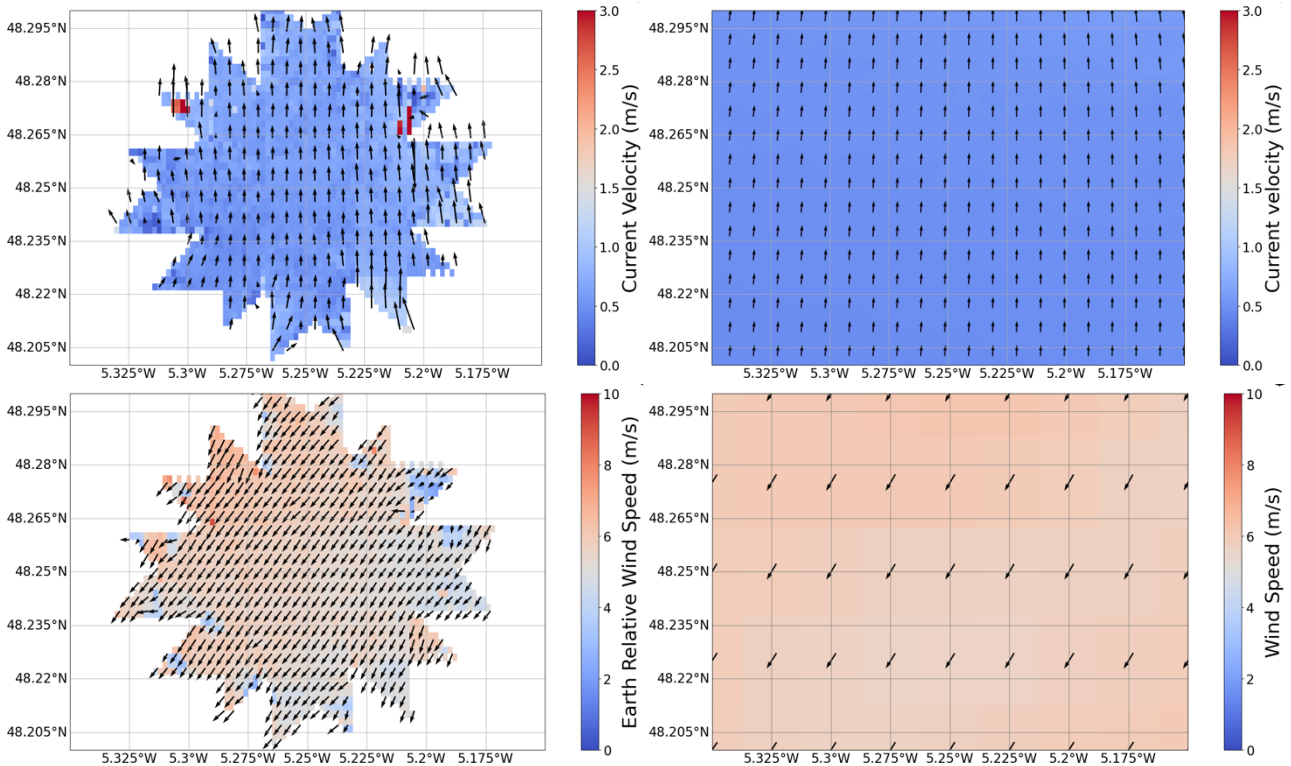
Figure 7.9: (top) Total Surface Current Vectors and (bottom) Ocean Surface Vector Winds during the star pattern flights over Trefle mooring on 22 May 2022. (Left) Measured by OSCAR at 200m resolution using simultaneous inversion (200m pixels, arrows subset to 400m). (Right) Predicted by MARS2D high-resolution ocean model (200m pixels, arrows subset to 400m) and AROME atmospheric model (0.025 degrees pixels and vectors, ~ 2km) (Credits: National Oceanography Centre, D. McCann – MetaSensing, A. Meta)

7.3.1.2. OSCAR results over strong tidal currents and current gradients in Ouessant

The TSCV and OSVW fields measured by OSCAR for a single track over Ouessant on 17 May 2022 are shown in Figure 7.10 (left), side-by-side with output from state-of-the-art high-resolution ocean and atmosphere models (Figure 7.10 right). Both datasets depict the intense tidal jets north and south of the island that are typical of the region. Once again, OSCAR data show excellent agreement in directions and magnitudes of both TSCV and OSVW with model data. Closer examination reveals differences at fine scales however, notably in the position of tidal jets and the small-scale variability of the wind field near headlands that is absent in the model.

That OSCAR correctly positions the tidal jet further north than seen in the model is confirmed by a NovaSAR-1 satellite NRCS image obtained within 1 hour of the OSCAR acquisition (Figure 7.11 left). The satellite NRCS, overlaid with OSCAR TSCV, reports strong backscatter modulation by current gradients where OSCAR measures strong tidal jets, further from land than predicted by the model.

In the right panel in Figure 7.11, independent TSCV measurements from the X-band radar on La Jument lighthouse serve to validate the current jet detected by OSCAR south of the island. The scatter plot in Figure 7.12 demonstrates excellent quantitative agreement between TSCV velocities measured by OSCAR and those from the X-band radar on La Jument lighthouse.
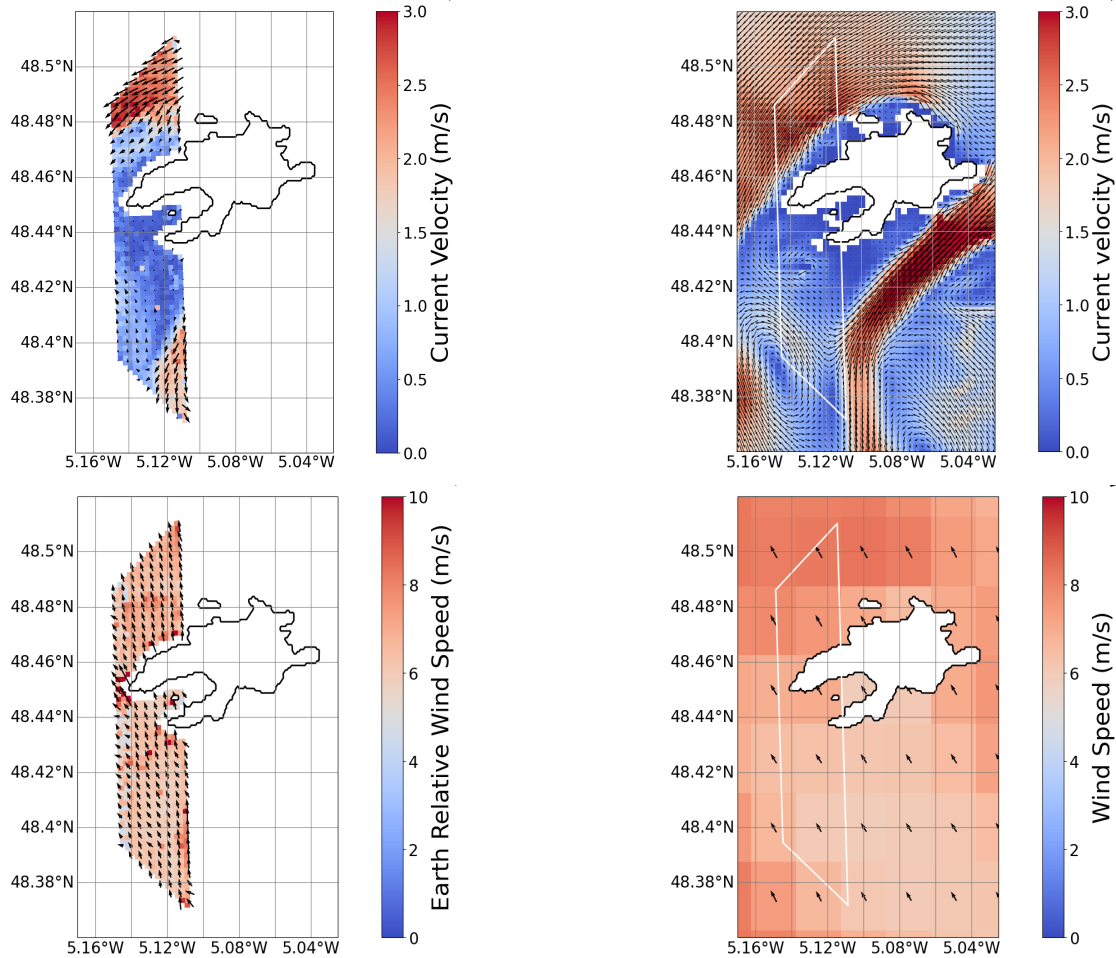
Figure 7.10: (top) Total Surface Current Vectors and (bottom) Ocean Surface Vector Winds over Ouessant on 17 May 2022. (Left) Measured by OSCAR at 200m resolution using simultaneous inversion (200m pixels, arrows subset to 400m). (Right) Predicted by MARS2D high-resolution ocean model (200m pixels, arrows subset to 400m) and AROME atmospheric model (0.025 degrees pixels and vectors, ~ 2km) (Credits: National Oceanography Centre, D. McCann – MetaSensing, A. Meta).
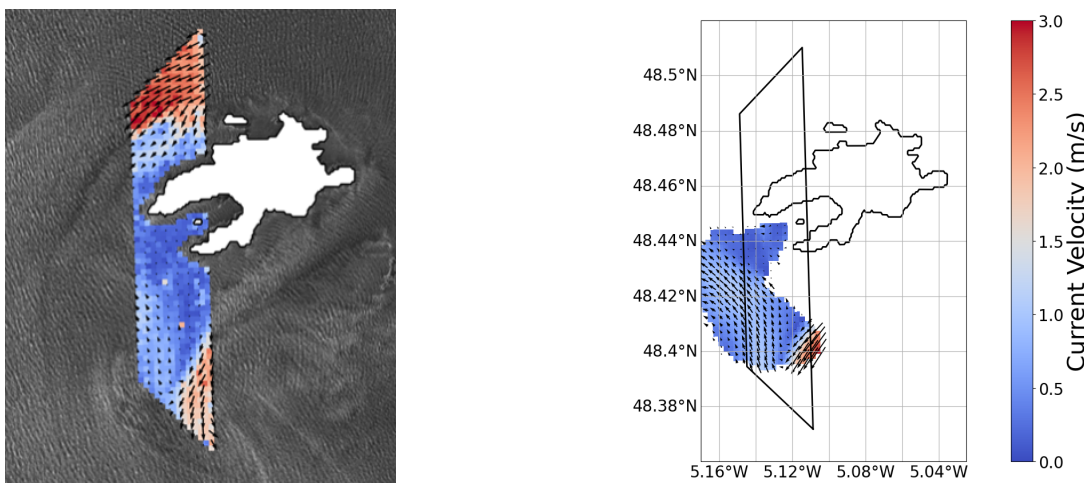
Figure 7.11: (Left) OSCAR Total Surface Current Vector field over Ouessant on 17 May 2022 at 09:30 UTC superimposed on NovaSAR-1 S-band SAR NRCS at 10:30 UTC. (Credits: National Oceanography Centre, D. McCann – SSTL and Airbus UK, Martin Cohen) (Right) Total Surface Current Vector field measured with X-band marine radar from La Jument Lighthouse (Credits: National Oceanography Centre, D. McCann – Hereon, R. Carrasco)
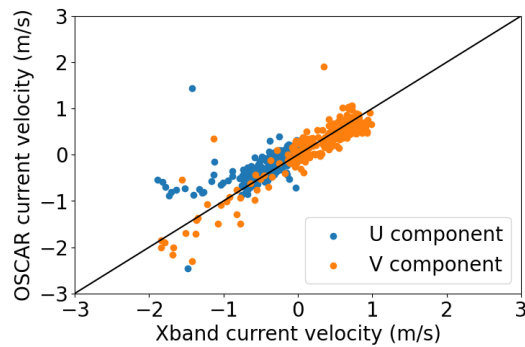
Figure 7.12: Comparison of OSCAR Total Surface Current Vector components (U = East; V = North) with coincident X-band marine radar data (Credits: National Oceanography Centre, D. McCann)

7.3.2. Performance with OSCAR airborne campaign data in the Western Mediterranean Sea collocated with SWOT 1-day repeat

A second airborne campaign was carried out with OSCAR during Phase 0, in May 2023 in the Western Mediterranean Sea. The opportunity arose for OSCAR to underfly SWOT along one of the satellite tracks north of Menorca during the 1-day repeat Cal/Val phase. The campaign also opened the possibility of benefiting from in situ oceanographic data acquired during the BioSWOT-Med ship campaign in the area (https://www.swot-adac.org/blogs/bioswot-med/).

Since only preliminary results are available from the OSCAR-Med campaign so far, we present those in Chapter 8 as an illustration of the vibrant International Context in which Seastar is being proposed.

7.4. Validation concept

The validation concept for Seastar uses principles similar to those used to validate OSCAR data in previous sections. In coastal regions, TSCV validation will use ground-truth from HF radar, X-band radar and ocean instruments (ADCP, drifters, autonomous vehicles) supported by data from high-resolution models and satellites. Validation in shelf seas and close to sea ice will be more challenging and will require in situ campaigns including dedicated drifter releases.

Independent validation of OSVW is more challenging, particularly at high-resolution. Wind measurements from buoy- or platform-based anemometers are the baseline, but more advanced remote sensing techniques like lidar profiling should also be considered to resolve 2D wind field variability that cannot be captured by point measurements. As for TSCV, high-resolution models and observations from other satellites are relevant to support evaluations. In particular, drawing from the virtual scatterometer constellation, OSVWs on scales down to 5 km are validated and expected to be available during the Seastar mission.

8. SYNERGIES AND INTERNATIONAL CONTEXT

Seastar has a minimum lifetime of 3 years with a goal of 7 years. The target launch window for EE11 is 2032/33.

Seastar is a self-contained single-satellite mission with no dependencies on other satellites. However, Seastar has strong scientific affinities with high-resolution measurements of sea surface temperature, ocean colour, sea surface height, sea state, winds and Doppler radial velocity.

8.1. Relation to existing and planned missions

8.1.1. Seastar and Copernicus programmes

As shown in Chapter 2, there are important synergies with the **Copernicus Sentinels**, particularly the optical and thermal imagers on Sentinel-3 (OLCI, SLSTR) and Sentinel-2 MSI and high-resolution altimeters on Sentinel-3 and Sentinel-6MF/Jason-CS (Figure 2.1, Figure 2.4, Figure 2.6). Seastar will support deeper interpretation of the water column properties observed by these sensors, providing large-sale fine-resolution information about ocean mixing, transport and air-sea interactions at small scales, to pin down more precisely the information they contain about fluxes and export of carbon, nutrients and other waterborne materials.

By the 2030s, the current generation of Copernicus Sentinels will be in Extended life but still be operational. The observing capability provided today by Copernicus Sentinels has assured continuity and will be enhanced through the Copernicus **Sentinel Next Generation (NG)** satellites currently under development for launch in the 2030-2040 timeframe (Figure 8.1).

It is anticipated that, with the advent of Copernicus NG missions in the 2030-40 timeframe, the availability of daily images at very-high-resolution of ocean colour, sea surface temperature, sea surface height, sea state and sea ice will be the norm, emphasising yet again, the urgent need for Seastar's high-temporal high-spatial imaging of total currents, winds and waves to complement and support the exploitation of observations from Copernicus NG sensors.
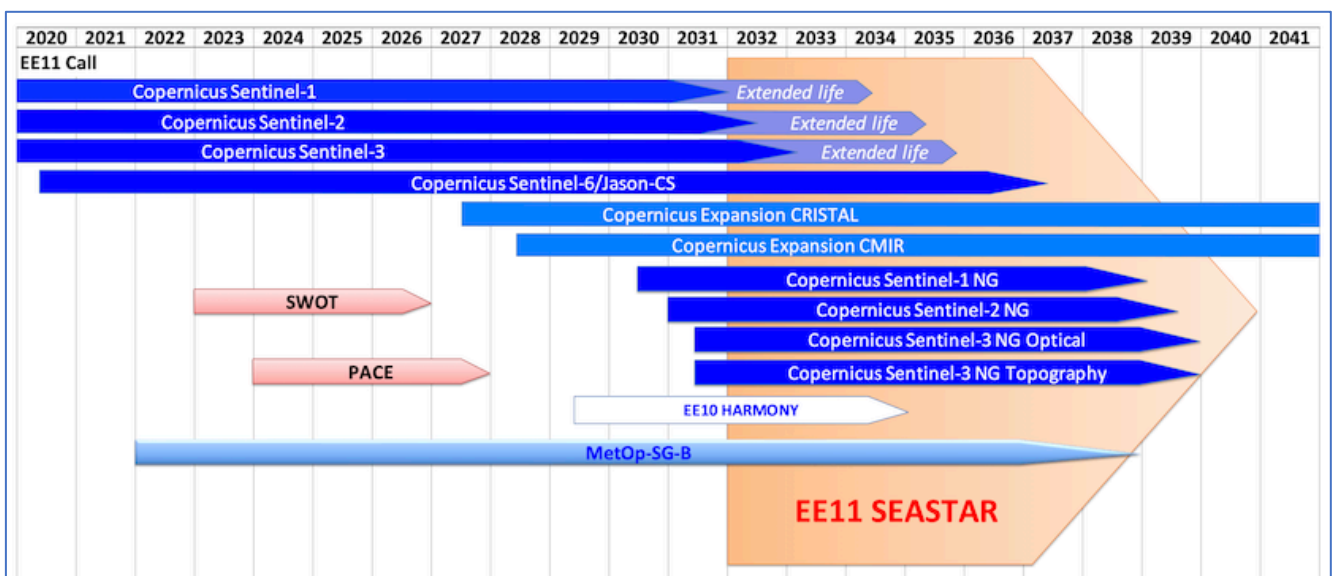

Figure 8.1: Seastar mission duration and relation to other missions.

In the same timeframe (2030s), Seastar would fly alongside the new generation of **Copernicus Sentinel Expansion Missions**, notably CRISTAL (Copernicus Polar Ice and Snow Topography Altimeter) and CIMR (Copernicus Imaging Microwave Radiometer), which would offer particularly valuable synergy with Seastar at high latitudes. With a launch planned in 2027, CRISTAL will measure sea ice thickness, ice sheet elevations and snow coverage and support applications in coastal and inland waters. Its advanced multi-frequency altimeter follows the ground-breaking footsteps of the Cryosat-2 Earth Explorer mission which demonstrably brought new capabilities for oceanography and coastal applications and the observation of ocean topography with its high along-track resolution.

8.1.2. Seastar and high-resolution wide-swath ocean topography

There are also direct scientific complementarities between Seastar and high-resolution wide-swath ocean topography measurements such as provided by **SWOT (Surface Water & Ocean Topography)**. High-resolution images of total currents, winds, waves coincident with high-resolution sea surface height images would bring significant benefits to study the interactions between geostrophic and ageostrophic processes at meso- and submesoscales in ways that have never been possible so far.

Figure 8.2 shows an example of synergy between OSCAR, SWOT and other high-resolution datasets during the OSCAR airborne campaign in the Western Mediterranean Sea in May 2023 (Section 7.3.2). Here, OSCAR flew a circular rose pattern (red circle) coincident in time and space with the left swath of SWOT 1-day repeat pass No. 003 north of Menorca. The high-resolution SWOT Ka-band NRCS data (Row 1) are shown with special permission from CNES. Also shown are daily SST products (courtesy CLS/IPSL) and C-band SAR images from coincident overflights by the Canadian RADARSAT Constellation Mission on all three days. Although OSCAR data are only preliminary, similar patterns in different datasets underline the benefits of multi-sensor synergy for greater depth of understanding about fast-evolving processes and their impacts on transports, exchanges and marine ecosystems.

SWOT was launched in December 2022 and has a nominal lifetime of 3 years. It is therefore unlikely to be operational in the 2031/32 timeframe when Seastar would be launched. Opportunities for synergy with high-resolution wide-swath ocean topography will materialise with the Copernicus **Sentinel-3 Next Generation Ocean Topography (S3NG-T)** mission. The primary objectives of the S3NG-T mission are to ensure measurement continuity of the current Sentinel-3 constellation and to provide enhanced coverage and revisit time of the altimetric measurements. The S3NG-T mission comprises a constellation of two satellites embarking wide-swath across-track interferometers and nadir-looking SAR altimeters. With a tentative launch date of 2032, the same timeframe as Seastar, the opportunities for synergy with the S3NG-T mission are very significant.

8.1.3. Seastar and side-looking SAR imagers

Data from all SAR missions flying in the 2030s, including **national SAR missions and commercial SAR data providers** (e.g., Capella) will provide valuable opportunities for cross-comparisons, validation and joint scientific exploitation of Seastar data. **Sentinel-1 C-band SAR** data are relevant to Seastar to validate ocean wave products (with shared heritage) and compare high-resolution images of NRCS and Radial Surface velocity in different environmental conditions. The combination of Seastar with classical broadside-only SAR data will bring new understanding to interpret the diversity of surface signatures observed in high-resolution SAR NRCS and Radial Surface Velocity images over the ocean, and their connections with ocean and atmospheric processes.
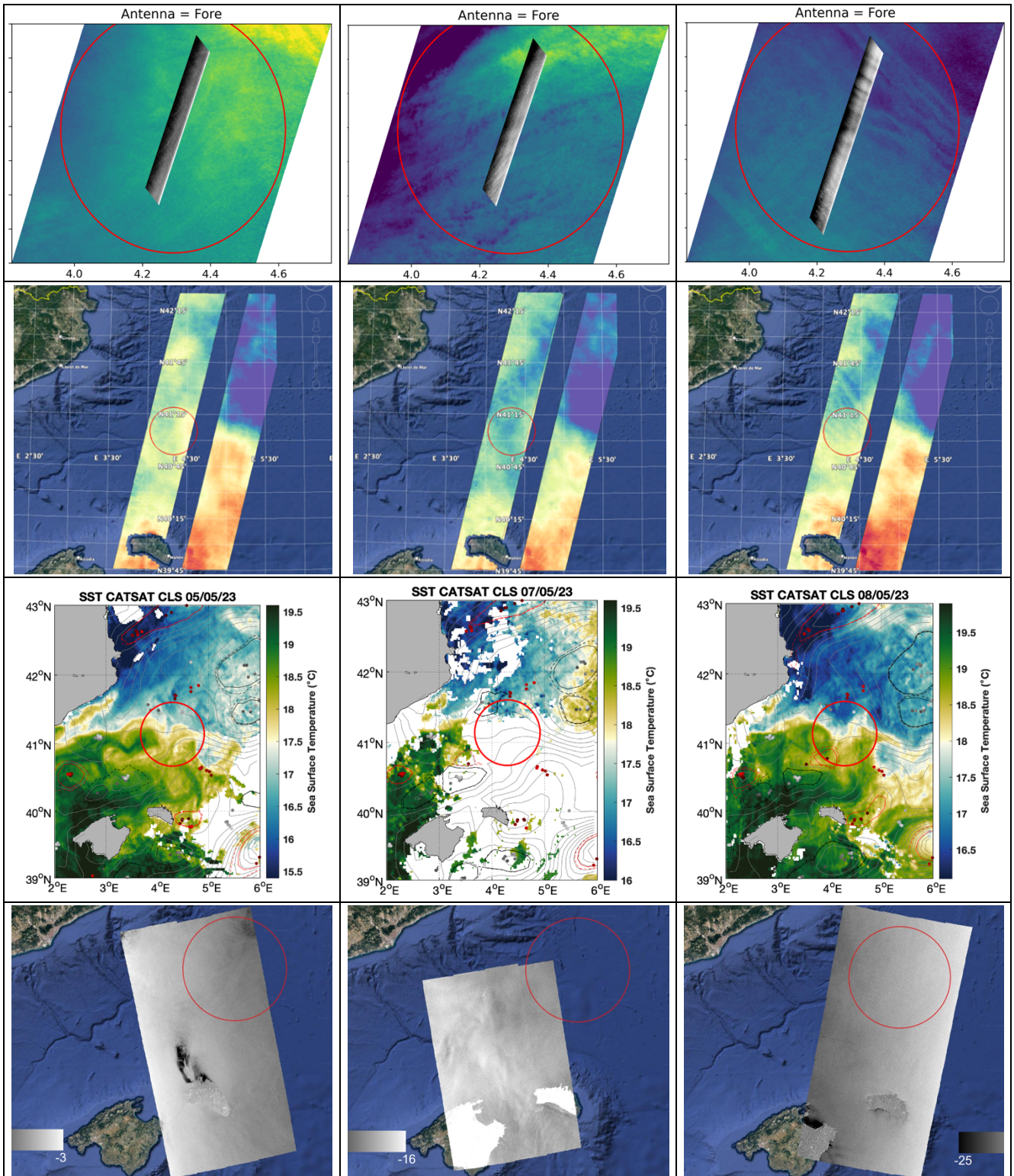
Figure 8.2: Synergy during the OSCAR airborne campaign in Western Mediterranean in May 2023. Panels right to left show data for 05, 07 and 08 May 2023: (Row 1) OSCAR fore antenna Ku-band NRCS image over coincident SWOT 250m resolution Ka-band Sigma0. (Row 2) SWOT 2km resolution Sea Surface Height from 1-day repeat pass No. 003 (Row 3) Daily SST from CLS CATSAT service. (Row 4) Coincident RADARSAT Constellation Mission C-band NRCS. [Credits: NOC, D. McCann - Noveltis/CNES, E. LeMerle, A. Martin – AVISO+ https://bulletin.aviso.altimetry.fr/html/produits/swot/adac – CLS/IPSL, R. Laxenaire, S. Speich – Environment and Climate Change Canada, M. Dabboor]

8.1.4. Seastar and scatterometry

In the 2031-2036 timeframe, Seastar will fly with a number of C- and Ku-band ocean wind vector missions (CEOS, 2014), including the next generation of European scatterometers (MetOp-SG-B-SCA) which will provide continuous operational service with up to 3 satellites from 2025 to 2043.

Seastar will benefit greatly from the high SRL processing, quality control, calibration and validation methods developed for SCA and Ku-band scatterometers (Vogelzang *et al.*, 2011; de Kloe *et al.*, 2017; Rivas *et al.*, 2017; Stoffelen *et al.*, 2017; Wang *et al.*, 2017; Vogelzang & Stoffelen, 2018; Gade & Stoffelen, 2019; Stoffelen *et al.*, 2019; Xu & Stoffelen, 2019; Verhoef & Stoffelen, 2021) that are all relevant for the production and evaluation of Seastar wind vector products.

Conversely, Seastar's high-resolution capability close to land and sea ice margins will complement the global medium-resolution observations of scatterometers and enable new understanding about the impacts of subpixel variability on operational wind products. With its daily days revisit, and multiple observations at different times of day at some latitudes, Seastar will bring unprecedented insight into the sub-daily variability of ocean winds, for example in response to diurnal warming or cloud cover, which are topics of growing importance for forecasting and climate projections.

8.1.5. Seastar and Harmony

There is also strong complementarity between Seastar and Harmony. Harmony was selected as ESA's 10th Earth Explorer (EE10) in September 2022. It will fly two companion satellites in multi-static formation with Sentinel-1 (López-Dekker et al., 2021). Its objectives span across several domains, including air-sea interactions, cryosphere and solid earth, using various combinations of formation flying with Sentinel-1.

Most directly relevant to Seastar are Harmony's objectives for air-sea interactions, which focus on interactions between the atmosphere and the ocean over large current systems in the open ocean. As already explained in Section 4.2.2, the Seastar science goals and mission objectives focus on fast-evolving small-scale processes in ocean margins, for which daily revisits, high performance and systematic observations of coastal, shelf and marginal ice zones are critical. Thus, whilst Harmony will also provide measurements of currents and winds, its temporal sampling, spatial coverage and uncertainty levels are not compatible with the observational needs of the Seastar mission.

The complementarity of Seastar and Harmony is most evident when considering the acquisition masks of Harmony and Seastar (Figure 8.3). Harmony's data acquisitions over oceans are determined by Sentinel-1 operation modes (Interferometric Wide swath, Extra-Wide swath or Wave mode) and its fixed 12-day repeat orbit. In contrast, as a self-contained mission, Seastar has the flexibility to transition from exact-repeat to slow-drifting orbits over its mission lifetime. This capability allows Seastar to fulfill its objectives of capturing fast-changing ocean processes and providing the first high-resolution description of ocean circulation across global ocean margins.

With Harmony's expected launch in 2029 timeframe, the opportunity for Seastar to fly concurrently with Harmony presents several advantages for both missions: Seastar can benefit from Harmony's in-flight experience, including calibration, processing, and validation, as well as access to its globally distributed data. In return, Harmony can leverage Seastar's finer temporal sampling, spatial resolution, and reduced uncertainties to enhance its observations and interpretations. Seastar can also assist in calibrating Harmony's measurements of currents and winds, which Harmony focuses on relatively, without strict requirements on total uncertainty (biases). Moreover, this collaboration opens doors for enhanced cooperation and joint initiatives between the user communities of both missions.
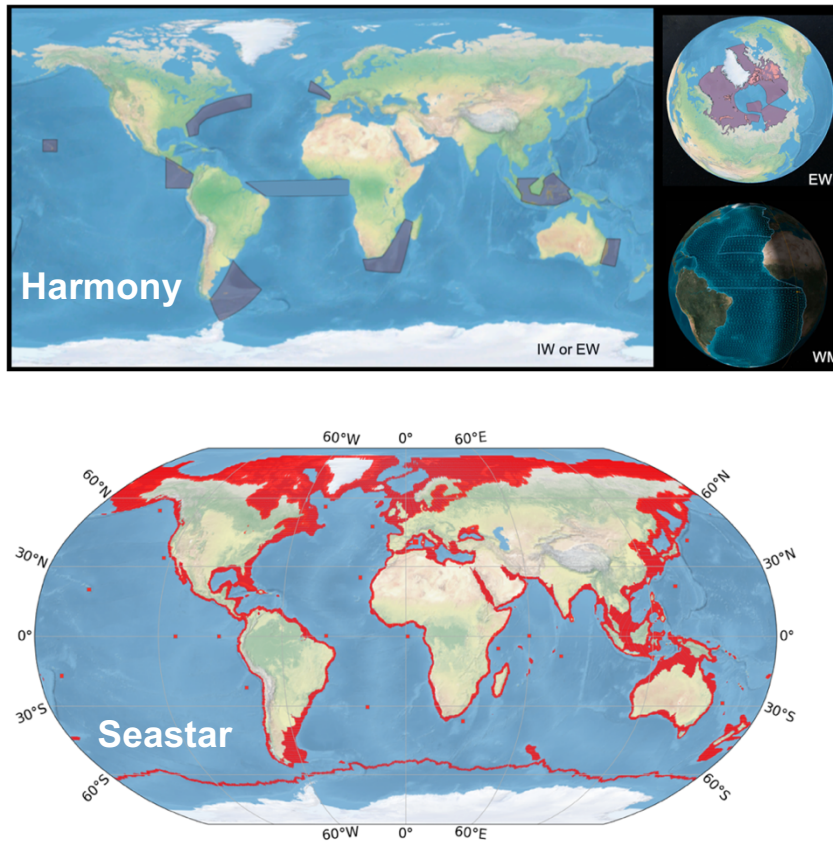
Figure 8.3: Acquisition masks for (top) Harmony and (bottom) Seastar showing the full complementarity in spatial coverage between the two missions.

8.2. Relation to proposed mission concepts

The urgent calls by the scientific community and users in recent years for new satellite observations of total surface currents has inspired several other relevant mission concepts.

DopSCAT is a long-standing Europe-led concept that proposes to add Doppler capability to scatterometers to measure marine winds and surface currents simultaneously (Fois *et al.*, 2015). The mission would deliver global daily monitoring with a spatial resolution around 25 km and errors better than 0.2 m/s. DopSCAT is driven by operational weather and ocean forecasting needs that differ from the scientific objectives of Seastar. DopSCAT remains in a research phase and its plans and prospects are under investigation.

OdySea is a joint US/France Doppler-enabled scatterometer concept recently submitted to the NASA Earth Explorer 2023 call. Previously known as WaCM (Winds and Currents Mission), Odysea would provide global sub-daily monitoring of wind and current vectors over a wide-swath (Bourassa *et al.*, 2016;Wineteer *et al.*, 2020). OdySea targets 0.1 m/s uncertainties at 25 x 25 km^2 spatial resolution, or 0.5 m/s at 5 x 5 km^2. As stated previously (Section 2.3.3, Section 7.2.1.2, Section 7.2.1.3), these capabilities are not appropriate to address the Seastar science objectives.

APPENDICES

Appendix A. Science Readiness Assessment

A.1. Science Readiness Level Criteria

The SRL requirements for EE11 is for candidates to reach SRL4 by the end of Phase 0. The Science Readiness Level 4 corresponds to the 'Proof of concept' stage and is defined as (ESA, 2015a):

'The measurement concept is validated. A model linking geophysical parameters and measurements is established. Sensitivity of the measurements to the targeted geophysical parameter is demonstrated through extensive analyses by means of dedicated experiments but at least through simulations.'

The SRL assessment takes the form of a series of key questions that are presented and addressed in Table 8.1 and Table 8.2. The table summarises SRL status of Seastar at the end of Phase 0.

Table 8.1: Science Readiness Level assessment for the Seastar candidate mission at the end of Phase 0.

SRL 4 Key Question	Answer
Are the science goal(s) translated into mission objectives, mission requirements and system requirements in a fully traceable way?	Yes. The Seastar mission objectives, mission requirements and system requirements have been translated into the MATER and reviewed by the Seastar MAG and the SciRec team.
Is a model (software package) available that allows the computation of measurements based on observation input data?	Yes. A prototype was developed during SciRec to produce L1B observables (NRCS, Radial Surface Velocity) from ocean input for single pixels, 1D tracks and 2D images at 1 km resolution. The software is open source and available on GitHub.
Is the model technically and scientifically adequate and has it been independently reviewed?	Yes. The simultaneous inversion model was published in the peer-reviewed literature for the two-look squinted interferometer configuration (Martin *et al.*, 2018). The same approach was applied to the three-look instrument configuration during SciRec and results have been submitted for publication as a peer-reviewed paper (Martin *et al.*, 2023).
Has the sensitivity of the measurements to the targeted geophysical parameter been demonstrated based on representative measurement data (e.g., campaign data) or in any other way?	Yes. The sensitivity of the measurements to the Seastar primary products (TSCV, OSVW) has been demonstrated with the three-look simultaneous inversion applied to numerical data during SciRec (Martin *et al.*, 2023) and to airborne data from the Seastarex OSCAR scientific campaign in Iroise Sea in May 2022 (McCann *et al.*, 2023a).
Has an information content analysis been performed and have the geophysical parameters contributing to the measurement data been identified?	Yes. The OSCAR Iroise Sea TSCV measurements were validated against X-band radar data (Ouessant) and ADCP data (Trefle star pattern). The OSCAR Iroise Sea OSVW measurements were validated against high-resolution model data (missing ground truth for wind). The validation results have been presented at conferences (Martin et al., 2022a; Martin et al., 2022b; McCann

	et al., 2023b) and have been submitted for publication in the peer-reviewed literature (McCann et al., 2023a).
Has a scientific risk analysis been performed?	The main scientific risk is the consolidation of the joint retrieval algorithms of TSCV, OSVW and waves. This is however mitigated by experimental campaigns performed during phase-0, showing that by applying the algorithms published in the literature, the joint estimation of these parameters can be achieved.
Has a demonstration data set of measurements been produced?	Yes. The Wavemill PoC data are available on request. The simulation data are an output of the ESA SciRec project. The OSCAR airborne data are an output of the ESA Seastarex project and have been shared with external collaborators who requested access (with ESA permission).
Has the mission concept been discussed with respect to complementary and / or alternative missions?	Yes. This was done throughout this report, and specifically in Section 4.2.2 and Chapter 8.

Table 8.2: Evidenced required for successful evaluation of SRL-4 at the end of Phase-0

Evidence required	Answer
Draft MRD	All mission requirements are consolidated in MATER V6.0. First version of MRD produced.
Software code for the model and documentation	Yes. Prototype software was developed during SciRec to produce L1B observables (NRCS, Radial Surface Velocity) from ocean input for single pixels, 1D tracks and 2D images at 1 km resolution. The software is open source and available on GitHub with available documentation delivered as output of the SciRec project. The software and documentation are input to the ongoing ESA STEEPS End-to-End Simulator study.
Peer reviewed scientific literature	Yes. The simultaneous inversion model was published in the peer-reviewed literature for the two-look squinted interferometer configuration (Martin et al., 2018). The same approach was applied to the three-look instrument configuration during SciRec and results have been submitted for publication as a peer-reviewed paper (Martin et al., 2023). The results of the Seastarex OSCAR scientific campaign in Iroise Sea in May 2022 have been submitted for publication in the peer-reviewed literature (McCann et al., 2023a).
Clear roadmap of activities to be pursued.	Yes. A roadmap of activities to achieve SRL-5 by the end of phase A is provided in this chapter.
Scientific Risk Register	The development of the End-to-End simulator mitigates the scientific risks associated with achieving SRL-5 at the end of phase-A.

A.2. Scientific roadmap towards SRL-5

Science Readiness Level 4 has been achieved and there are no identified show-stopper to SRL5 by the end of Phase A.

SRL 5 corresponds to the "End-to-End Performance Simulations" stage, described as (ESA, 2015a):

An end-to-end measurement performance simulator is developed, tested and validated using realistic and/or actual measurements. The performance model used is applicable to a predefined range of conditions (including realistic uncertainties of natural and observational nature) and can be used to address the needs originating from the science requirements in an end-to-end manner. Retrieval algorithms applicable for a realistic range of error sources (both geophysical and technical) are demonstrated against a pre- defined performance metric reflecting observation and measurement requirements.

The development of an End-to-End (E2E) simulator for Seastar is well underway and progressing rapidly as part of the ESA STEEPS activity. The activity benefits greatly from existing ESA investments in developing simulation capability for the EE9 SKIM and EE10 Harmony missions.

The scientific roadmap towards SRL5 is shown in Figure 8.4 and includes:

A/ Perform OSCAR scientific validation campaign in marginal ice zones.

B/ Develop, test and validate E2E simulator using Level-2 inversions (simultaneous and sequential) (progressing in STEEPS Phase 0/A)

C/ Perform Observing System Simulation Experiment (OSSE) to quantify benefits of the Seastar space-time sampling in different orbits.

Figure 8.4: Seastar scientific roadmap to reach SRL5 by end of Phase A

Appendix B. Relevance to evaluation criteria

B.1. Relevance to ESA research objectives for Earth Observation

Relevance to ESA Earth Observation Science Strategy – Seastar is directly relevant to many objectives of the ESA EO Science Strategy (ESA 2015a, ESA 2015b), which states (p39):

"A <u>very-high-resolution description of ocean circulation</u> is required, in particular, <u>to better understand and quantify the major role of</u> mesoscale and <u>sub-mesoscale circulation in heat, energy transport and biogeochemical cycles</u>. <u>Understanding and forecasting the evolution of marine ecosystems and coastal systems</u> in response to natural and anthropogenic changes are also specific challenges with very high societal relevance".

where we <u>underline</u> those aspects addressed directly by Seastar.

More specifically, Seastar is relevant to: **Ocean Challenges O1** *"<u>Evolution of coastal ocean systems, including the interactions with land, in response to natural and human-induced environmental perturbations</u>";* **Ocean Challenges O2** *"Mesoscale and <u>sub-mesoscale circulation</u> and the <u>role of the vertical ocean pump and its impact on energy transport and biogeochemical cycles</u>";* **Ocean Challenges O3** *"<u>Responses of the marine ecosystem and the associated ecosystem services to natural and anthropogenic changes</u>"; and* **Ocean Challenges O4** *"<u>Physical and biogeochemical air–sea interaction processes on different spatiotemporal scales and their fundamental roles in weather and climate</u>".* In addition, Seastar also relates to: **Land Surface Challenge L2** *"Improving scientific understanding of the <u>interactions between terrestrial ecosystems and other components of the Earth system and between water and other biogeochemical cycles [..]</u>"; and,* **Cryosphere Challenge C1** *"Regional and seasonal distribution of sea-ice mass and the <u>coupling between sea ice, climate, marine ecosystems and biogeochemical cycling in the ocean</u>."*

ESA EO priorities for global trends and societal benefits – Seastar applies to ESA's strategic priorities on "Global Trends" including *"climate change"* (ocean transports, carbon uptake), *"increased exposure to disasters"* (coastal management, navigation and shipping, marine hazards), *"decreasing biodiversity"* (biophysical interactions, impacts on habitats and ecosystems) and *"increasing demand for water, food and energy"* (renewables, fisheries and aquaculture, water quality, pollution). Seastar's focus on coastal, shelf seas and Marginal Ice Zones brings a **high level of societal relevance**. Coastal and shelf seas represent less than 10% of the total ocean (< 500m depth) but have a comparatively large impact on many aspects of the marine environment and human activities. These areas of exceptionally high biologically productivity are responsible for the production of most of the marine food harvested by humans (Gruber, 2015). Changes to upper ocean dynamics could affect marine productivity in some regions, with huge implications for **food security** and the fishing industry. Coastal and shelf seas also mediate the transfer of terrestrial material from land to the open ocean, including carbon, fertilisers, oil, plastics and other pollutants. It is estimated that 90% of plastic polluting the oceans originate from just 10 rivers (Gray, 2018). Anthropogenic pollution of the oceans has direct consequences for coastal **water quality**, fisheries and aquaculture, marine habitats and biodiversity. Coastal, shelf seas and Marginal Ice Zones provide vital resources and services to society including also **energy** (oil & gas, renewables), transport (international shipping, ferries) and recreation (sailing, tourism), whilst presenting mankind with some of the most challenging environmental hazards e.g., coastal flooding (Staneva *et al.*, 2016). In polar waters, sea ice extent is a key climate change indicator, responsible for major climate feedbacks through the Earth surface albedo and air-sea heat fluxes. Sea ice extent and dynamics also introduce important strategic and economic considerations associated

with the navigability and accessibility of the Arctic with less or no ice in summer (Stephenson *et al.*, 2011; Aksenov *et al.*, 2017). Seastar has direct bearing on all these issues.

ESA priorities for EO technology and digital innovations – Seastar relates to ESA's strategic ambitions of stimulating European economic growth and technological innovation, putting forward **innovative technology** that complements existing international observing systems (e.g., Copernicus Expansion, Copernicus NG, METOP), consolidates Europe's international leadership in Earth Observation technology and demonstrates EO capability to prepare future operational missions. Seastar also applies to **Digital Twins** initiatives like Destination Earth (DestinE, 2022), the Ocean Decade Digital Twins of the Ocean (DITTO, 2021) or NASA's Earth System Digital Twin (ESTO, 2023). In this context, Digital Twins are virtual representations of the Earth System, designed to integrate a wide range of data sources to transform data into knowledge, and connect, engage and empower citizens, governments and industries by giving them the capacity to make informed decisions. Seastar data about fast ocean processes at the interfaces of the Earth System are central to the correct representation of interactions and exchanges. By adopting emerging digital twins standards, Seastar will ensure the interoperability of its data across different systems, helping to bridge the scales gap between infrequent or low-resolution data from other data sources and the small, local scales that are relevant to users. In the data-rich environment of the 2030s (Section 8.1), Seastar will provide new opportunities for synergy across multiple data sources, harnessing existing methods and advanced **AI technologies** to contribute to the advancement of knowledge in a new digital age.

B.2. Need, usefulness and excellence

Seastar addresses an urgent need for high-resolution ocean current data. Ocean surface currents are the most frequently requested ocean parameter in marine user surveys, as shown by the detailed requirements collated by various international bodies. The Global Ocean Observing System (GOOS) and the Global Climate Observing System (GCOS) programme of the World Meteorological organisation (WMO) all identify surface currents as Essential Climate Variables (ECV), together with sea state, ocean surface vector stress and sea ice drift (WMO, 2018). GCOS explicitly recognise the importance of small-scale ocean dynamics, stating: *"Convergences/divergences, spiralling eddies, and filaments all contribute to vertical motions and mass exchange. Surface currents impact the steepness of surface waves and are thus important for generating accurate marine sea state forecasts"* (GCOS, 2016). GCOS spells out the data needs in coastal seas, recognising that *"Coastal regions are where boundary currents and upwelling regimes modulate fluxes of heat, carbon and other properties, with small-scale phenomena highly impacting the climate globally and locally, and also ecosystems"* (WMO, 2022). The WMO Observing Systems Capability Analysis and Review Tool (OSCAR; https://space.oscar.wmo.int) sets **user requirements for ocean surface current vectors** that highlight the need for high spatial resolution (**1 km goal/5 km breakthrough**) and high accuracy (**0.05 m/s goal/0.1 m/s breakthrough**). These requirements are fully aligned with the Seastar capabilities and cannot be met by any other existing or planned mission.

Seastar's high-resolution capability in coastal, shelf and polar seas align with priorities set out by Horizon Europe that foresees the "*evolution of Copernicus Marine Service global and regional systems to better describe ocean phenomenon with high dynamics at fine spatial scales to provide enhanced boundary conditions to coastal models (both physics, biogeochemistry or marine ecosystems)*". The Copernicus Marine Environment Monitoring Service (CMEMS) Evolution project highlights similar issues, including *"Ocean circulation, ocean-wave and ocean-ice coupling"*, *"Biogeochemistry and ecosystems in the marine environment"* and *"Seamless interactions between CMEMS and coastal systems"* – topics where Seastar would play a decisive role.

Seastar attends to ocean data needs identified by Community White Papers of the decadal OceanObs'2019 conference (OO'19, 2019), notably for winds, currents and waves (Villas Bôas *et al.*, 2019). Likewise, Seastar relates to several Programmes and Actions of the United Nations Decade of Ocean Science for Sustainable Development (https://oceandecade.org) including CoastPredict, GlobalCoast (Pinardi, 2021), ForeSea, OceanPredict (Chassignet, 2021) and OASIS (Cronin, 2021; Cronin *et al.*, 2023). Finally, Seastar is directly relevant to the ambitions of the United Nations 17 Sustainable Development Goals (SDGs), most specifically SDG #7 (Affordable and Clean Energy), SDG #14 (Life below water) and SDG #13 (Climate Action).

B.3. Uniqueness and complementarity

Uniqueness – Seastar offers unique new capability to map vectorial fields of currents, winds and waves, simultaneously, with unprecedented temporal sampling, spatial resolution and accuracy, in all coastal, shelf and marginal ice zones.

Outside satellites, surface currents are measured by a multitude of means, including current-meters, Acoustic Doppler Current Profilers (ADCP), surface drifters, Argo floats, airborne systems and HF radars. Whilst surface drifters provide the most comprehensive representation of global ocean surface currents (Maximenko *et al.*, 2012; Laurindo *et al.*, 2017), the products are generally sparce and coarse (~50 km), although some provide fine temporal resolution (Elipot *et al.*, 2016). Mapping two-dimensional vectorial fields of ocean surface currents using *in situ* means is very challenging. Dedicated oceanographic campaigns have used moorings, ships, floats, gliders and drifters (Martin & Richards, 2001, Poje *et al.*, 2014, Buckingham *et al.*, 2016, D'Asaro *et al.*, 2020b) but the logistics are complex, and campaigns localised and short-lived. Airborne surveys can help (Shcherbina *et al.*, 2015, Rodríguez *et al.*, 2018) but are inherently expensive and unsustainable. Ground-based HF radars provide regular high-quality surface current vector data and the means to monitor sub-hourly km-scale variability (Parks *et al.*, 2009; Stanev *et al.*, 2015**)**. But, whilst the international HF radar network continues to grow, coverage outside industrialised countries is poor. With HF radars difficult to deploy and maintain in poor, remote or harsh environments, much of the world's coastal ocean circulation has never been observed. Seastar will give the first comprehensive high-resolution description of total ocean currents, winds and waves and the hazards they pose in global coastal seas, with HF radars providing essential ground-truth to validate Seastar in instrumented coastal regions.

Regarding spaceborne capability, satellite altimetry is the best-known source of global ocean current data. All altimeters also measure wind speed and significant wave height, providing rare and valuable wind and wave information at regular intervals along their narrow tracks. Nadir-pointing altimeters measure along-track sea surface height (SSH) gradients from which geostrophic current in the across-track direction are estimated. Conventional pulse-limited altimeters only resolve scales above ~70 km (Dibarboure *et al.*, 2014), with SAR mode altimetry as used on Cryosat-2, Sentinel-3 SRAL and Sentinel-6MF retrieving details as fine as 20 km (Heslop *et al.*, 2017). Recent developments of Fully-Focused SAR techniques present particular interest close to land and ice margins (Egido & Smith, 2016; Schlembach *et al.*, 2023). Geostrophic current vector fields are produced from altimeter SSH by optimally interpolating data from a lattice of narrow ground tracks over 7-30 days assuming a priori spatial and temporal decorrelation scales, producing gridded products with resolutions around 25 km (Dohan & Maximenko, 2010; Johannessen *et al.*, 2016). The Surface Water and Ocean Topography (SWOT) mission launched in December 2022 is expected to address the need for 2D high-resolution SSH imaging (Fu *et al.*, 2010; Fu *et al.*, 2017). SWOT uses Across-Track Interferometry (XTI) to produce 1-km gridded SSH over two 60 km swaths, from which geostrophic currents at 10-15 km scales may be retrieved. In both cases, SSH-derived currents from nadir altimeters or from SWOT only represent the geostrophic part of the total circulation, ignoring contributions from tides, wind (Ekman),

near-inertial motions, waves (Stokes drift) and other ageostrophic motions (Isern-Fontanet *et al.*, 2017). Moreover, the geostrophic approximation breaks down in shallow waters and where spatial scales reach below the Rossby radius of deformation, making SSH-derived currents unsuitable to address the data needs in coastal and high latitude ocean margins identified by Seastar.

Mapping total ocean surface currents with satellites is already possible today. Maximum Cross Correlation (MCC) methods derive vectorial fields of total ocean currents from sequences of satellite images using intrinsic water properties (e.g., SST) as passive tracers of underlying currents. This works best in regions where ocean properties and structures are conserved (e.g., no heating/cooling for SST) and where cloud-free images are available relatively frequently. The method works also with SAR images where features remain coherent between successive images. But MCC does not work everywhere and produces spatially and temporally averaged currents that do not capture the fast-evolving small-scale surface dynamics observed by Seastar.

SAR Doppler velocity data have also been put forward to obtain direct observations of ocean surface currents. Doppler shifts in reflected microwave radar signals sense the motion of the ocean surface relative to the sensor in the line-of-sight of the radar (Graber *et al.*, 1996). The method has been demonstrated extensively with airborne and spaceborne SAR data in what is known as the Doppler Centroid Anomaly (DCA) method (Shuchman & Meadows, 1980; Rufenach *et al.*, 1983; Chapron *et al.*, 2005; Romeiser *et al.*, 2014). SAR signals need careful calibration and correction for satellite navigation and attitude errors, which can otherwise obscure ocean current signals (Martin *et al.*, 2022). The lack of azimuth diversity in traditional side-looking SAR makes it difficult to retrieve both current and wind from one line-of-sight direction. Seastar will overcome these limitations of SAR systems by measuring backscatter amplitude and Doppler shift in three lines-of-sight, yielding new understanding about the relation of SAR backscatter and Doppler signals with ocean currents, winds and waves, leading to improved retrievals for existing side-looking SAR systems.

In future, the EE10 Harmony mission will concentrate on providing direct observations of currents and winds over western boundary current systems, eastern boundary upwelling systems, and other regions of interest, but as shown in Section 8.1.5, Harmony and Seastar offer complementary capabilities, given the spatial coverage, resolution, total uncertainty levels and temporal revisit that Seastar would bring into the European Earth Observation portfolio.

Seastar's high-resolution capability close to land and sea ice margins will also complement the global medium-resolution observations of scatterometers and enable new understanding about the impacts of subpixel variability on operational wind products. In addition, with its daily revisit, and multiple observations at different times of day at some latitudes, Seastar will bring unprecedented insight into the sub-daily variability of ocean winds, for example in response to diurnal warming or cloud cover, which are topics of growing importance for forecasting and climate projections.

Seastar's innovative self-contained single-satellite concept makes it uniquely able to satisfy the challenging but well-defined scientific requirements for frequent revisit, fine resolution, high accuracy, wide swath and systematic sampling of coastal, shelf and marginal ice zones identified in Chapter 2. These requirements are aligned with the observational needs of forecasting and coupled modelling systems over the typical width of the MIZs and estuaries/coastal/open ocean transitions. The capabilities offered by Seastar are unmatched by any existing, planned or proposed mission. Seastar's stringent requirements on spatial resolution and accuracy will make it possible to obtain valuable two-dimensional maps of high-order derivative products (vorticity, divergence, strain, gradient) for TSCV and OSVW to allow direct comparison with similar diagnostic tools used routinely in theoretical and numerical studies of sub-mesoscale dynamics. As shown in Chapter 7, the scientific value of these derivative products can only be realised with the fine spatial resolution and high accuracy proposed by

Seastar. Its advanced capability will bring a new level of information about fast-evolving ocean dynamics that has never been available from any mission before.

Complementarity – As stated in Section 8.1, Seastar's 1 km resolution TSCV and OSVW images are directly complementary with high-resolution ocean colour, SST and SAR backscatter images from Copernicus Sentinels and Sentinels Next Generation, including multi-azimuth images and ultra-high-resolution data from Sentinel-2 such as sun-glitter and current gradients products. Seastar presents great scientific complementarity also with ocean topography, wind and waves data from high-resolution altimeters such as Cryosat-2, Sentinel-3 SRAL, Sentinel-6/Jason-CS, particularly in coastal and sea ice regions. Seastar's measurements in coastal regions and major river estuaries are relevant to the ongoing developments of advanced altimetry products for coastal oceanography and inland waters (e.g., river discharge) and SWOT high-resolution products. As stated in Section 8.1.2, Seastar is directly relevant to the wide-swath across-track interferometers of the Copernicus Sentinel-3 next Generation Ocean Topography constellation, which would launch in the same timeframe as Seastar and present very significant scientific benefits and opportunities for synergy.

As demonstrated in Section 8.1.5, there is strong complementarity between Seastar and Harmony, in terms of temporal sampling, spatial coverage and L2 total uncertainty levels (accuracy), with substantial benefits to both missions and the science community from the possibility of Seastar and Harmony flying in the same timeframe.

With its high-inclination orbit, Seastar presents particularly valuable synergy at high latitudes with ocean topography, sea ice thickness and surface temperature from CRISTAL and CIMR Sentinel Expansion missions, where additional knowledge of high-resolution surface forcing from Seastar will bring new insights about the mechanisms governing sea ice motion, formation and break up in both the Arctic and the Southern Ocean. In addition, Seastar will bring unique new high-resolution observations in coastal regions of the Arctic, where coastal currents, winds, directional waves and freshwater plumes from major rivers are all directly relevant to permafrost loss and the evolution of Arctic sea ice.

B.4. Degree of innovation and contribution to the advancement of European Earth Observation capabilities

Innovative data products – Seastar provides a new class of ocean surface observations that will reveal, for the first time, the day-to-day evolution of ocean surface dynamics at fine scales. Seastar delivers high-quality estimates of key ocean dynamic properties that have never before been measured from space with such fine spatial resolution, accuracy, sensitivity and temporal sampling. Seastar will provide new synoptic measurements across all coastal, shelf and polar seas where in situ and spaceborne capability lags the data needs of the ocean, atmosphere, cryosphere, coastal and climate communities. Seastar will produce the first comprehensive high-resolution description of currents, winds and waves in the global ocean margins, to contribute new environmental intelligence and improve understanding and forecasting where scientific and societal needs are greatest and most pressing.

Seastar unprecedented spatial resolution and accuracy will make it possible to produce valuable two-dimensional maps of high-order derivatives, including divergence and vorticity, available for the first time with such level of detail. Seastar will develop new secondary products for the MIZs and coastal regions, including high-accuracy instantaneous sea ice vectors, full directional wave spectra (including wind waves), added-value data about localised surface phenomena (fronts, wave breaking) and new observations of the pathways and dispersion of river plumes and pollutants.

Working in synergy with high-resolution products from other satellites, Seastar will complete the portfolio of satellite observations of the atmosphere-ocean interface to yield new knowledge about

transports and exchanges between the ocean, atmosphere, cryosphere, land and the marine biosphere. Seastar's daily to multi-annual sampling for up to 7 years (goal) of all coastal seas, shelf seas and MIZs will encourage uptake of spaceborne SAR data by the wider international community of scientists, users and modellers, and build on scientific endeavours arising from high-resolution ocean data from SWOT and Copernicus satellites. Seastar's focus on key interfaces of the Earth System will bring together communities from traditionally divided scientific disciplines (coastal, atmosphere, ocean, cryosphere, land, hydrology, biogeochemistry) and inspire new collaborative efforts to understand interactions and exchanges between different components of the Earth System. Seastar would create new opportunities to engage and exploit powerful disruptive technologies like AI and represent an essential component for the development of data-driven representations of the Earth and Digital Twins.

Innovative observing and technology – One of several innovative aspects of Seastar is to apply the principle of ATI in two highly squinted directions fore and aft of broadside from a single satellite. This unique capability makes it possible to retrieve two components of ocean surface motion vectors in a single satellite pass with high accuracy. Conventional single-pass Along-Track Interferometry only measures in one azimuth direction in the radar line of sight (typically in the instrument broadside direction) which limits it to measuring only one component of the ocean surface motion vector. The EE10 Harmony mission achieves dual observation interferometry from two passive SAR systems as bistatic observations with Sentinel-1, achieving an angular diversity of 20 degrees fore and aft, which causes anisotropy in data uncertainties. Seastar will be the first mission to implement high-squint along-track interferometry from a single platform, the first instrument and mission of its kind. By operating at Ku-band on a single satellite, Seastar achieves optimal angular diversity that delivers quasi-orthogonality (~ 90 degrees) between the two squinted look directions. This technological innovation is what gives Seastar its unique ability to satisfy the stringent requirements on spatial resolution and uncertainties driven by its science goals and mission objectives.

The inclusion of a broadside beam is another innovation for spaceborne ATI, adding a third observation in azimuth to support unambiguous simultaneous retrieval of wind and current vectors. The addition of a third line-of-sight in the broadside direction gives Seastar the combined benefits of a scatterometer-type three-look sensitivity to wind vectors (Stoffelen & Portabella, 2006) with the fine spatial resolution of SAR imagers.

B.5. Feasibility and level of maturity

B.5.2. Scientific Maturity, Critical Areas and Risks

Seastar presents high levels of scientific maturity thanks to extensive heritage from scatterometry, SAR (Envisat, Sentinel-1) and ATI (TerraSAR-X, TanDEM-X, Harmony) and sustained research investments by ESA and the UK Space Agency/Centre for Earth Observation Instrumentation (CEOI) in high-squint along-track interferometry concepts (ESA Wavemill, ESA Ocean Surface Current Mission, CEOI Seastar+, ESA OSCAR, etc.).

Seastar's outstanding performance and unique capabilities have been demonstrated extensively with numerical simulations and multiple airborne campaigns, including two validation campaigns during Phase 0, with results and capabilities being communicated widely to the science and user community through conference interventions and peer-reviewed publications.

The concept is attracting high levels of interest across many countries, domains and scientific disciplines, from scientists to modellers, engineers, operators and decision makers and industry (e.g., Gommenginger *et al.*, 2019). Seastar clearly addresses an urgent and widespread need for frequent high-resolution measurements of total currents, winds and waves in coastal, shelf and polar seas, an

observational gap that no existing, planned or proposed mission can satisfy. Seastar data products are fully aligned with the challenging but well-defined user requirements expressed through multiple forums, publications, international entities and programmes (GCOS, WMO, Horizon Europe, OceanDecade).

B.5.2. Technical Maturity, Critical Areas and Risks

During the Phase 0 preparatory activities, each industrial consortium has defined a system concept with the capability of fulfilling Seastar's mission objectives and requirements. Phase 0 has also identified the main technical risks and mission critical elements. A technology pre-development plan has been put forward to mitigate these risks and increase the TRL of critical elements to at least 5 by the end of phase B1. No technical showstoppers have been identified thus far to proceed to Phase A.

Satellite and Platform: Consortium A and Consortium B are proposing a technical solution for the platform based on the reuse or adaptation of the avionics and the reuse, adaptation or re-design of equipment and subsystems of the current generation of existing EO platforms or under development within the Copernicus programme. A custom-made structure is proposed to accommodate the antenna. Concept A is baselining the Astrobus avionics and the LSTM equipment while concept B is proposing the avionics and equipment under development for CO2M. All the platform equipment proposed for Seastar are considered to be at a Technological Readiness Level (TRL) not requiring any specific technology pre-development.

Pointing requirements are key mission drivers, specifically the need for short-term stability to reduce the impact on the radial velocity standard deviation and pointing bias during the scene acquisition. AOCS drift or antenna/baseline deformations produced by the Thermoelastic distortion affect the instrument pointing performance. Phase 0 results for both consortia show that current satellite architecture together with the external calibration strategy may be sufficient to achieve the instrument performance without a metrology system on-board.

Consortium B has also analysed during Phase-0 an alternative mission solution at an orbit of 560 km capable of providing similar Radial Velocity Standard Deviation as per the solution described in this report at an orbit of 412 km with a revisit time of about 1 day. However, the consolidation of this solution is ongoing and will be the focus of the activities during any potential phase A.

Seastar is compatible with margins with the maximum launchable mass of Vega-C as per user manual and has the potential to accommodate unforeseen design evolutions up to ~5% of current mass estimate for Concept B and ~ 3% for Concept A. Seastar, however, uses all the available envelope. Whilst this is not considered a showstopper, it represents a technical and programmatic risk and in the case of Concept B a limiting factor for the mission lifetime since the volume is driven by the size of the propellant tanks (and stowed antenna). Additionally, Seastar complies with ESA's debris regulations applicable at the time of the call. However, adopting the stricter new ESA regulations could lead to technical and programmatic impacts, to be investigated in future mission phases.

Payload: The Seastar baseline payload is an Along-Track Interferometry (ATI) SAR instrument which operates with a carrier frequency of 13.5 GHz at Ku-band. The system is designed to perform an ATI velocity measurement of the sea surface in both a fore and aft squinted looking direction.

For concept A the beamforming network, the antenna assembly, the HPA's, the Tx and Rx switching Matrix, the Duplexing circulator and the LNA's protection switch are considered the critical elements. For Concept B, the TRM's, the antenna assembly, the frequency generator and the Ku upconverted hybrid are considered critical elements. For these elements, it is considered a priority to initiate pre-developments in Phase A to retire risks and reach TRL 5 at the end of Phase B1. Other elements that

would require to build engineering models to retire risks and reach TRL 5/6 adaptation are the ICU/UPM and TxRx electronics elements of the radar electronics.

For concept A the ICU/UPM, Tx and RX module, timing control receiver, synth module and power converter module are based on adapted modules from Sentinel 1 and, Biomass or based on ROSE-L ongoing developments. HPA's are based on adaptation of MetOp-SG SCA HPA's while the switching matrix will benefit from the lessons learned from MetOP-SG SCA and the on-going R&D activity. Previous Wavemill pre-developments and MetOP-SG SCA lessons learned are to be used for the adaptation of the design for the antenna panels and Beamforming Network (BFN).

For concept B, TRM's and RM's will benefit from the heritage of TAS Italy on X- and L-band TRMs (e.g., ROSE-L). Similar heritage applies for the Ku-band upconverters and frequency generators. Manufacturing of antenna panels relies on the existing heritage from the initially selected potential provider for the antenna panels. The antenna Interface Unit is an adaptation of existing Ku-band ferrite switch and routing networks at Honeywell. OHB has heritage on the proposed deployment mechanisms.

Plan to raise TRL to 5 by the end of Phase B1 of critical elements: Both consortia are proposing pre-development activities for the critical elements of the instrument to reach TRL 5 by end of phase B1. These pre-development activities are focused on the antenna, Radar electronics, HPA and LNA. Pre-developments on the switch matrix is proposed for Concept A. Pre-developments on the Ku upconverter hybrid and the frequency generator are also proposed for Concept B.

Antenna Assembly: It will cover the design and manufacturing of squinted and broadside antenna panels and any beamforming/distribution network. The selection of the manufacturing process, the definition of manufacturing tolerances and the overall technology characterisation will be also part of the activity.

HPA's: only proposed for Concept A, the HPA pre-development aims to cover both EIK and EPC. It will include the consolidation of the requirement for HPA and breadboarding for evaluation test to validate the achievable performance.

Switching matrix: only proposed for Concept A, will cover the consolidation of the topology and the de-risking in terms of multipactor and thermal issues through the manufacturing of breadboards.

TRM's: only proposed for Concept B, will cover the selection of suitable MMIC and overall TRM topology and the characterisation of the MMIC for different bias points and temperatures.

Beamforming network: The pre-development will cover the design, manufacturing and performance assessment.

B.6. Timeliness

The satellite portfolio of ocean observations stands incomplete at present, lacking central information about fast-evolving small-scale dynamics and the fine-scale ocean circulation in the global ocean margins. Seastar represents the missing piece of the puzzle that can shed new light on ocean signals seen in other satellite data in order to bring added scientific knowledge about fluxes and transports between different parts of the Earth System from synergistic exploitation of multiple satellite products.

The timing of Seastar, a few years after SWOT and into the bountiful era of Copernicus Sentinel Expansion and Copernicus Sentinel Next Generation missions, means its data will reach a user community with much greater awareness and need for daily high-resolution data, whilst coinciding with

wider availability and uptake of high-resolution coupled models, Digital Twins and Machine Learning analytical techniques.

Concept A and Concept B platform designs are built upon ongoing developments for the ESA/EU Copernicus missions, specifically LSTM and CO2M. The Qualification Acceptance Review for LSTM is scheduled for 2028 while for CO2M is scheduled in early 2026.

B.7. Programmatics

Pre-development plan to reach TRL 5: During Phase 0, critical areas and risks have been identified. To mitigate these risks, risk retirement activities have been initiated and a technology pre-development plan has been established with the goal of advancing the TRL to at least TRL 5 by the end of Phase B1. This plan is considered suitable to address the identified risks and achieve the target TRL by the end of Phase B1, provided that sufficient financial resources are available.

Development approach: Seastar will follow a phased development process (Phases B2/C/D/E1) with reviews to verify the status of the design, development, procurement and integration of the development and flight models. Both industrial consortia have proposed parallel development activities on the instrument, platform, and satellite levels, with instrument integration performed during the Satellite Assembly, Integration and Test (AIT) phase to optimise schedule and cost.

The development approach and model philosophy at platform and satellite level is in general terms common to both concepts. For the platform the equipment re-used without modification will follow a direct Flight Model (FM) approach, while most of those modified will go through a delta-qualification or will follow a Proto-Flight Model (PFM) approach. At satellite level both consortia are proposing to undergo early mechanical tests with consortium B developing an STM specifically for this purpose.

For the payload a mix of STM and EM models will be developed which will undergo the necessary mechanical test, TVAC, acoustic and TED testing procedures, to demonstrate both feasibility and performance. The electrical and functional verification at satellite level will be performed on a satellite Engineering Model consisting of the platform engineering model (that can be based on electrical and functional simulation models of the existing and re-used units and engineering models of the modified equipment) and of the Seastar Radar Backend Electronics Unit EM allowing an electric and functional verification of the payload/platform interfaces.

Schedule: The Seastar schedule is driven by the instrument development. The schedule assumes a Phase B1 to start in Q2 2026 and a Phase B2/C/D/E1 starting in Q4 2027 following the bidding and negotiation phase. Under these assumptions a launch in 2032/2033 timeframe would require an optimisation of the development approach to be consolidated in following phases.

Other programmatic considerations: Seastar adheres to the relevant ECSS standards for the Earth Explorer program and follows the debris regulations in effect at the time of the EE11 call in 2020. There are no known ITU regulatory issues. During Phase 0, no technical mission showstoppers were identified that would prevent proceeding to Phase A.

REFERENCES

Ahsbahs, T., N. G. Nygaard, A. Newcombe, and M. Badger. 2020. Wind farm wakes from SAR and doppler radar. *Remote Sensing* 12 (3): 462.

Aksenov, Y., E. E. Popova, A. Yool, A. G. Nurser, T. D. Williams, L. Bertino, and J. Bergh. 2017. On the future navigability of Arctic sea routes: High-resolution projections of the Arctic Ocean and sea ice. *Marine Policy* 75: 300-317.

Andersen, O. B. 1999. Shallow water tides in the northwest European shelf region from TOPEX/POSEIDON altimetry. *Journal of Geophysical Research: Oceans* 104 (C4): 7729-7741.

Ardhuin, F., A. Roland, F. Dumas, A.-C. Bennis, A. Sentchev, P. Forget, J. Wolf, F. Girard, P. Osuna, and M. Benoit. 2012. Numerical wave modeling in conditions with strong currents: Dissipation, refraction, and relative wind. *Journal of Physical Oceanography* 42 (12): 2101-2120.

Ardhuin, F., J. Stopa, B. Chapron, F. Collard, M. Smith, J. Thomson, M. Doble, B. Blomquist, O. Persson, and C. O. Collins III. 2017. Measuring ocean waves in sea ice using SAR imagery: A quasi-deterministic approach evaluated with Sentinel-1 and in situ data. *Remote sensing of Environment* 189: 211-222.

Ardhuin, F., M. Otero, S. Merrifield, A. Grouazel, and E. Terrill. 2020. Ice breakup controls dissipation of wind waves across southern ocean sea ice. *Geophysical Research Letters* 47 (13): e2020GL087699.

Armitage, T. W., G. E. Manucharyan, A. A. Petty, R. Kwok, and A. F. Thompson. 2020. Enhanced eddy activity in the Beaufort Gyre in response to sea ice loss. *Nature Communications* 11 (1): 761.

Belcher, S. E., A. L. Grant, K. E. Hanley, B. Fox-Kemper, L. Van Roekel, P. P. Sullivan, W. G. Large, A. Brown, A. Hines, and D. Calvert. 2012. A global perspective on Langmuir turbulence in the ocean surface boundary layer. *Geophysical Research Letters* 39 (18).

Biddle, L., and S. Swart. 2020. The observed seasonal cycle of submesoscale processes in the Antarctic marginal ice zone. *Journal of Geophysical Research: Oceans* 125 (6): e2019JC015587.

Blockley, E., M. Martin, A. McLaren, A. Ryan, J. Waters, D. Lea, I. Mirouze, K. Peterson, A. Sellar, and D. Storkey. 2014. Recent development of the Met Office operational ocean forecasting system: an overview and assessment of the new Global FOAM forecasts. *Geoscientific Model Development* 7 (6): 2613-2638.

Bourassa, M. A., E. Rodriguez, and D. Chelton. 2016. Winds and currents mission: Ability to observe mesoscale AIR/SEA coupling. Geoscience and Remote Sensing Symposium (IGARSS), 2016 IEEE International.

Brannigan, L., D. P. Marshall, A. Naveira-Garabato, and A. G. Nurser. 2015. The seasonal cycle of submesoscale flows. *Ocean Modelling* 92: 69-84.

Brewin, R. J., S. Sathyendranath, G. Kulk, M.-H. Rio, J. A. Concha, T. G. Bell, A. Bracher, C. Fichot, T. L. Frölicher, and M. Galí. 2023. Ocean carbon from space: Current status and priorities for the next decade. *Earth-science reviews*: 104386.

Buck, C. 2005. An extension to the wide swath ocean altimeter concept. Geoscience and Remote Sensing Symposium, 2005. IGARSS'05. Proceedings. 2005 IEEE International.

Buckingham, C. E., A. C. Naveira Garabato, A. F. Thompson, L. Brannigan, A. Lazar, D. P. Marshall, A. George Nurser, G. Damerell, K. J. Heywood, and S. E. Belcher. 2016. Seasonality of submesoscale flows in the ocean surface boundary layer. *Geophysical Research Letters* 43 (5): 2118-2126.

Bulczak, A. I., S. Bacon, A. C. Naveira Garabato, A. Ridout, M. J. Sonnewald, and S. W. Laxon. 2015. Seasonal variability of sea surface height in the coastal waters and deep basins of the Nordic Seas. *Geophysical Research Letters* 42 (1): 113-120.

Capet, X., J. C. McWilliams, M. J. Molemaker, and A. Shchepetkin. 2008. Mesoscale to submesoscale transition in the California Current System. Part I: Flow structure, eddy flux, and observational tests. *Journal of Physical Oceanography* 38 (1): 29-43.

Capet, X., G. Roullet, P. Klein, and G. Maze. 2016. Intensification of upper-ocean submesoscale turbulence through Charney baroclinic instability. *Journal of Physical Oceanography* 46 (11): 3365-3384.

Carmack, E., I. Polyakov, L. Padman, I. Fer, E. Hunke, J. Hutchings, J. Jackson, D. Kelley, R. Kwok, and C. Layton. 2015. Toward quantifying the increasing role of oceanic heat in sea ice loss in the new Arctic. *Bulletin of the American Meteorological Society* 96 (12): 2079-2105.

CEOS. 2014. The Ocean Surface Vector Wind Virtual Constellation. http://ceos.org/ourwork/virtual-constellations/osvw/

Chapron, B., F. Collard, and F. Ardhuin. 2005. Direct measurements of ocean surface velocity from space: Interpretation and validation. *Journal of Geophysical Research: Oceans* 110 (C7).

Chassignet, E. P. 2021. ForeSea – the ocean prediction capacity of the future (https://oceandecade.org/actions/foresea-the-ocean-prediction-capacity-of-the-future/).

Chelton, D. B., R. A. DeSzoeke, M. G. Schlax, K. El Naggar, and N. Siwertz. 1998. Geographical variability of the first baroclinic Rossby radius of deformation. *Journal of Physical Oceanography* 28 (3): 433-460.

Chelton, D. B., M. G. Schlax, R. M. Samelson, J. T. Farrar, M. J. Molemaker, J. C. McWilliams, and J. Gula. 2019. Prospects for future satellite estimation of small-scale variability of ocean surface velocity and vorticity. *Progress in Oceanography* 173: 256-350.

Chen, M., C. B. Pattiaratchi, A. Ghadouani, and C. Hanson. 2020. Influence of storm events on chlorophyll distribution along the oligotrophic continental shelf off south-western Australia. *Frontiers in Marine Science* 7: 287.

Collard, F., F. Ardhuin, and B. Chapron. 2005. Extraction of coastal ocean wave fields from SAR images. *IEEE Journal of Oceanic Engineering* 30 (3): 526-533.

Copernicus Arctic Regional Reanalysis Service. 2023. https://climate.copernicus.eu/copernicus-arctic-regional-reanalysis-service).

Cronin, M., S. Swart, C. A. Marandino, C. Anderson, P. Browne, S. Chen, W. Joubert, U. Schuster, R. Venkatesan, and C. I. Addey. 2023. Developing an observing air–sea interactions strategy (OASIS) for the Global Ocean. *ICES Journal of Marine Science* 80 (2): 367-373.

Cronin, M. F. 2021. OASIS - Observing Air-Sea Interactions Strategy (https://oceandecade.org/actions/observing-air-sea-interactions-strategy-oasis/).

D'Asaro, E. A., D. F. Carlson, M. Chamecki, R. R. Harcourt, B. K. Haus, B. Fox-Kemper, M. J. Molemaker, A. C. Poje, and D. Yang. 2020a. Advances in Observing and Understanding Small-Scale Open Ocean Circulation During the Gulf of Mexico Research Initiative Era. *Frontiers in Marine Science*.

D'Asaro, E. A., D. F. Carlson, M. Chamecki, R. R. Harcourt, B. K. Haus, B. Fox-Kemper, M. J. Molemaker, A. C. Poje, and D. Yang. 2020b. Advances in observing and understanding small-scale open ocean circulation during the Gulf of Mexico Research Initiative Era. *Frontiers in Marine Science* 7: 349.

Daewel, U., N. Akhtar, N. Christiansen, and C. Schrum. 2022. Offshore wind farms are projected to impact primary production and bottom water deoxygenation in the North Sea. *Communications Earth & Environment* 3 (1): 292.

Dai, H.-J., J. C. McWilliams, and J.-H. Liang. 2019. Wave-driven mesoscale currents in a marginal ice zone. *Ocean Modelling* 134: 1-17.

Dai, M., J. Su, Y. Zhao, E. E. Hofmann, Z. Cao, W.-J. Cai, J. Gan, F. Lacroix, G. G. Laruelle, and F. Meng. 2022. Carbon fluxes in the coastal ocean: synthesis, boundary processes, and future trends. *Annual Review of Earth and Planetary Sciences* 50: 593-626.

Dammann, D. O., L. E. B. Eriksson, J. M. Jones, A. R. Mahoney, R. Romeiser, F. J. Meyer, H. Eicken, and Y. Fukamachi. 2019. Instantaneous sea ice drift speed from TanDEM-X interferometry. *The Cryosphere* 13 (4): 1395-1408. https://doi.org/10.5194/tc-13-1395-2019. https://tc.copernicus.org/articles/13/1395/2019/.

Davidson, F., A. Alvera-Azcarate, A. Barth, G. B. Brassington, E. P. Chassignet, E. Clementi, P. De Mey-Frémaux, P. Divakaran, C. Harris, and F. Hernandez. 2019. Synergies in operational oceanography: the intrinsic need for sustained ocean observations. *Frontiers in Marine Science* 6: 450.

de Kloe, J., A. Stoffelen, and A. Verhoef. 2017. Improved use of scatterometer measurements by using stress-equivalent reference winds. *IEEE Journal of Selected Topics in Applied Earth Observations and Remote Sensing* 10 (5): 2340-2347.

De Mey-Frémaux, P., N. Ayoub, A. Barth, R. Brewin, G. Charria, F. Campuzano, S. Ciavatta, M. Cirano, C. A. Edwards, and I. Federico. 2019. Model-observations synergy in the coastal ocean. *Frontiers in Marine Science* 6: 436.

de Rosnay, P., P. Browne, E. de Boisséson, D. Fairbairn, Y. Hirahara, K. Ochi, D. Schepers, P. Weston, H. Zuo, and M. Alonso-Balmaseda. 2022. Coupled data assimilation at ECMWF: Current status, challenges and future developments. *Quarterly Journal of the Royal Meteorological Society* 148 (747): 2672-2702.

DestinE. 2022. Destination Earth, https://destination-earth.eu.

Dibarboure, G., F. Boy, J. Desjonqueres, S. Labroue, Y. Lasne, N. Picot, J. Poisson, and P. Thibaut. 2014. Investigating short-wavelength correlated errors on low-resolution mode altimetry. *Journal of Atmospheric and Oceanic Technology* 31 (6): 1337-1362.

DITTO. 2021. Ocean Decade Digital Twins of the Ocean, https://oceandecade.org/actions/digital-twins-of-the-ocean-ditto.

Dohan, K., and N. Maximenko. 2010. Monitoring ocean currents with satellite sensors. *Oceanography* 23 (4): 94-103.

Dong, H., M. Zhou, R. P. Raj, W. O. Smith Jr, S. L. Basedow, R. Ji, C. Ashjian, Z. Zhang, and Z. Hu. 2022. Surface chlorophyll anomalies induced by mesoscale eddy-wind interactions in the northern Norwegian Sea. *Frontiers in Marine Science* 9: 1002632.

Donlon, C. 2013. Ocean Total Surface Current Velocity (TSCV) Mission Assumption and preliminary Technical Requirement (MATER). *ESA Reference EOP-SM/2513/CD-cd, Issue 1, Rev 4, Issued 30 May 2013, 70pp*.

Dorrell, R. M., C. J. Lloyd, B. J. Lincoln, T. P. Rippeth, J. R. Taylor, C.-c. P. Caulfield, J. Sharples, J. A. Polton, B. D. Scannell, and D. M. Greaves. 2022. Anthropogenic mixing in seasonally stratified shelf seas by offshore wind farm infrastructure. *Frontiers in Marine Science* 9: 830927.

Egido, A., and W. H. Smith. 2016. Fully focused SAR altimetry: Theory and applications. *IEEE Transactions on Geoscience and Remote Sensing* 55 (1): 392-406.

Elipot, S., R. Lumpkin, R. C. Perez, J. M. Lilly, J. J. Early, and A. M. Sykulski. 2016. A global surface drifter data set at hourly resolution. *Journal of Geophysical Research: Oceans* 121 (5): 2937-2966.

Elyouncha, A., L. E. Eriksson, R. Romeiser, and L. M. Ulander. 2019. Measurements of Sea Surface Currents in the Baltic Sea Region Using Spaceborne Along-Track InSAR. *IEEE Transactions on Geoscience and Remote Sensing* 57 (11): 8584-8599.

Engen, G., and H. Johnsen. 1995. SAR-ocean wave inversion using image cross spectra. *IEEE transactions on geoscience and remote sensing* 33 (4): 1047-1056.

ESA. 2015a. *Scientific Readiness Levels (SRL) Handbook*. EOP-SM/2776/MDru-mdru, Prepared by M. Drusch, C. Donlon, K. Scipal, D. Schuettemeyer & B. Veiheilmann. Issue 1 Rev. 1, Issued 17/06/2015p.

ESA. 2015b. *ESA's Living Planet Programme: Scientific Achievements and Future Challenges – Scientific Context of the Earth Observation Science Strategy for ESA.ESA SP-1329/2, February 2015.* http://esamultimedia.esa.int/multimedia/publications/SP-1329_2/p.

ESA. 2015c. *Earth Observation Science Strategy for ESA: A New Era for Scientific Advances and Societal Benefits.* http://esamultimedia.esa.int/multimedia/publications/SP-1329_1/: ESA SP-1329/1, February 2015p.

ESA. 2023. Antarctica vulnerable to extreme events Observing the Earth: https://www.esa.int/ESA_Multimedia/Images/2023/08/Antarctic_sea-ice_concentration.

Esposito, G., M. Berta, L. Centurioni, T. S. Johnston, J. Lodise, T. Özgökmen, P.-M. Poulain, and A. Griffa. 2021. Submesoscale vorticity and divergence in the Alboran Sea: Scale and depth dependence. *Frontiers in Marine Science* 8: 678304.

ESTO. 2023. Earth System Digital Twin, https://esto.nasa.gov/earth-system-digital-twin.

European Commission. 2023. "Energy and the European Green Deal. Available: https://commission.europa.eu/strategy-and-policy/priorities-2019-2024/european-green-deal/energy-and-green-deal_en".

Farquharson, G., W. N. Junek, A. Ramanathan, S. J. Frasier, R. Tessier, D. J. McLaughlin, M. A. Sletten, and J. V. Toporkov. 2004. A pod-based dual-beam SAR. *IEEE Geoscience and Remote Sensing Letters* 1 (2): 62-65.

Fischereit, J., X. G. Larsén, and A. N. Hahmann. 2022. Climatic Impacts of Wind-Wave-Wake Interactions in Offshore Wind Farms. *Frontiers in Energy Research* 10: 881459.

Flato, G., J. Marotzke, B. Abiodun, P. Braconnot, S. C. Chou, W. J. Collins, P. Cox, F. Driouech, S. Emori, and V. Eyring. 2013. Evaluation of Climate Models. In: Climate Change 2013: The Physical Science Basis. Contribution of Working Group I to the Fifth Assessment Report of the Intergovernmental Panel on Climate Change. *Climate Change 2013* 5: 741-866.

Fois, F., P. Hoogeboom, F. Le Chevalier, A. Stoffelen, and A. Mouche. 2015. DopSCAT: A mission concept for simultaneous measurements of marine winds and surface currents. *Journal of Geophysical Research: Oceans* 120 (12): 7857-7879.

Fox-Kemper, B., and R. Ferrari. 2008. Parameterization of mixed layer eddies. Part II: Prognosis and impact. *Journal of Physical Oceanography* 38 (6): 1166-1179.

Fox-Kemper, B., G. Danabasoglu, R. Ferrari, S. Griffies, R. Hallberg, M. Holland, M. Maltrud, S. Peacock, and B. Samuels. 2011. Parameterization of mixed layer eddies. III: Implementation and impact in global ocean climate simulations. *Ocean Modelling* 39 (1-2): 61-78.

Fox-Kemper, B., H. T. Hewitt, C. Xiao, G. Aðalgeirsdóttir, S. S. Drijfhout, T. L. Edwards, N. R. Golledge, M. Hemer, R. E. Kopp, G. Krinner, A. Mix, D. Notz, S. Nowicki, I. S. Nurhati, L. Ruiz, J.-B. Sallée, A. B. A. Slangen, and Y. Yu. 2021. Ocean, Cryosphere and Sea Level Change. In *Climate Change 2021: The Physical Science Basis. Contribution of Working Group I to the Sixth Assessment Report of the Intergovernmental Panel on Climate Change*, edited by V. Masson-Delmotte, P. Zhai, A. Pirani, S.L. Connors, C. Péan, S. Berger, N. Caud, Y. Chen, L. Goldfarb, M.I. Gomis, M. Huang, K. Leitzell, E. Lonnoy, J.B.R. Matthews, T.K. Maycock, T. Waterfield, O. Yelekçi, R. Yu, and B. Zhou, 1211–1362, doi: 10.1017/9781009157896.011. Cambridge University Press, Cambridge, United Kingdom and New York, NY, USA.

Frasier, S. J., and A. J. Camps. 2001. Dual-beam interferometry for ocean surface current vector mapping. *IEEE Transactions on Geoscience and Remote Sensing* 39 (2): 401-414.

Fu, L.-L., D. B. Chelton, P.-Y. Le Traon, and R. Morrow. 2010. Eddy dynamics from satellite altimetry. *Oceanography* 23 (4): 14-25.

Fu, L.-L., R. Morrow, T. Pavelsky, and J.-F. Cretaux. 2017. Summary report of the 2nd SWOT Sciene Team Meeting 2017. *26-28 June 2017, Meteo-France Conference Centre, Toulouse, Available from https://spark.adobe.com/page/iuFI7X6PBlVYT/.*

Futch, V., and A. Allen. 2019. Search and rescue applications: on the need to improve ocean observing data systems in offshore or remote locations. *Frontiers in Marine Science* 6: 301.

Gade, M., and A. Stoffelen. 2019. An introduction to microwave remote sensing of the Asian Seas. *Remote Sensing of the Asian Seas*: 81-101.

Gao, S., J. Schwinger, J. Tjiputra, I. Bethke, J. Hartmann, E. Mayorga, and C. Heinze. 2023. Riverine impact on future projections of marine primary production and carbon uptake. *Biogeosciences* 20 (1): 93-119.

Garabato, A. C. N., A. Forryan, P. Dutrieux, L. Brannigan, L. C. Biddle, K. J. Heywood, A. Jenkins, Y. L. Firing, and S. Kimura. 2017. Vigorous lateral export of the meltwater outflow from beneath an Antarctic ice shelf. *Nature* 542 (7640): 219-222.

GCOS. 2016. The Global Observing System for Climate: Implementation needs. GCOS-200 (GOOS-214). *World Meteorological Organization. Available from https://public.wmo.int/en/programmes/global-climate-observing-system*.

Gebert, N., A. Martin , V. Navarro, and M. Portabella. 2018. Ocean surface current airborne radar (OSCAR) demonstrator. Doppler Oceanography from Space (DOfS), From science to technology and applications, 10-12 October 2018, Brest, France.

Giles, K. A., S. W. Laxon, A. L. Ridout, D. J. Wingham, and S. Bacon. 2012. Western Arctic Ocean freshwater storage increased by wind-driven spin-up of the Beaufort Gyre. *Nature Geoscience* 5 (3): 194.

Godø, O. R., A. Samuelsen, G. J. Macaulay, R. Patel, S. S. Hjøllo, J. Horne, S. Kaartvedt, and J. A. Johannessen. 2012. Mesoscale eddies are oases for higher trophic marine life. *PloS one* 7 (1): e30161.

Goldstein, R. M., and H. A. Zebker. 1987. Interferometric radar measurement of ocean surface currents. *Nature* 328 (6132): 707-709.

Goldstein, R. M., T. P. Barnett, and H. A. Zebker. 1989. Remote sensing of ocean currents. *Science* 246 (4935): 1282-1286.

Gommenginger, C. P., B. Chapron, A. Hogg, C. Buckingham, B. Fox-Kemper, L. Eriksson, F. Soulat, M.-H. Rio, C. Ubelmann, F. Ocampo-Torres, B. Buongiorno Nardelli, D. Griffin, P. Lopez-Dekker, P. Knudsen, O. Andersen, L. Stenseng, N. Stapleton, W. Perrie, N. Violante-Carvalho, J. Schulz-Stellenfleth, D. Woolf, J. Isern-Fontanet, F. Ardhuin, P. Klein, A. Mouche, A. Pascual, X. Capet, D. Hauser, A. Stoffelen, R. Morrow, L. Aouf, O. Breivik, L.-L. Fu, J. Johannessen, Y. Aksenov, L. M. Bricheno, J. Hirschi, A. C. H. Martin, A. P. Martin, G. Nurser, J. Polton, J. Wolf, H. Johnsen, A. Soloviev, G. Jacobs, F. Collard, S. Groom, V. Kudryavstev , J. Wilkin, V. Navarro, A. Babanin, M. Martin, J. Siddorn, A. Saulter, T. Rippeth, B. Emery, N. Maximenko, R. Romeiser, H. Graber, A. Alvera Azcarate, C. Hughes, D. Vandemark, J. da Silva, P.-J. van Leeuwen, A. Naveira-Gabarato, J. Gemmrich, A. Mahadevan, J. Marquez, Y. Munro, S. Doody, and G. Burbidge. 2019. Developing new spaceborne observations of submesoscale ocean dynamics and small scale atmosphere-ocean processes in coastal, shelf and polar seas. *OceanObs'2019, Frontiers in Marine Science* 6(457): 1.

Graber, H. C., D. R. Thompson, and R. E. Carande. 1996. Ocean surface features and currents measured with synthetic aperture radar interferometry and HF radar. *Journal of Geophysical Research: Oceans* 101 (C11): 25813-25832.

Graham, J. A., E. O'Dea, J. Holt, J. Polton, H. T. Hewitt, R. Furner, K. Guihou, A. Brereton, A. Arnold, and S. Wakelin. 2018. AMM15: a new high-resolution NEMO configuration for operational simulation of the European north-west shelf. *Geoscientific Model Development* 11 (2): 681-696.

Gray, A. 2018. 90% of plastic polluting our oceans comes from just 10 rivers. *World Economic Forum. https://www.weforum.org/agenda/2018/06/90-of-plastic-polluting-our-oceans-comes-from-just-10-rivers/*.

Gruber, N. 2015. Ocean biogeochemistry: Carbon at the coastal interface. *Nature* 517 (7533): 148.

Halsne, T., P. Bohlinger, K. H. Christensen, A. Carrasco, and Ø. Breivik. 2022. Resolving regions known for intense wave–current interaction using spectral wave models: A case study in the energetic flow fields of Northern Norway. *Ocean Modelling* 176: 102071.

Heslop, E., A. Sánchez-Román, A. Pascual, D. Rodríguez, K. Reeve, Y. Faugère, and M. Raynal. 2017. Sentinel-3A Views Ocean Variability More Accurately at Finer Resolution. *Geophysical Research Letters* 44 (24).

Holt, J., P. Hyder, M. Ashworth, J. Harle, H. T. Hewitt, H. Liu, A. L. New, S. Pickles, A. Porter, and E. Popova. 2017. Prospects for improving the representation of coastal and shelf seas in global ocean models. *Geoscientific Model Development* 10 (1): 499-523.

Horvat, C., E. Tziperman, and J. M. Campin. 2016. Interaction of sea ice floe size, ocean eddies, and sea ice melting. *Geophysical Research Letters* 43 (15): 8083-8090.

Howell, S. E., T. Wohlleben, M. Dabboor, C. Derksen, A. Komarov, and L. Pizzolato. 2013. Recent changes in the exchange of sea ice between the Arctic Ocean and the Canadian Arctic Archipelago. *Journal of Geophysical Research: Oceans* 118 (7): 3595-3607.

IPCC AR6. 2021. Sixth Assessment Report Working Group 1: the Physical Science Basis (https://www.ipcc.ch/assessment-report/ar6/wg1/).

Isachsen, P. E. 2015. Baroclinic instability and the mesoscale eddy field around the Lofoten Basin. *Journal of Geophysical Research: Oceans* 120 (4): 2884-2903.

Isern-Fontanet, J., J. Ballabrera-Poy, A. Turiel, and E. García-Ladona. 2017. Remote sensing of ocean surface currents: a review of what is being observed and what is being assimilated. *Nonlinear Processes in Geophysics* 24: 613 - 643.

Jacobs, S. S. 2004. Bottom water production and its links with the thermohaline circulation. *Antarctic Science* 16 (4): 427-437.

Johannessen, J., B. Chapron, F. Collard, M. Rio, J. Piollé, L. Gaultier, G. Quartly, J. Shutler, R. Raj, and C. Donlon. 2016. GlobCurrent: Multisensor synergy for surface current estimation.

Johannessen, J., and O. Andersen. 2017. The high latitudes and polar ocean. *Satellite Altimetry over Oceans and Land Surfaces; Stammer, D., Cazenave, A., Eds*: 271-294.

Johannessen, J. A., S. Sandven, K. Lygre, E. Svendsen, and O. Johannessen. 1989. Three-dimensional structure of mesoscale eddies in the Norwegian Coastal Current. *Journal of Physical Oceanography* 19 (1): 3-19.

Josey, S., M. De Jong, M. Oltmanns, G. Moore, and R. Weller. 2019. Extreme variability in Irminger Sea winter heat loss revealed by ocean observatories initiative mooring and the ERA5 reanalysis. *Geophysical Research Letters* 46 (1): 293-302.

Josey, S. A., and K. Schroeder. 2023. Declining winter heat loss threatens continuing ocean convection at a Mediterranean dense water formation site. *Environmental Research Letters* 18 (2): 024005.

Kai, E. T., V. Rossi, J. Sudre, H. Weimerskirch, C. Lopez, E. Hernandez-Garcia, F. Marsac, and V. Garçon. 2009. Top marine predators track Lagrangian coherent structures. *Proceedings of the National Academy of Sciences* 106 (20): 8245-8250.

King, R. R., J. While, M. J. Martin, D. J. Lea, B. Lemieux-Dudon, J. Waters, and E. O'Dea. 2018. Improving the initialisation of the Met Office operational shelf-seas model. *Ocean Modelling* 130: 1-14.

Klein, P., G. Lapeyre, G. Roullet, S. Le Gentil, and H. Sasaki. 2011. Ocean turbulence at meso and submesoscales: connection between surface and interior dynamics. *Geophysical & Astrophysical Fluid Dynamics* 105 (4-5): 421-437.

Klein, P., G. Lapeyre, L. Siegelman, B. Qiu, L. L. Fu, H. Torres, Z. Su, D. Menemenlis, and S. Le Gentil. 2019. Ocean-scale interactions from space. *Earth and Space Science* 6 (5): 795-817.

Kleinherenbrink, M., P. Lopez-Dekker, B. Chapron, and A. Mouche. 2021. Ocean wave spectra estimation with the Earth Explorer 10 candidate Harmony. EGU General Assembly Conference Abstracts.

Klocker, A., A. Naveira Garabato, F. Roquet, C. De Lavergne, and S. Rintoul. 2023. Generation of the internal pycnocline in the subpolar Southern Ocean by wintertime sea ice melting. *Journal of Geophysical Research: Oceans* 128 (3): e2022JC019113.

Koutsokosta, E., and L. Chadwick. 2023. European countries sign declaration to make North Sea wind power hub. *Euronews.com*.

Kozlov, I. E., A. V. Artamonova, G. E. Manucharyan, and A. A. Kubryakov. 2019. Eddies in the Western Arctic Ocean from spaceborne SAR observations over open ocean and marginal ice zones. *Journal of Geophysical Research: Oceans* 124 (9): 6601-6616.

Labrousse, S., G. Williams, T. Tamura, S. Bestley, J.-B. Sallée, A. D. Fraser, M. Sumner, F. Roquet, K. Heerah, and B. Picard. 2018. Coastal polynyas: Winter oases for subadult southern elephant seals in East Antarctica. *Scientific Reports* 8 (1): 3183.

Lapeyre, G., and P. Klein. 2006a. Dynamics of the upper oceanic layers in terms of surface quasigeostrophy theory. *Journal of Physical Oceanography* 36 (2): 165-176.

Lapeyre, G., and P. Klein. 2006b. Impact of the small-scale elongated filaments on the oceanic vertical pump. *Journal of marine research* 64 (6): 835-851.

Laurindo, L. C., A. J. Mariano, and R. Lumpkin. 2017. An improved near-surface velocity climatology for the global ocean from drifter observations. *Deep Sea Research Part I: Oceanographic Research Papers* 124: 73-92.

Lea, D., I. Mirouze, M. Martin, R. King, A. Hines, D. Walters, and M. Thurlow. 2015. Assessing a new coupled data assimilation system based on the Met Office coupled atmosphere–land–ocean–sea ice model. *Monthly Weather Review* 143 (11): 4678-4694.

Lévy, M., P. Klein, and M. Ben Jelloul. 2009. New production stimulated by high-frequency winds in a turbulent mesoscale eddy field. *Geophysical Research Letters* 36 (16).

Lévy, M., P. Klein, A.-M. Tréguier, D. Iovino, G. Madec, S. Masson, and K. Takahashi. 2010. Modifications of gyre circulation by sub-mesoscale physics. *Ocean Modelling* 34 (1): 1-15.

Lévy, M., R. Ferrari, P. J. Franks, A. P. Martin, and P. Rivière. 2012. Bringing physics to life at the submesoscale. *Geophysical Research Letters* 39 (14).

Li, Z., A. Verhoef, A. Stoffelen, J. Shang, and F. Dou. 2023. First Results from the WindRAD Scatterometer on Board FY-3E: Data Analysis, Calibration and Wind Retrieval Evaluation. *Remote Sensing* 15 (8): 2087.

Liu, X., C. A. Stock, J. P. Dunne, M. Lee, E. Shevliakova, S. Malyshev, and P. C. Milly. 2021. Simulated global coastal ecosystem responses to a half-century increase in river nitrogen loads. *Geophysical Research Letters* 48 (17): e2021GL094367.

López-Dekker, P., P. Prats, F. De Zan, S. Wollstadt, D. Schulze, G. Krieger, and A. Moreira. 2011. Demonstration of SAR interferometry under crossing orbits using TerraSAR-X and TanDEM-X. Geoscience and Remote Sensing Symposium (IGARSS), 2011 IEEE International.

López-Dekker, P., J. Biggs, B. Chapron, A. Hooper, A. Kääb, S. Masina, J. Mouginot, B. B. Nardelli, C. Pasquero, and P. Prats-Iraola. 2021. The Harmony mission: End of phase-0 science overview. 2021 IEEE International Geoscience and Remote Sensing Symposium IGARSS.

Lozier, M. S., F. Li, S. Bacon, F. Bahr, A. S. Bower, S. Cunningham, M. F. de Jong, L. de Steur, B. deYoung, and J. Fischer. 2019. A sea change in our view of overturning in the subpolar North Atlantic. *Science* 363 (6426): 516-521.

Luijendijk, A., and A. van Oudenhoven. 2019. *The Sand Motor: A nature-based response to climate change: findings and reflections of the Interdisciplinary Research Program NatureCoast*. Delft University Publishersp.

Lumpkin, R., T. Özgökmen, and L. Centurioni. 2017. Advances in the application of surface drifters. *Annual review of marine science* 9: 59-81.

Lyard, F. H., D. J. Allain, M. Cancet, L. Carrère, and N. Picot. 2021. FES2014 global ocean tide atlas: design and performance. *Ocean Sci.* 17 (3): 615-649. https://doi.org/10.5194/os-17-615-2021. https://os.copernicus.org/articles/17/615/2021/.

Lyzenga, D., R. Shuchman, and C. Rufenach. 1982. Synthetic aperture radar measurements of ocean surface currents. *Geophysical Research Letters* 9 (7): 747-750.

MacLeod, M., H. P. H. Arp, M. B. Tekman, and A. Jahnke. 2021. The global threat from plastic pollution. *Science* 373 (6550): 61-65.

Manucharyan, G. E., and A. F. Thompson. 2017. Submesoscale sea ice-ocean interactions in marginal ice zones. *Journal of Geophysical Research: Oceans* 122 (12): 9455-9475.

Márquez, J., B. Richards, and C. Buck. 2010. Wavemill: A novel instrument for ocean circulation monitoring. EUSAR 2010, 8th European Conference on Synthetic Aperture Radar, Aachen, Germany, 07-10 June 2010.

Martin , A., N. Gebert, C. Trampuz, M. Portabella, V. Navarro, and C. Gommenginger. 2019. Ocean Surface Current Airborne Radar (OSCAR) Demonstrator. Living Planet Symposium 2019, 13-17 May 2019, Milan.

Martin, A. C., C. P. Gommenginger, B. Jacob, and J. Staneva. 2022. First multi-year assessment of Sentinel-1 radial velocity products using HF radar currents in a coastal environment. *Remote Sensing of Environment* 268: 112758.

Martin, A. C. H., C. P. Gommenginger, J. Marquez, S. Doody, V. Navarro, and C. Buck. 2016. Wind-wave-induced velocity in ATI SAR ocean surface currents: First experimental evidence from an airborne campaign. *J. Geophys. Res. Oceans* 121 (doi:10.1002/2015JC011459).

Martin, A. C. H., and C. P. Gommenginger. 2017. Towards wide-swath high-resolution mapping of Total Ocean Surface Current Vectors from space: airborne proof-of-concept and validation. *Remote Sensing of Environment, under revision.*

Martin, A. C. H., C. Gommenginger, and Y. Quilfen. 2018. Simultaneous ocean surface current and wind vectors retrieval with squinted SAR interferometry: geophysical inversion and performance assessment. *Remote Sensing of the Environment* 216 (October 2018): 798-808. https://doi.org/https://doi.org/10.1016/j.rse.2018.06.013.

Martin , A. C. H., D. McCann, K. Macedo, A. Meta, C. P. Gommenginger, M. Portabella, L. Marié, J. Horstmann, J.-F. Filipot, J. Marquez, P. Martin-Iglesias, and T. Casal. 2022a. "Ocean Surface Current Airborne Radar (OSCAR): a new instrument to measure ocean surface dynamics at the sub-mesoscale." 5th Oceans from Space Symposium, 24-28 October 2022, Scuola Grande di San Marco, Venice, Italy.

Martin , A. C. H., C. Trampuz, H. Keryhuel, K. Macedo, R. Hu, A. Meta, M. Portabella, L. Marié, C. P. Gommenginger, J.-F. Filipot, J. Horstmann, J. Marquez, P. Martin-Iglesias, and T. Casal. 2022b. "Ocean Surface Current Airborne Radar (OSCAR) Demonstrator & SEASTARex campaign." Living Planet Symposium 2022, 23-27 May 2022, Bonn, Germany.

Martin, A. C. H., C. P. Gommenginger, D. Andrievskaia, P. Martin-Iglesias, and A. Egido. 2023. Evaluating the performance of the Earth Explorer 11 SeaSTAR mission candidate for simultaneous retrieval of total surface current and wind vectors. *Remote Sensing (sub judice)*.

Martin, A. P., and K. J. Richards. 2001. Mechanisms for vertical nutrient transport within a North Atlantic mesoscale eddy. *Deep Sea Research Part II: Topical Studies in Oceanography* 48 (4): 757-773.

Maximenko, N., J. Hafner, and P. Niiler. 2012. Pathways of marine debris derived from trajectories of Lagrangian drifters. *Marine pollution bulletin* 65 (1-3): 51-62.

Mayot, N., C. Le Quéré, C. Rödenbeck, R. Bernardello, L. Bopp, L. M. Djeutchouang, M. Gehlen, L. Gregor, N. Gruber, and J. Hauck. 2023. Climate-driven variability of the Southern Ocean CO2 sink. *Philosophical Transactions of the Royal Society A* 381 (2249): 20220055.

McCann, D. L., A. C. H. Martin , K. Macedo, R. Carrasco Alavarez, J. Horstmann, L. Marié, J. Marquez, M. Portabella, A. Meta, C. P. Gommenginger, P. Martin-Iglesias, and T. Casal. 2023a. A new airborne system for simultaneous high-resolution ocean vector current and wind mapping: first demonstration of the SeaSTAR mission concept in the macrotidal Iroise Sea. *Ocean Science (sub judice)*.

McCann, D. L., A. C. H. Martin, K. Macedo, C. P. Gommenginger, L. Marié, A. Meta, P. Martin-Iglesias, and T. Casal. 2023b. "OSCAR: validation of 2D total surface current vector fields during the

SEASTARex airborne campaign in Iroise Sea, May 2022 (oral presentation)." European Geophysical Union General Assembly 2023, Vienna, Austria.

McWilliams, J. C. 2016. Submesoscale currents in the ocean. *Proc. R. Soc. A* A 472: 20160117. http://dx.doi.org/10.1098/rspa.2016.0117.

Meta, A., S. Placidi, C. Trampuz, V. Navarro, A. Repucci, C. P. Gommenginger, and A. C. H. Martin. 2015. Ocean Surface Current Airborne Radar Demonstrator (OSCAR). *Proposal submitted in response to ESA AO/1-8309/15/NL/BJ (Re-Issue of AO/1-7994/14/NL/BJ)*.

Meybeck, M., and C. Vörösmarty. 1999. Global transfer of carbon by rivers. *Global Change Newsletter* 37: 18-19.

Miller, R. L., B. A. Mckee, and E. J. D'sa. 2007. Monitoring bottom sediment resuspension and suspended sediments in shallow coastal waters. In *Remote Sensing of Coastal Aquatic Environments: Technologies, Techniques and Applications*, 259-276. Springer.

Moiseev, A. 2021. Ocean surface currents derived from Sentinel-1 SAR Doppler shift measurements. Doctoral thesis, The University of Bergen (https://hdl.handle.net/11250/2838477).

Morrison, A., A. M. Hogg, M. H. England, and P. Spence. 2020. Warm Circumpolar Deep Water transport toward Antarctica driven by local dense water export in canyons. *Science Advances* 6 (18): eaav2516.

Mouche, A. A., F. Collard, B. Chapron, K.-F. Dagestad, G. Guitton, J. A. Johannessen, V. Kerbaol, and M. W. Hansen. 2012. On the use of Doppler shift for sea surface wind retrieval from SAR. *IEEE Transactions on Geoscience and Remote Sensing* 50 (7): 2901-2909.

Nielsen, D. M., P. Pieper, A. Barkhordarian, P. Overduin, T. Ilyina, V. Brovkin, J. Baehr, and M. Dobrynin. 2022. Increase in Arctic coastal erosion and its sensitivity to warming in the twenty-first century. *Nature Climate Change* 12 (3): 263-270.

Nurser, A., and S. Bacon. 2014. The rossby radius in the arctic ocean. *Ocean Science* 10 (6): 967-975.

Oke, P. R., and P. Sakov. 2008. Representation error of oceanic observations for data assimilation. *Journal of Atmospheric and Oceanic Technology* 25 (6): 1004-1017.

OO'19. 2019. Oceanobs'19: An Ocean of Opportunity (https://oceanobs19.net). *Honolulu, USA, 16–20 September 2019*

OSI SAF. 2022. *Algorithm Theoretical Basis Document for the scatterometer wind products.* (EUMETSAT Ocean and Sea Ice Satellite Application Facility (OSI SAF), Version 2.1, 12/10/2022. https://scatterometer.knmi.nl/publications/pdf/osisaf_ss3_atbd.pdf).

Parks, A., L. Shay, W. Johns, J. Martinez-Pedraja, and K. W. Gurgel. 2009. HF radar observations of small-scale surface current variability in the Straits of Florida. *Journal of Geophysical Research: Oceans* 114 (C8).

Pinardi, N. 2021. Coastpredict – observing and predicting the global coastal ocean (https://oceandecade.org/actions/coastpredict-observing-and-predicting-the-global-coastal-ocean/).

Platis, A., S. K. Siedersleben, J. Bange, A. Lampert, K. Bärfuss, R. Hankers, B. Cañadillas, R. Foreman, J. Schulz-Stellenfleth, and B. Djath. 2018. First in situ evidence of wakes in the far field behind offshore wind farms. *Scientific reports* 8 (1): 2163.

Pleskachevsky, A., B. Tings, S. Wiehle, J. Imber, and S. Jacobsen. 2022. Multiparametric sea state fields from synthetic aperture radar for maritime situational awareness. *Remote Sensing of Environment* 280: 113200.

Poje, A. C., T. M. Özgökmen, B. L. Lipphardt, B. K. Haus, E. H. Ryan, A. C. Haza, G. A. Jacobs, A. Reniers, M. J. Olascoaga, and G. Novelli. 2014. Submesoscale dispersion in the vicinity of the Deepwater Horizon spill. *Proceedings of the National Academy of Sciences* 111 (35): 12693-12698.

Portabella, M. 2002. Wind field retrieval from satellite radar systems. PhD dissertation, University of Barcelona (Available: http://www.knmi.nl/scatterometer).

Poulain, P.-M., A. Bussani, R. Gerin, R. Jungwirth, E. Mauri, M. Menna, and G. Notarstefano. 2013. Mediterranean surface currents measured with drifters: From basin to subinertial scales. *Oceanography* 26 (1): 38-47.

Quach, B., Y. Glaser, J. E. Stopa, A. A. Mouche, and P. Sadowski. 2020. Deep learning for predicting significant wave height from synthetic aperture radar. *IEEE Transactions on Geoscience and Remote Sensing* 59 (3): 1859-1867.

Raj, R., I. Halo, S. Chatterjee, T. Belonenko, M. Bakhoday-Paskyabi, I. Bashmachnikov, A. Fedorov, and J. Xie. 2020. Interaction between mesoscale eddies and the gyre circulation in the Lofoten Basin. *Journal of Geophysical Research: Oceans* 125 (7): e2020JC016102.

Regnier, P., L. Resplandy, R. G. Najjar, and P. Ciais. 2022. The land-to-ocean loops of the global carbon cycle. *Nature* 603 (7901): 401-410.

Renault, L., P. Marchesiello, S. Masson, and J. C. Mcwilliams. 2019. Remarkable control of western boundary currents by eddy killing, a mechanical air-sea coupling process. *Geophysical Research Letters* 46 (5): 2743-2751.

Richter, M. E., W.-J. von Appen, and C. Wekerle. 2018. Does the East Greenland current exist in the northern Fram Strait? *Ocean Science* 14 (5): 1147-1165.

Ricker, R., F. Girard-Ardhuin, T. Krumpen, and C. Lique. 2018. Satellite-derived sea ice export and its impact on Arctic ice mass balance. *The Cryosphere* 12 (9): 3017-3032.

Rivas, M. B., A. Stoffelen, J. Verspeek, A. Verhoef, X. Neyt, and C. Anderson. 2017. Cone metrics: a new tool for the intercomparison of scatterometer records. *IEEE Journal of Selected Topics in Applied Earth Observations and Remote Sensing* 10 (5): 2195-2204.

Rodríguez, E., A. Wineteer, D. Perkovic-Martin, T. Gál, B. W. Stiles, N. Niamsuwan, and R. Rodriguez Monje. 2018. Estimating ocean vector winds and currents using a Ka-band pencil-beam Doppler scatterometer. *Remote Sensing* 10 (4): 576.

Romeiser, R. 2005. Current measurements by airborne along-track InSAR: Measuring technique and experimental results. *IEEE Journal of Oceanic Engineering* 30 (3): 552-569.

Romeiser, R., J. Johannessen, B. Chapron, F. Collard, V. Kudryavtsev, H. Runge, and S. Suchandt. 2010. Direct surface current field imaging from space by along-track InSAR and conventional SAR. In *Oceanography from Space*, 73-91. Springer.

Romeiser, R., H. Runge, S. Suchandt, R. Kahle, C. Rossi, and P. S. Bell. 2014. Quality assessment of surface current fields from TerraSAR-X and TanDEM-X along-track interferometry and Doppler centroid analysis. *IEEE Transactions on Geoscience and Remote Sensing* 52 (5): 2759-2772.

Roobaert, A., G. G. Laruelle, P. Landschützer, N. Gruber, L. Chou, and P. Regnier. 2019. The spatiotemporal dynamics of the sources and sinks of CO2 in the global coastal ocean. *Global Biogeochemical Cycles* 33 (12): 1693-1714.

Rossby, T., M. Prater, and H. Søiland. 2009. Pathways of inflow and dispersion of warm waters in the Nordic seas. *Journal of Geophysical Research: Oceans* 114 (C4).

Rufenach, C. L., R. A. Shuchman, and D. R. Lyzenga. 1983. Interpretation of synthetic aperture radar measurements of ocean currents. *Journal of Geophysical Research: Oceans* 88 (C3): 1867-1876.

Rynders, S. 2017. Impact of waves on sea ice and oceans in the Marginal Ice Zone. *PhD Thesis, University of Southampton*.

Sandu, I., P. Bechtold, L. Nuijens, A. Beljaars, and A. Brown. 2020. On the causes of systematic forecast biases in near-surface wind direction over the oceans. In *ECMWF Technical Memo*.

Schlembach, F., F. Ehlers, M. Kleinherenbrink, M. Passaro, D. Dettmering, F. Seitz, and C. Slobbe. 2023. Benefits of fully focused SAR altimetry to coastal wave height estimates: A case study in the North Sea. *Remote Sensing of Environment* 289: 113517.

Schulz-Stellenfleth, J., and E. Stanev. 2016. Analysis of the upscaling problem–A case study for the barotropic dynamics in the North Sea and the German Bight. *Ocean Modelling* 100: 109-124.

SeaSTAR MATER. 2023. *EE11 SeaSTAR Mission Assumptions And Technical Requirements (MATER).* ESA Reference EOP-ΦMP/2021-11-2315, Version 5.0, Issued 13/06/2023.

Shcherbina, A. Y., M. A. Sundermeyer, E. Kunze, E. D'Asaro, G. Badin, D. Birch, A.-M. E. Brunner-Suzuki, J. Callies, B. T. Kuebel Cervantes, and M. Claret. 2015. The LatMix summer campaign: submesoscale stirring in the upper ocean. *Bulletin of the American Meteorological Society* 96 (8): 1257-1279.

Shemer, L., M. Marom, and D. Markman. 1993. Estimates of currents in the nearshore ocean region using interferometric synthetic aperture radar. *Journal of Geophysical Research: Oceans* 98 (C4): 7001-7010.

Shin, Y., L. Deike, and L. Romero. 2022. Modulation of Bubble-Mediated CO2 Gas Transfer Due To Wave-Current Interactions. *Geophysical Research Letters* 49 (22): e2022GL100017.

Shuchman, R., and G. Meadows. 1980. Airborne synthetic aperture radar observation of surf zone conditions. *Geophysical Research Letters* 7 (11): 857-860.

Shutler, J. D., R. Wanninkhof, P. D. Nightingale, D. K. Woolf, D. C. Bakker, A. Watson, I. Ashton, T. Holding, B. Chapron, and Y. Quilfen. 2020. Satellites will address critical science priorities for quantifying ocean carbon. *Frontiers in Ecology and the Environment* 18 (1): 27-35.

Siegelman, L., P. Klein, P. Rivière, A. F. Thompson, H. S. Torres, M. Flexas, and D. Menemenlis. 2020. Enhanced upward heat transport at deep submesoscale ocean fronts. *Nature Geoscience* 13 (1): 50-55.

Siegert, M. J., M. J. Bentley, A. Atkinson, T. J. Bracegirdle, P. Convey, B. Davies, R. Downie, A. E. Hogg, C. Holmes, and K. A. Hughes. 2023. Antarctic extreme events. *Frontiers in Environmental Science* 11: 1229283.

Sperrevik, A. K., K. H. Christensen, and J. Röhrs. 2015. Constraining energetic slope currents through assimilation of high-frequency radar observations. *Ocean Science* 11 (2): 237-249.

Stanev, E., F. Ziemer, J. Schulz-Stellenfleth, J. Seemann, J. Staneva, and K.-W. Gurgel. 2015. Blending surface currents from HF radar observations and numerical modeling: tidal hindcasts and forecasts. *Journal of Atmospheric and Oceanic Technology* 32 (2): 256-281.

Stanev, E. V., M. Dobrynin, A. Pleskachevsky, S. Grayek, and H. Günther. 2009. Bed shear stress in the southern North Sea as an important driver for suspended sediment dynamics. *Ocean Dynamics* 59 (2): 183-194.

Staneva, J., K. Wahle, H. Günther, and E. Stanev. 2016. Coupling of wave and circulation models in coastal–ocean predicting systems: a case study for the German Bight. *Ocean Science* 12 (3): 797-806.

Staneva, J., V. Alari, Ø. Breivik, J.-R. Bidlot, and K. Mogensen. 2017. Effects of wave-induced forcing on a circulation model of the North Sea. *Ocean Dynamics* 67 (1): 81-101.

Stephenson, S. R., L. C. Smith, and J. A. Agnew. 2011. Divergent long-term trajectories of human access to the Arctic. *Nature Climate Change* 1 (3): 156.

Stoffelen, A., and M. Portabella. 2006. On Bayesian scatterometer wind inversion. *IEEE Transactions on Geoscience and Remote Sensing* 44 (6): 1523-1533.

Stoffelen, A., J. A. Verspeek, J. Vogelzang, and A. Verhoef. 2017. The CMOD7 geophysical model function for ASCAT and ERS wind retrievals. *IEEE Journal of Selected Topics in Applied Earth Observations and Remote Sensing* 10 (5): 2123-2134.

Stoffelen, A., R. Kumar, J. Zou, V. Karaev, P. S. Chang, and E. Rodriguez. 2019. Ocean surface vector wind observations. In *Remote sensing of the Asian Seas*, edited by V. Barale and M. Gade, 429-447. https://doi.org/10.1007/978-3-319-94067-0_24: Springer.

Stoffelen, A. C. M. 1998. Scatterometry. Ph.D. dissertation, University of Utrecht, The Netherlands.

Stopa, J. E., P. Sutherland, and F. Ardhuin. 2018. Strong and highly variable push of ocean waves on Southern Ocean sea ice. *Proceedings of the National Academy of Sciences* 115 (23): 5861-5865.

Storto, A., M. J. Martin, B. Deremble, and S. Masina. 2018. Strongly coupled data assimilation experiments with linearized ocean–atmosphere balance relationships. *Monthly Weather Review* 146 (4): 1233-1257.

Strand, K. O., M. Huserbråten, K.-F. Dagestad, C. Mauritzen, B. E. Grøsvik, L. A. Nogueira, A. Melsom, and J. Röhrs. 2021. Potential sources of marine plastic from survey beaches in the Arctic and Northeast Atlantic. *Science of the Total Environment* 790: 148009.

Tonani, M., P. Sykes, R. R. King, N. McConnell, A.-C. Péquignet, E. O'Dea, J. A. Graham, J. Polton, and J. Siddorn. 2019. The impact of a new high-resolution ocean model on the Met Office North-West European Shelf forecasting system. *Ocean Science* 15 (4): 1133-1158.

Toporkov, J. V., D. Perkovic, G. Farquharson, M. A. Sletten, and S. J. Frasier. 2005. Sea surface velocity vector retrieval using dual-beam interferometry: First demonstration. *IEEE transactions on geoscience and remote sensing* 43 (11): 2494-2502.

Trampuz, C., N. Gebert, S. Placidi, L. C. Izzy Hendricks, F. Speziali, V. Navarro, A. C. H. Martin, C. P. Gommenginger, M. Suess, and A. Meta. 2018. "OSCAR - The airborne interferometric and scatterometric radar instrument for accurate sea current and wind retrieval." EUSAR 2018, the 12th European Conference on Synthetic Aperture Radar., Aachen, 4-7 June 2018.

Tucker, M. J., and E. G. Pitt. 2001. *Waves in ocean engineering*. Vol. 5. *Elsevier Ocean Engineering Book Series*: Elsevier. 550p.

US Department of State. 2021. "The Long-Term Strategy of the United States: Pathways to Net-Zero Greenhouse Gas Emissions by 2050. Available: https://www.whitehouse.gov/wp-content/uploads/2021/10/US-Long-Term-Strategy.pdf".

van den Bremer, T. S., and Ø. Breivik. 2018. Stokes drift. *Philosophical Transactions of the Royal Society A: Mathematical, Physical and Engineering Sciences* 376 (2111): 20170104.

Vellinga, M., D. Copsey, T. Graham, S. Milton, and T. Johns. 2020. Evaluating benefits of two-way ocean–atmosphere coupling for global NWP forecasts. *Weather and Forecasting* 35 (5): 2127-2144.

Verhoef, A., and A. Stoffelen. 2021. *Advances in Ku-Band Scatterometer Quality Control.* EUMETSAT report SAF/OSI/CDOP3/KNMI/SCI/TN/404, Version 1.1. https://knmi-scatterometer-website-prd.s3-eu-west-1.amazonaws.com/publications/osisaf_cdop3_ss3_tn_advances_in_ku-band_qc_1.1.pdf.

Villas Bôas, A. B., F. Ardhuin, A. Ayet, M. A. Bourassa, P. Brandt, B. Chapron, B. D. Cornuelle, J. T. Farrar, M. R. Fewings, and B. Fox-Kemper. 2019. Integrated observations of global surface winds, currents, and waves: requirements and challenges for the next decade. *Frontiers in Marine Science* 6: 425.

Vogelzang, J., A. Stoffelen, A. Verhoef, and J. Figa-Saldaña. 2011. On the quality of high-resolution scatterometer winds. *Journal of Geophysical Research: Oceans* 116 (C10).

Vogelzang, J., and A. Stoffelen. 2018. Improvements in Ku-band scatterometer wind ambiguity removal using ASCAT-based empirical background error correlations. *Quarterly Journal of the Royal Meteorological Society* 144 (716): 2245-2259.

Vogelzang, J., and A. Stoffelen. 2022. On the accuracy and consistency of quintuple collocation analysis of in situ, scatterometer, and NWP winds. *Remote Sensing* 14 (18): 4552.

Wang, R., W. Zhu, X. Zhang, Y. Zhang, and J. Zhu. 2023. Comparison of Doppler-Derived Sea Ice Radial Surface Velocity Measurement Methods From Sentinel-1A IW Data. *IEEE Journal of Selected Topics in Applied Earth Observations and Remote Sensing* 16: 2178-2191. https://doi.org/10.1109/JSTARS.2023.3241978.

Wang, Z., A. Stoffelen, F. Fois, A. Verhoef, C. Zhao, M. Lin, and G. Chen. 2017. SST dependence of Ku-and C-band backscatter measurements. *IEEE Journal of Selected Topics in Applied Earth Observations and Remote Sensing* 10 (5): 2135-2146.

Wang, Z., J. Zou, A. Stoffelen, W. Lin, A. Verhoef, X. Li, Y. He, Y. Zhang, and M. Lin. 2021. Scatterometer sea surface wind product validation for HY-2C. *IEEE Journal of Selected Topics in Applied Earth Observations and Remote Sensing* 14: 6156-6164.

Wineteer, A., H. S. Torres, and E. Rodriguez. 2020. On the surface current measurement capabilities of spaceborne Doppler scatterometry. *Geophysical Research Letters* 47 (21): e2020GL090116.

Winterfeld, M., G. Mollenhauer, W. Dummann, P. Köhler, L. Lembke-Jene, V. D. Meyer, J. Hefter, C. McIntyre, L. Wacker, and U. Kokfelt. 2018. Deglacial mobilization of pre-aged terrestrial carbon from degrading permafrost. *Nature Communications* 9 (1): 3666.

WMO. 2018. Observing Systems Capability Analysis and Review Tool (OSCAR): Requirements for Ocean Surface Currents (vector). https://www.wmo-sat.info/oscar/variables/view/116.

WMO. 2022. *The 2022 GCOS Implementation Plan.* (https://library.wmo.int/records/item/58104-the-2022-gcos-implementation-plan-gcos-244).

Wolf, J., and D. Prandle. 1999. Some observations of wave–current interaction. *Coastal Engineering* 37 (3-4): 471-485.

Wolf, J. 2009. Coastal flooding: impacts of coupled wave–surge–tide models. *Natural Hazards* 49 (2): 241-260.

Woodson, C. B., and S. Y. Litvin. 2015. Ocean fronts drive marine fishery production and biogeochemical cycling. *Proceedings of the National Academy of Sciences* 112 (6): 1710-1715.

Xu, X., and A. Stoffelen. 2019. Improved rain screening for ku-band wind scatterometry. *IEEE Transactions on Geoscience and Remote sensing* 58 (4): 2494-2503.

Yague-Martinez, N., J. Márquez, M. Cohen, D. Lancashire, and C. Buck. 2012. Wavemill proof-of-concept campaign. processing algorithms and results. EUSAR 2012. 9th European Conference on Synthetic Aperture Radar, Nuremberg, Germany, 23-26 April 2012

Yu, P., A. L. Kurapov, G. D. Egbert, J. S. Allen, and P. M. Kosro. 2012. Variational assimilation of HF radar surface currents in a coastal ocean model off Oregon. *Ocean Modelling* 49: 86-104.

Yurovsky, Y. Y., V. N. Kudryavtsev, S. A. Grodsky, and B. Chapron. 2019. Sea surface Ka-band Doppler measurements: Analysis and model development. *Remote Sensing* 11 (7): 839.

Zhang, Y., W. Huang, X. Liu, C. Zhang, G. Xu, and B. Wang. 2021. Rip current hazard at coastal recreational beaches in China. *Ocean & Coastal Management* 210: 105734.

Zhong, Y., A. Bracco, J. Tian, J. Dong, W. Zhao, and Z. Zhang. 2017. Observed and simulated submesoscale vertical pump of an anticyclonic eddy in the South China Sea. *Scientific Reports* 7.

ACRONYMS

ADCP	Acoustic Doppler Current Profiler
AMOC	Atlantic Meridional Overturning Circulation
AOCS	Attitude and Orbit Control
AIU	Antenna Interface Unit
ATI	Along-track Interferometry
CoG	Center of Gravity
CosMIZ	Coastal Seas, Continental Shelf Seas and Marginal Ice Zones
CTT	Central Thrust Tube
DBI	Dual-Beam Interferometry
DCA	Doppler Centroid Anomaly
DCG	Digital Chirp Generator
DGE	Digital Electronic
DEM	Digital Elevation Model
DN	Distribution Network
DOWS	Directional Ocean Wave Spectrum
DWD	Dominant Wave Direction
DWNCO	Down-conversion
EE11	Earth Explorer 11
EFE	Electronic Front End
EIK	Extended Interaction Klystron
EPC	Electronic Power Conditioner
ESA	European Space Agency
EC	European Commission
EO	Earth Observation
EOL	End of Life
ERF	Estuarine River Flow
ESOC	European Space Operations Center
FG	Frequency Generator

FEM	Finite Element Model
FOCC	Flight Operations Control Center
FOS	Flight Operational Segment
FutureEO	Future Earth Observation
GCP	Ground Control Point
GMF	Geophysical Model Function
GNSS	Global Navigation Satellite System
HDRM	Hold Down and Release Mechanisms
HF	High Frequency
HODP	Higher Order Derivatives Products
HPA	High-Power Amplifier
ICU	Instrument Control Unit
IPCC	Intergovernmental Panel on Climate Change
LEO	Low Earth Orbit
LEOP	Launch and Early Orbit Phase
LNA	Low Noise Amplifier
LoS	Line of Sight
LSTM	Copernicus Land Surface Temperature Monitoring Mission
MATER	Mission Assumptions And Technical Requirements
Mbps	Megabits per second
MIZ	Marginal Ice Zones
ML	Machine Learning
NCC	Norwegian Coastal Current
NOP	Numerical Ocean Prediction
NRCS	Normalised Radar Cross Section
NWP	Numerical weather prediction
OCS	Orbit Control System
ORSSI	Ocean Regions of Special Scientific Interest
OSCAR	Ocean Surface Current Airborne Radar Demonstrator
OSCM	Ocean Surface Current Mission

OSVW	Ocean Surface Vector Wind
PCDU	Power Conditioning and Distribution Unit
PCM	Phase Change Material
PDGS	Payload Data Ground Segment
PDHT	Payload Data Handling and Transmission
PRF	Pulse Repetition Frequency
RCS	Reaction Control System
RF	Radio Frequency
RM	Receive Module
RMSE	Root Mean Square Error
RSV	Radial Surface Velocity
Rx	Receive
S3NG-TOPO	Sentine-3 Next Generation Topography Mission
SAR	Synthetic Aperture Radar
SAS	SAR Front-End Sub-system
SADM	Solar Array Drive Mechanism
SCORE	Scan On Receive
ScanSAR	Scanning Synthetic Aperture Radar
SES	SAR Electronic Sub-system
SFEES	SAR Front-End Electronic Sub-system
SG	Science Goals
SIDV	Sea Ice Drift Vectors
SNR	Signal to Noise Ratio
SSO	Sun-synchronous orbit
SST	Sea Surface Temperature
SLC	Single Look Complex
SRL	Science Readiness Level
STR	Star Tracker
SWH	Significant Wave Height
SWOT	Surface Water and Ocean Topography mission

TED	Thermo-elastic Distortion
TRM	Transmit and Receive Module
TSCV	Total Surface Current Vector
TT&C	Telemetry, Tracking and Command
Tx	Transmit
TWTA	Travelling Wave Tube Amplifier
UPCO	Up conversion
UPM	Universal Processing Modules
VCM	Variable Coding and Modulation
WASV	Wind-wave Artefact Surface Velocity
WMO	World Meteorological Organization